

Final Report

Technology for Neutron Instrumentation

(TECHNI)

Final Report

(1st March 2000 – 28th February 2004)

Contract No	HPRI-CT-1999-50005
Start Date of Contract	1 st March 2000
End Date of Contract	28 th February 2004
RTD Project Title	Technology for Neutron Instrumentation
Website Address	http://www.isis.rl.ac.uk/techni/
Name of Co-ordinator	Dr M W Johnson
E-mail Address	m.w.johnson@rl.ac.uk

Partnership Summary

<i>Participant Number</i> (co-ordinating partner as participant N°1)	<i>Name of Participating Organisation</i>	<i>Role in Project*</i>
1	Council for the Laboratories Research Council, UK	LSF-TMR
2	Technische Universiteit Delft, The Netherlands	OTHER
3	Hahn-Meitner-Institut, Germany	LSF
4	Institut Laue Langevin, France	LSF
5	Istituto Nazionale per la Fisica della Materia, Italy	OTHER
6	Forschungszentrum Jülich, Germany	LSF
7	Laboratoire Léon Brillouin, France	LSF
8	Kings College London, UK	OTHER
9	Paul Scherrer Institut, Switzerland	LSF
10	Riso National Laboratory, Denmark	OTHER
11	Universita degli studi di Milano-Bicocca, Italy	OTHER
12	Universita degli studi di Roma Tor Vergata, Italy	OTHER

- * LSF-IHP: a research infrastructure funded for access under the IHP programme
LSF-TMR: a research infrastructure funded for access under the TMR programme
LSF-OTH: a research infrastructure outside the IHP or TMR programmes
IND: an industrial or commercial enterprise
OTHER: other types of participant

Final Report

1. EXECUTIVE SUMMARY

The TECHNI programme is aimed at improving access to neutron scattering facilities throughout Europe by improving the quality of neutron instrumentation. The objectives of the TECHNI RTD project were therefore to:

- improve the technology used to build neutron instruments
- improve the instrumentation of European neutron facilities
- train young scientists in the techniques of neutron instrumentation

Since many of the research tasks within TECHNI should result in improved instrumentation technology, as well as specific devices, the list of resulting deliverables is considerable, and has included:

- higher spatial resolution detectors
- more efficient, and faster detectors
- cheaper, more effective position-sensitive detectors
- new focusing components
- more efficient neutron polarising supermirrors

The objectives of the project are best described by the following table (Table 1.1), which lists the research tasks to be undertaken and the technical objectives of each task. In the Annex (Table A1) the roles of each laboratory and the sub-tasks within each of the 9 research tasks are defined. The numbering scheme used in Table A1 is used in the following section to identify the work undertaken by each partner.

In summary the work of the entire programme has generally gone exceptionally well. Out of the nine areas of research, all have delivered their objectives, or made very significant progress towards them. A number of projects have produced results in excess of their objectives. The closure of the Riso reactor early in the TECHNI programme affected the work of their team, but their re-aligned programme was delivered in the final year of the programme. In some areas, it will be seen that recruitment difficulties or other staff difficulties have slowed progress. Overall the programme is met over 95% of its deliverables, and in some cases exceeded original specifications for the project.

	Research Task	Technical Objectives (Deliverables)
1	Millimetre and Sub-Millimetre Detectors	Construction of a second-generation Si microstrip and microstrip gas detectors (MSGC), using ^3He and ^{157}Gd converters. Establish the applicability of GEM technology to different MSGC designs. Report on the inter-comparison study of the three detector types following the evaluation of their characteristics and areas of applicability.
2	> 3 MHz count rate Area PSD	Demonstration of a large area multi-wire neutron PSD detector able to operate at sustained count rates in excess of 3 MHz. Report on the detectors performance and characteristics.
3	Image Plate Detectors	The development of a second generation of neutron image plates with an improved quantum efficiency and a fast, low resolution, online scanner. Develop storage phosphors with lower X-ray sensitivity. Report on the detectors performance and characteristics.
4	3mm scintillator strip detector	A linear scintillator position sensitive detector with >50% efficiency at 1\AA , high γ rejection ($< E-6$), and having a spatial resolution 3mm.
5	>10eV Energy Neutron detector	Build and test a new type of resonant neutron detector capable of efficiently detecting neutrons in the 100 eV energy range. Report on the detectors performance and characteristics.
6	Neutron Focussing Devices	Design and construction of three types of neutron focussing devices. Report on the inter-comparison of their characteristics and performance.
7	Neutron Polarisation	Design and manufacture of the next generation of remanent neutron supermirror polarisers which have a divergence suitable for use with thermal (i.e. $\lambda > 1\text{\AA}$) neutron beams. The design and manufacture of self-supporting multilayer films, and their integration into a practical, neutron beam-line component. Report on the inter-comparison of the performance of the two devices.
8	Neutron Energy Selection Devices	The production of a gradient crystal monochromator for thermal (i.e. $\lambda > 1\text{\AA}$) neutrons. Build an optimised neutron optical grating for neutron energy analysis. Report on the inter-comparison of the performance of the two devices.
9	NSE Radial Correction Coils	A successful new design of NSE radial correction coils

Table 1.1

Final Report

1. SCIENTIFIC & TECHNICAL PERFORMANCE

1.1. Specific Project Objectives

As noted above the completed TECHNI programme delivered ***% of its objectives on time and exceeded a number of the original technical specifications. A summary of the outcomes for each of the overall objectives defined in Table 1.1 are reported in Table 3.1 below.

In the section below we give a description of each of the major tasks reported by the teams involved.

1.2. Overview of Technical Progress

INFN: Milan / Perugia - Task 1

Millimetre and Sub-Millimetre Detectors

The capabilities of high space resolution at high counting rate, typical of the Si *p-n* junction diode, are the most appealing features from the perspective of operation under the intense neutron fluxes expected for next generation neutron sources. Of utmost interest is the maximum instantaneous data rate achievable since it influences the detector dead-time. Indeed, operation of the detector as a counter under an intense and pulsed neutron beam requires a dead-time notably less than 1 μ s and the capability of managing the time-information contained in the white neutron pulse. Side advantages, which can be exploited for some special neutron applications, are the shape flexibility and the operation of the Silicon detector, with its low-power front-end electronics, under vacuum and, if necessary, at low temperature. Neutron detection is accomplished by coupling the Si sensor to a converter with thickness and geometry optimized to maximize the neutron detection efficiency.

Under TECHNI, a number of prototype detectors (models from TEC_0 to TEC_3), all exploiting the concept of the microstrip Si sensor coupled to the Gd neutron converter, have been designed, fabricated and tested. Natural Gadolinium represents the best compromise between cost and detection efficiency, particularly under the test phase. The diverse detection schemes were optimized to match with the specific characteristics to be measured, such as neutron detection efficiency, background sensitivity and dead-time. Both linear (1-*d*) and two-dimensional (2-*d*) versions of high space resolution position sensitive prototypes have been developed, and the operation of 1-*d* detectors in powder diffraction and reflectometry applications was proved.

Together with the improvements in the detector performance, which can be achieved by changing the sensor geometry and its structural characteristics, it is of paramount importance to optimize the readout electronics coupled to the sensor. The overall performances of the neutron detector depend on the coupling of the sensor to highly performing ASICS chips. Parallel readout of a relatively large number of channels was necessary. Since the capability of reading out a large number of channels, with high speed and in parallel mode, is a fundamental demand for the construction of a large area detector with time stamp, special effort was devoted to the development of new electronics based on VLSI components for an easy handling of the detection event by the main computer. Moreover, as sensor and chips are ideally placed on the same PCB, a proper design of bondings and components mounting have to be anticipated for any further easy assembling of the PCB into modules of a larger size detector.

The results of the neutron test measurements on the different prototypes we developed, showed advantages and operational limits of the Si/Gd device as neutron counter. The measured pulse rise time and space resolution, were easily better than the corresponding values for standard gas or scintillator counters. Typical values of the rise time were smaller than 1 μ s, and 50 ns were obtained using a fast pre-amplifier chip, whereas position resolutions better than 0.5 mm were measured. At present, use of the natural Gadolinium converter confines the application to cold and thermal neutrons. Improvements in detector performances, like increasing the neutron detection efficiency and diminishing the γ -ray sensitivity, can be accomplished by using isotopic Gadolinium (^{155}Gd or ^{157}Gd) or a double converter (Gd-Si-Gd) configuration. The optimization of the detector design was also controlled by the Monte Carlo analysis, which enabled to simulate the detector performances associated to different choices of the construction parameters.

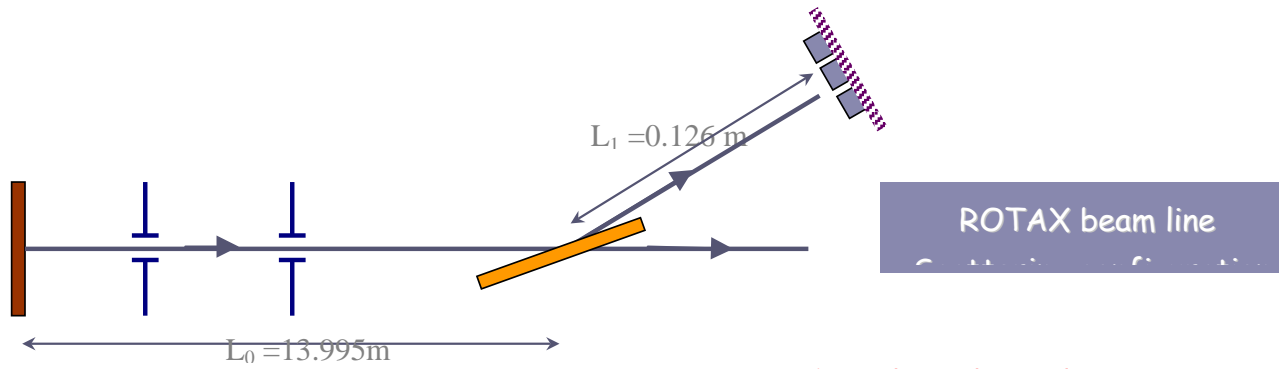
Final Report

The characteristics of the prototypes developed under the project, sensors and ASICS, are listed in the attached Table I. Major results from neutron test measurements are also shown in the Figures.

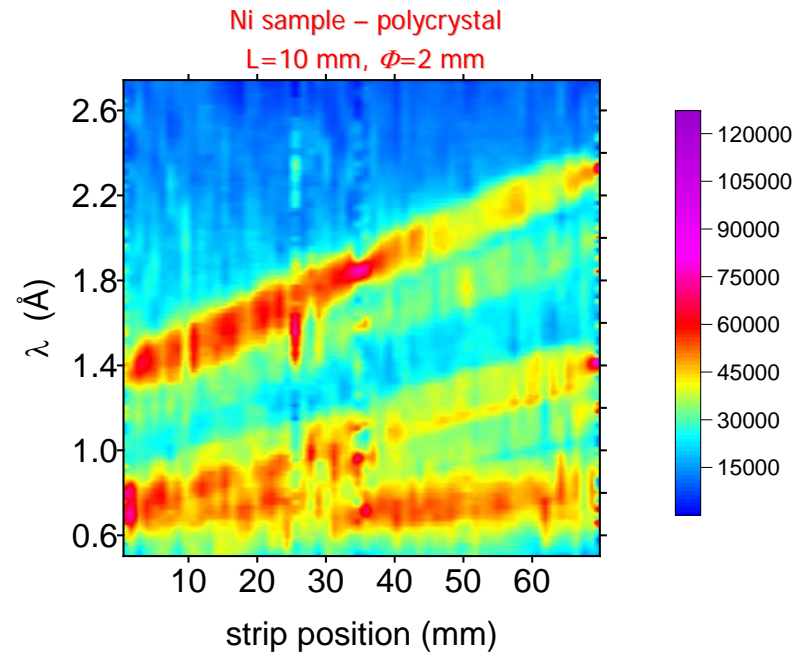
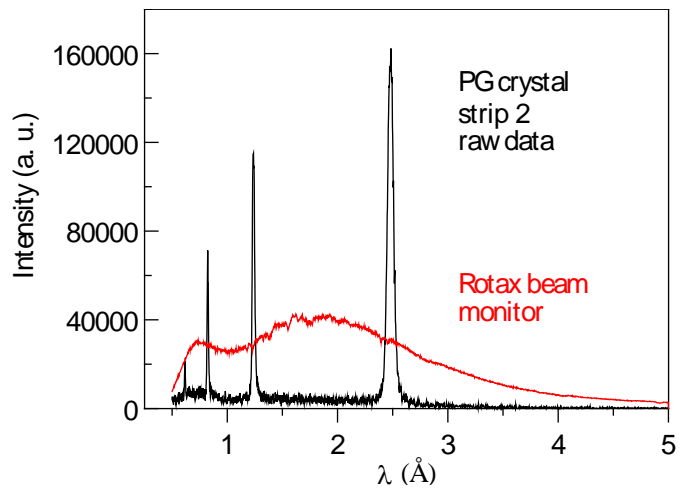
Table 1

Si/Gd Microstrip Detector		TEC_0	TEC_1	TEC_2	TEC_3
			<i>Upgraded design of the TEC_0 PCB</i>		
Converter characteristics		Natural Gd 1 metal foil, 0.25mm	Natural Gd 2 metal foils, 0.25mm back, 0.005mm front	Natural Gd 2 metal foils, 0.25mm back, 0.005mm front	Natural Gd 1 metal foil, 0.25mm
M E C H A N I C A L	Module size (mm ²)	40 x 70	40 x 70	40 x 70	20 x 20
	No. of detection planes	1	1	1	2
	Microstrip pitch (mm)	0.55	0.55	0.55	0.104
	No. of microstrips per module	128	128	128	192 x 192
	No. of ASICS per detection planes	16 VA2 (8ch) + 32 SMD, MAX908 + 16 SN74LS148	16 VA2 (8ch) + 32 SMD, MAX908 + 16 SN74LS148	4 VA32/TAN (32ch)	6 VA32/TAN (32 ch)
	Microstrip capacitance (pf)	20	20	20	5
E L E C T R I C A L	ENC achieved	165 e ⁻ + 6.1 e ⁻ /pF	165 e ⁻ + 6.1 e ⁻ /pF	300 e ⁻ + 25 e ⁻ /pF	300 e ⁻ + 25 e ⁻ /pF
	Signal readout	For all hits above the threshold, fast timing signal and address	For all hits above the threshold, fast timing signal and address	For all hits within the energy window, fast timing signal and address	For all hits within the energy window, fast timing signal and address
	Count rate/cm ² 10 % loss	500 kHz	500 kHz	2 MHz	90 MHz
	Count rate/ ASIC 10 % loss	---	---	1 MHz	1 MHz
	Count rate/ microstrip 10 % loss	100 kHz	100 kHz	1 MHz	1 MHz
	Peaking time (μs)	0.7	0.7	0.075 – 0.1	< 0.1

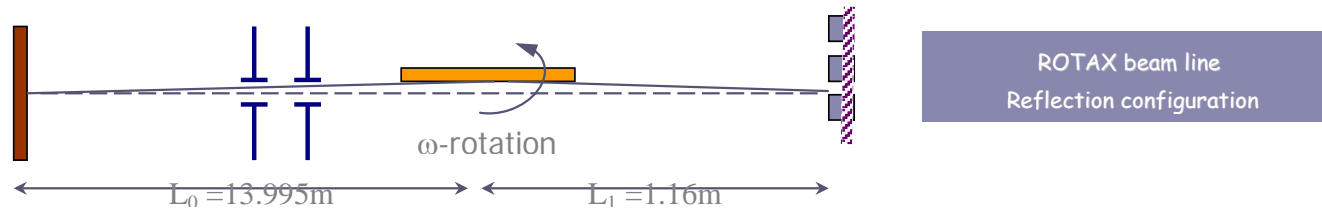
Final Report



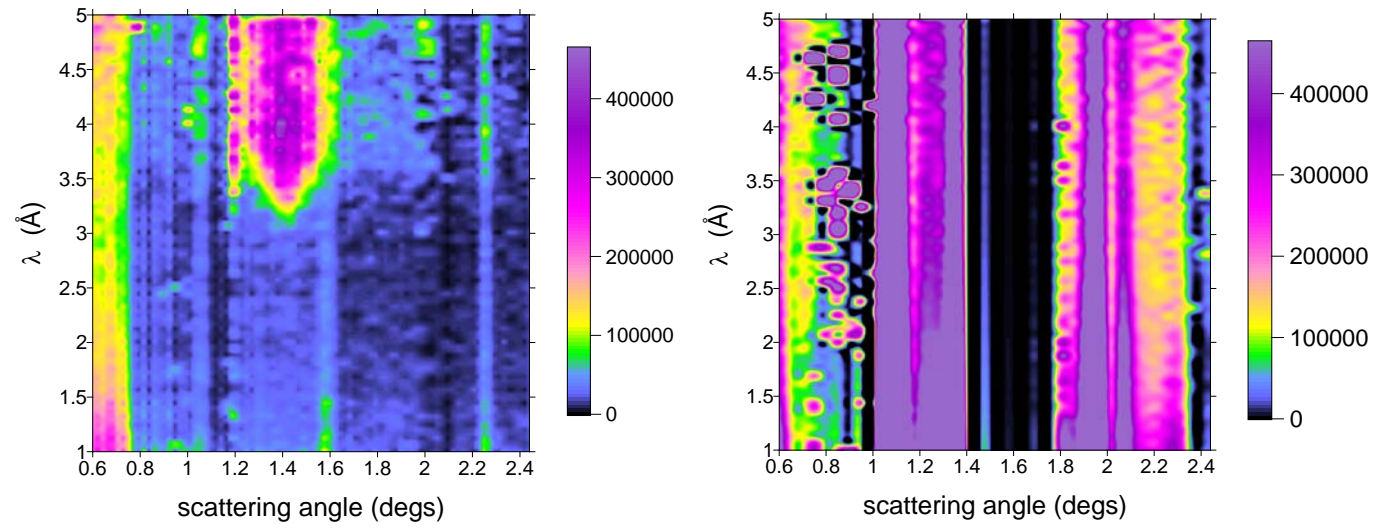
PG CRYSTAL



Final Report

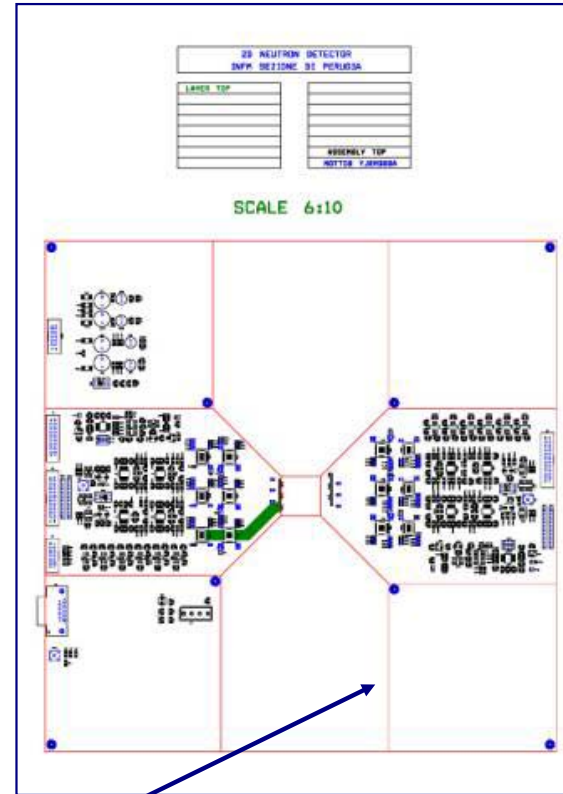
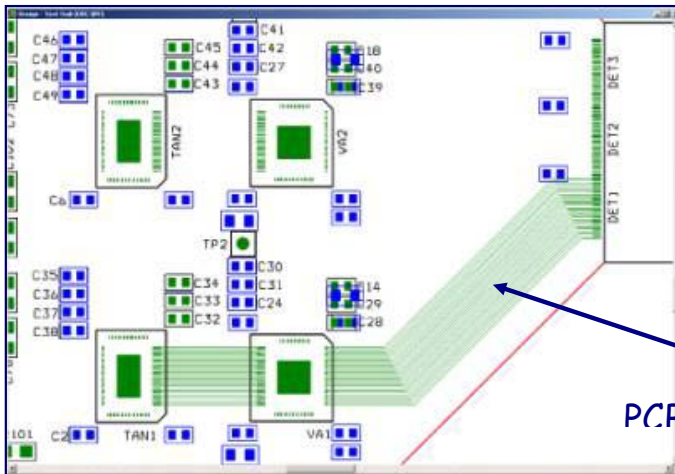
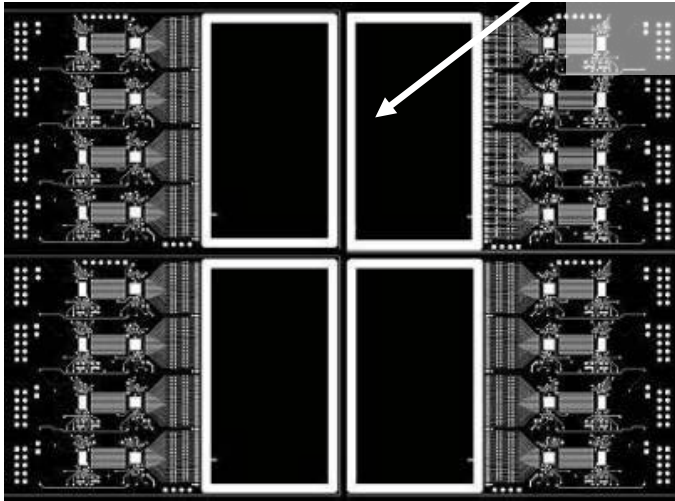


POLARISING MIRROR



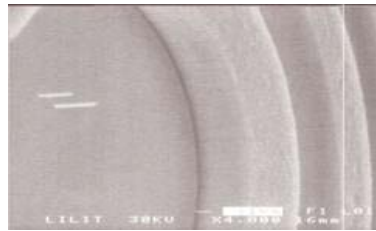
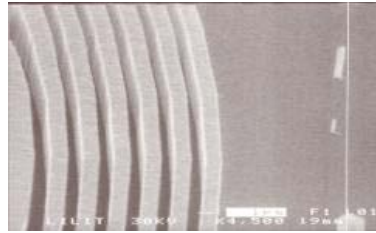
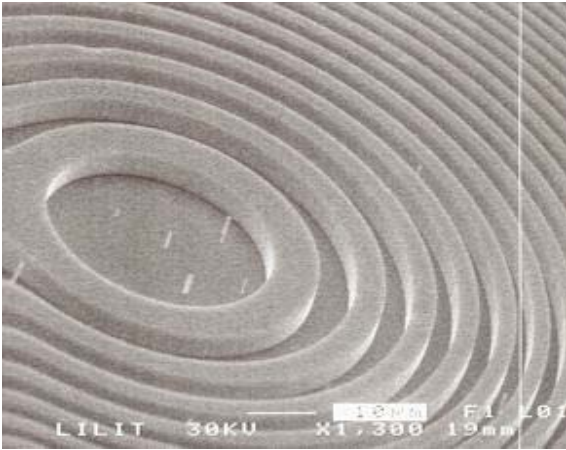
Final Report

Assembly of 4 TEC_1 modules - 1d detector
Sensor size 145 x 85 mm²
Pitch 0.55 mm
No. of channels 512

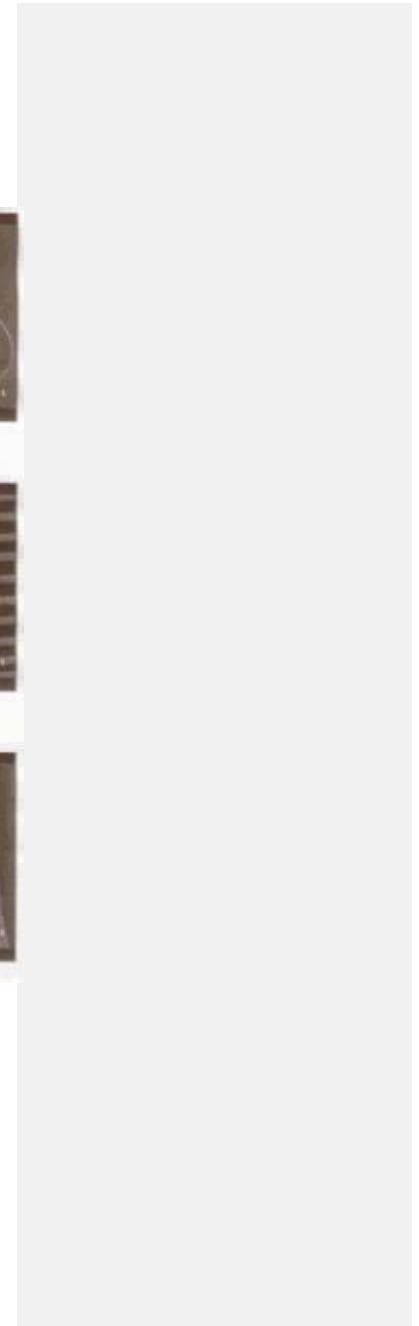
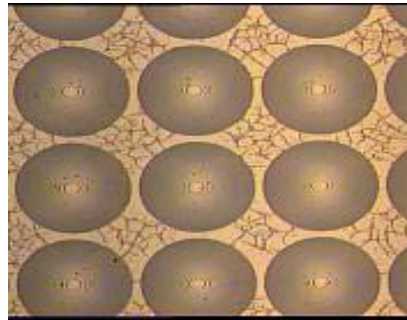
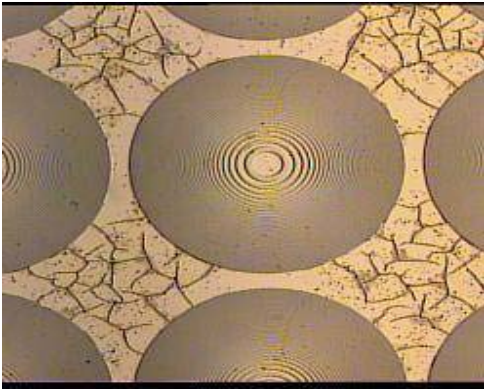
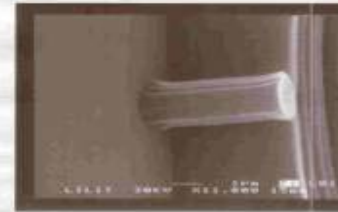
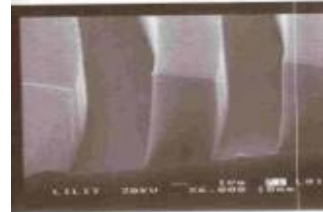
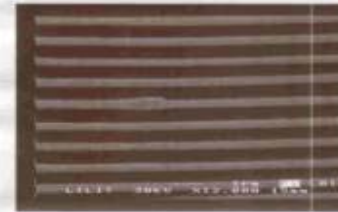
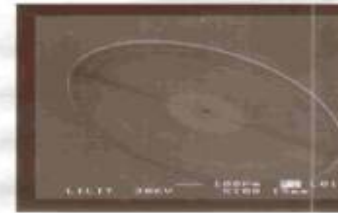


PCB of the 2d Si/Gd TFC 3 prototype

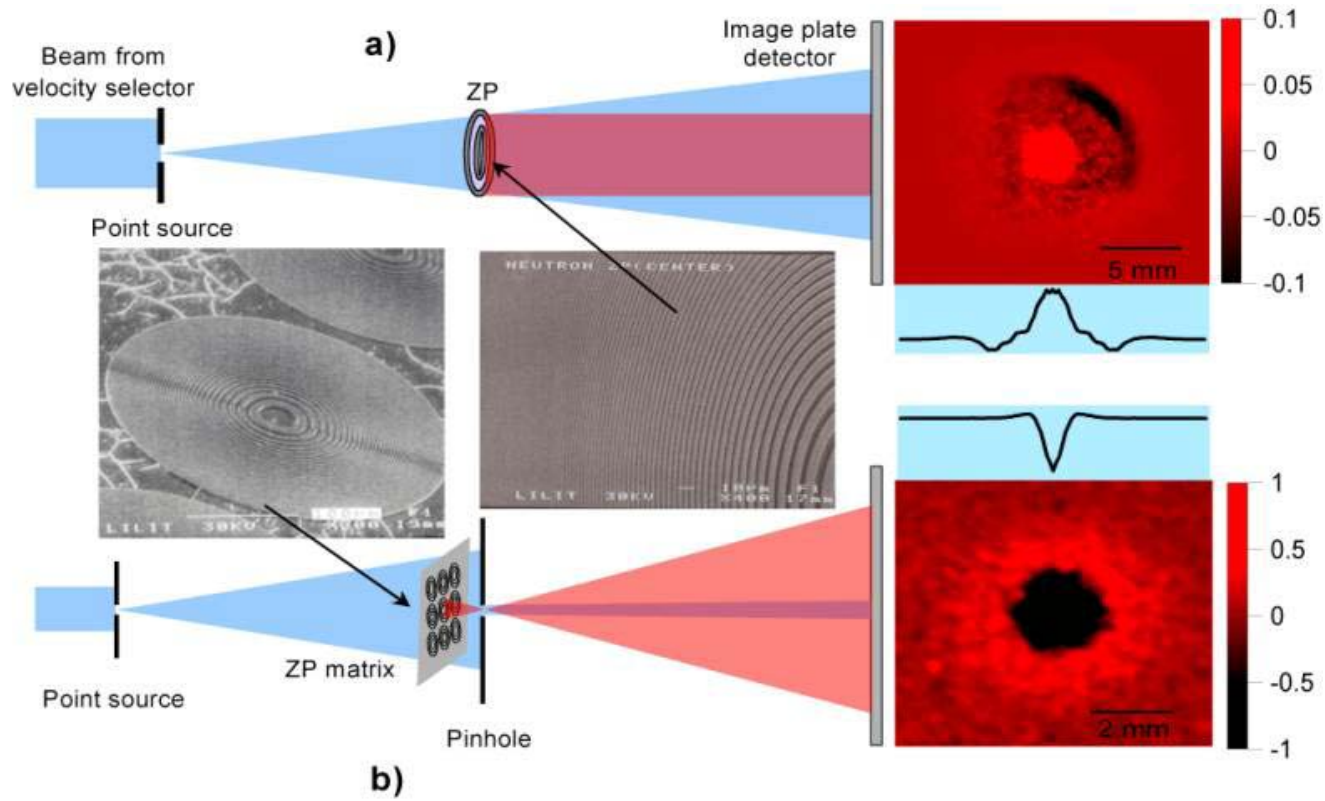
Final Report



Images of some of the Zone plates fabricated

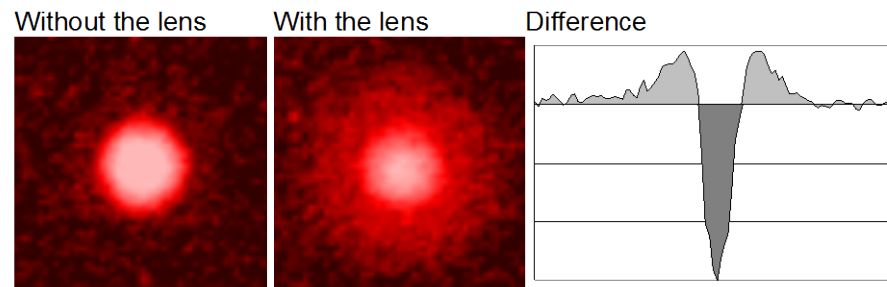
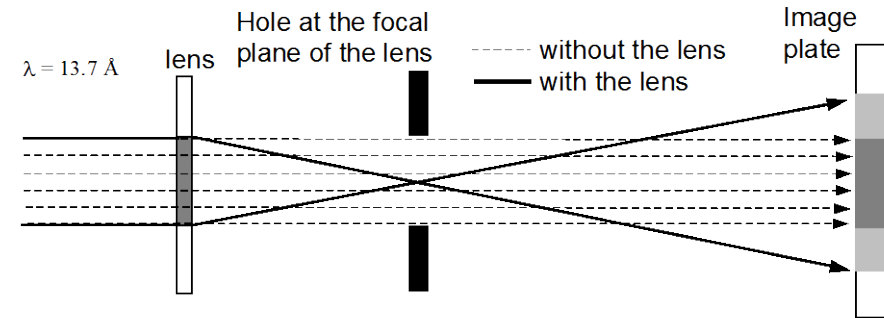


Final Report

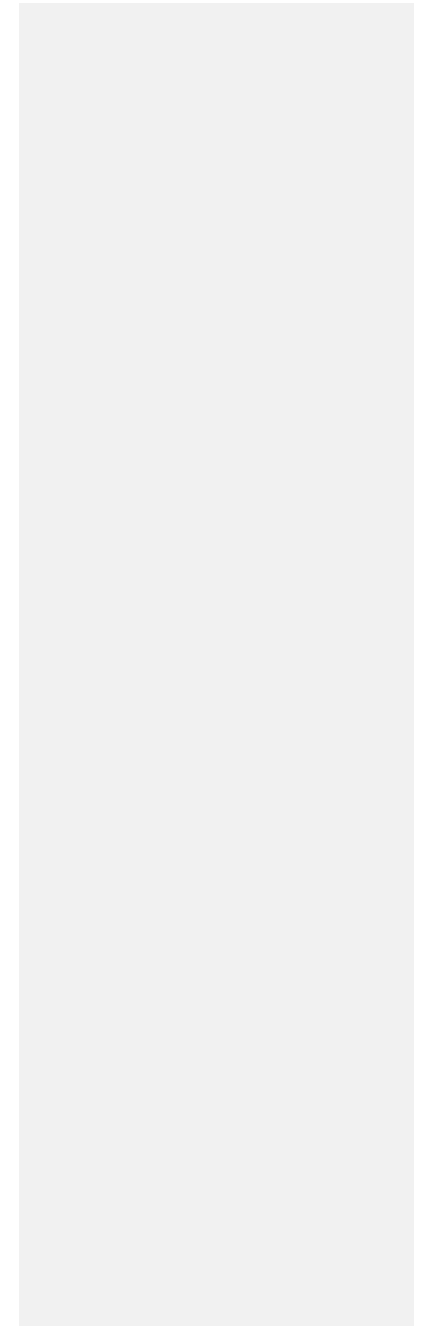


Neutron test measurements of the 5 mm Zone Plate, ZP_1, and the matrix ZP_3

Final Report

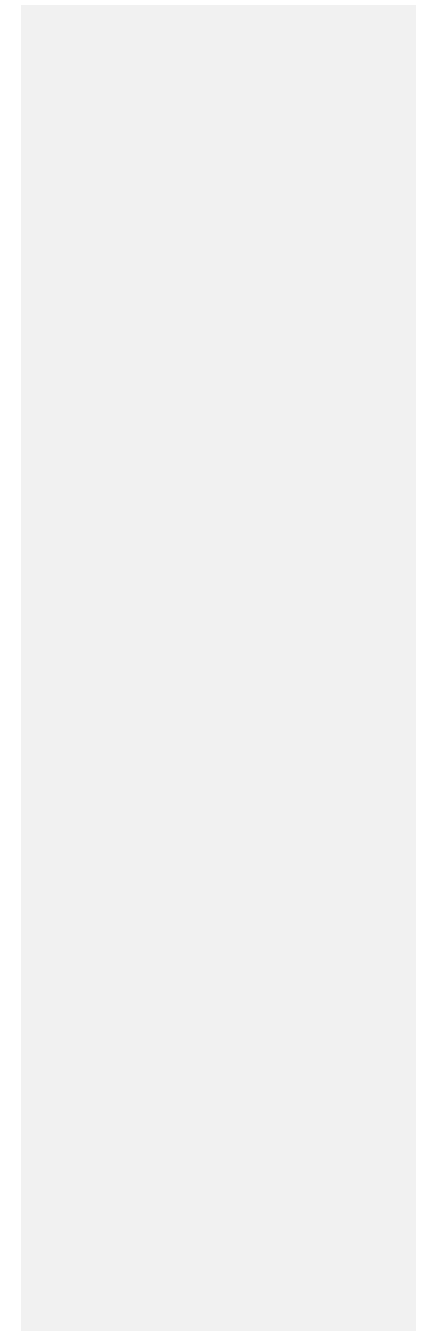
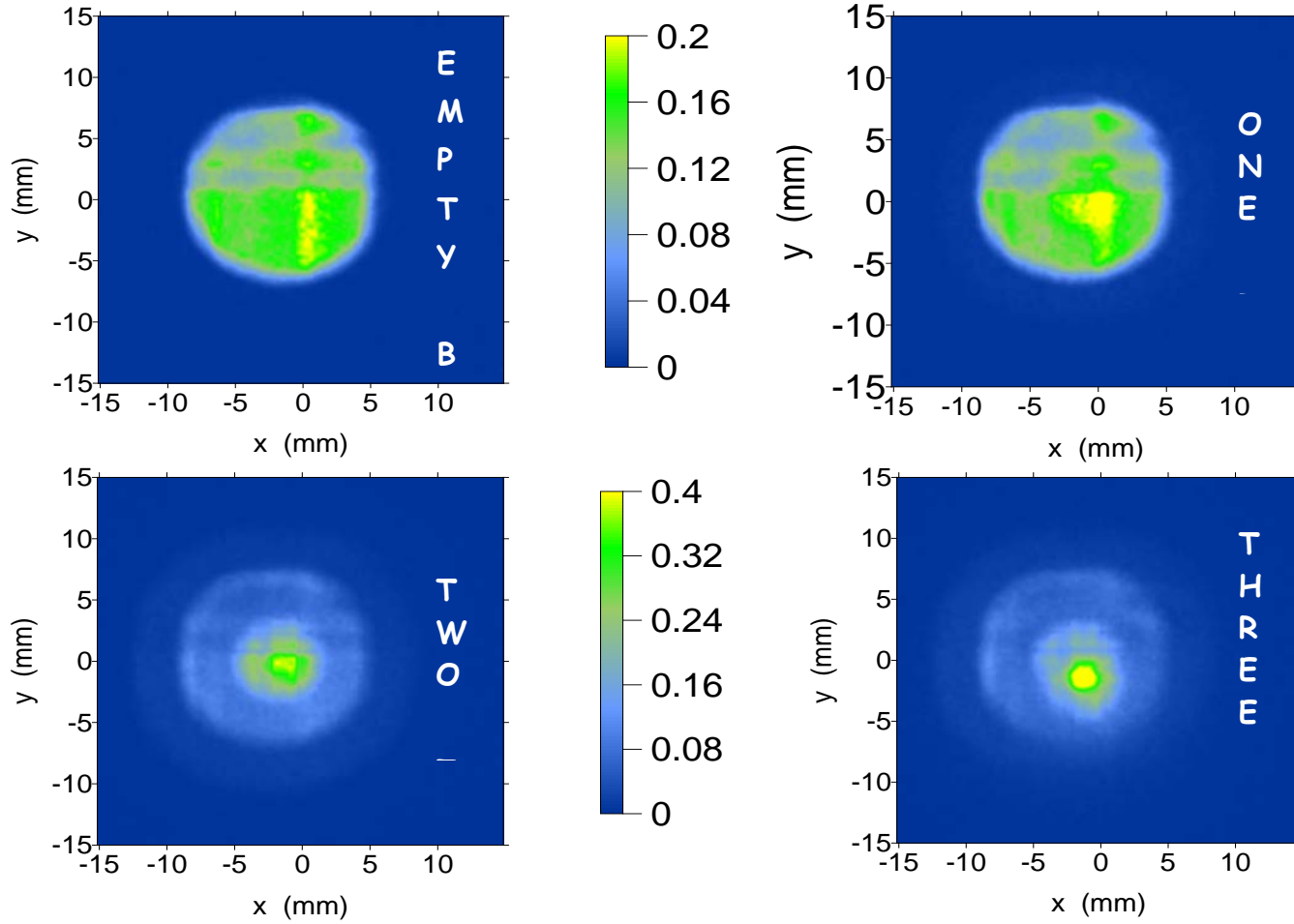


Neutron test measurements of the matrix ZP_3



Final Report

Neutron test measurements of the Zone Plate Stack SZP 1



Final Report

HMI: Task 1

The novel micro-strip gas chamber (MSGC) detector type developed at HMI improves the performance of present thermal neutron detectors considerably and delivers an adequate economic solution for fast high-resolution large-area detectors, even for the strongly rising requirements in experiments at next generation pulsed spallation neutron sources like ESS. Two-dimensional position resolutions of better than 0.3 mm (FWHM), time-of-flight resolutions of a few ns and count rates $>10^6$ cps per detector segment can be reached with a novel cost-effective high-rate multi-hit delay line readout technique developed at HMI based on subdivided delay lines connected via impedance matching amplifiers. A high-speed, high-resolution data acquisition board type developed in TECHNI and also in collaboration with JINR Dubna for this detector type is operational. A simpler board type based on the same technology for readout of multiwire chambers was also developed and built in series as a spin-off. For this board interest from several other institutes exist.

Prototype multi-layer MSGC plates for two-dimensional readout were fabricated in collaboration with Institute for Physics of Microstructures, Russian Academy of Sciences (IPM RAS). Composite Gd/CsI converters with columnar CsI secondary electron emitter structures of 1 μm height and the other detector components were developed at HMI in prototype size. For the development of full-size MSGC plates orders were placed at first at Fraunhofer Institute for Surface Engineering and Thin Films (FhG-IST), Germany, and then at IPM RAS, which, however, were not completed successfully due to high costs. Consequently it was decided to pursue these tasks at HMI, and a dedicated large-area UHV apparatus was developed as a vacuum envelope for all critical physical vapour deposition processes necessary for fabrication of full-size plates; this apparatus is now operational at HMI. However, the integration of all processes necessary for production of full-size MSGC detectors could not be achieved within TECHNI; this shall be accomplished during the next year.

Micro-strip Gas Detectors (MSGC)

Subtask 1.2.1 with the items:

“Development and fabrication of foil converters for MSGC and Si strip detectors” (in collaboration with INFEM)

This item is subdivided into two sub-items:

- Deposition of **Gd layers** of 2x 0.5-1.5 μm thickness either side of a Aramid plastic foil of a few μm thickness, and
- Deposition of **columnar CsI** secondary electron emitter (SEE) layers either side on top of the Gd layers.

At HMI the **deposition technology of Gd layers** of the required thickness onto 4-6 μm thick ARAMID (Kevlar) plastic foils was developed in prototype scale. ARAMID is the mechanically strongest plastic and it is also very heat resistant. However, a proper stretching of the ARAMID foils, an optimized sputter cycle and a homogeneous deposition from both sides are important for minimizing compressive stresses in the Gd layers and for compensating for the remaining stresses, respectively. For the deposition a small (2 inch) RF magnetron sputter source is operated with small power (50-100 W). The substrate is cooled on its rear side by a polished copper plate and a Peltier cell, which again is water-cooled on its rear side by means of a heat exchanger plate. Thus, via regulating the Peltier cell any required temperature can be chosen. The use of a small sputter source is essential, too, for using highly enriched ^{157}Gd in order to restrict the necessary amount of ^{157}Gd on the sputter target.

The same cooling technique is crucial for thermal evaporation of CsI in an Ar atmosphere of 10^{-3} mbar base pressure for deposition of columnar CsI SEE layers. By regulating the temperature and the deposition rate the structure width of the CsI columns can be optimised. Layers with columns of ~ 1 μm height and ~ 0.2 μm width were made. The layers were investigated with respect to their morphology and secondary electron emission properties.

This deposition work was performed in the detector laboratory of HMI in an existing high vacuum evaporation apparatus of 45 mm diameter, which was further equipped with the necessary additional tools, i.e. the sputter source, two thermal evaporation sources, the Peltier cooling and a gas regulation system.

Final Report

This apparatus had the following drawbacks: (i) It was only useful for prototype scale converter fabrication, since its small size did not allow travelling full-size (i.e. 28.5x28.5 cm²) converters over the set of sources in order to achieve the necessary deposition uniformity. (ii) It had no vacuum lock and transfer system for transferring the hygroscopic CsI samples from the chamber vacuum into a transport vessel filled with inert gas. (iii) The cleanliness of the base vacuum achieved was not sufficient for producing resistive layers needed for the multi-layer MSGC plate fabrication.

Therefore, a large-area (cross section 90x90 cm²) ultra-high vacuum apparatus with two-dimensional travel and transfer system with a lock to a glove box was designed. In this chamber full-size Gd/CsI composite converter foils can be made and all thermal evaporation and sputter deposition processes necessary for the fabrication of full-size detector segments can be performed in laboratory scale, i.e. for a limited number of samples (see below).

Construction of small-scale, low-pressure MSGC prototype using Gd converter design

For the development of low-pressure MSGC detectors in prototype scale (10 by 10 cm), except converter development, the following R&D work was completed at HMI:

1. Modelling, optimisation and CAD of prototype and full-size MSGC detectors:

This work was completed in a comprehensive style that was unparalleled in the literature so far using a combination of the codes MAXWELL for 2D and 3D electric field calculations, MSGCSIM for modelling of the gas multiplication process and of the signal induction, and SPICE and MOMENTUM for modelling the signal transport in the coupled MSGC multi-layer plates and the subsequent front-end electronics.

2. Development of the MSGC multi-layer technology:

The novel multi-layer MSGC plates are fabricated by deposition of the following layers on glass plates:

- Two micro-patterned metal layers with crossed strips with
- One insulating multi-layer stack and
- Three resistive layers of M Ω and 10¹⁴ Ω /square resistance on glass plates, respectively, in between.

The development of these multi-layer systems with integrated resistors and capacitors was pursued under coordination of HMI in two different collaborations using different technologies:

- At first in collaboration with the German Fraunhofer Institute for Surface Engineering and Thin Films FhG-IST, Braunschweig, and the Swiss firm IMT, Greifensee.
- Then in collaboration with Institute for Physics of Microstructures, Russian Academy of Sciences, IPM-RAS, Nizhny Novgorod.

By the first collaboration the development of the individual layers was successfully completed except for the insulating layer, where too many deficiencies remained. The further development of the multi-layer system thus proved as too time-consuming (17 production steps) and costly regarding the low delivery rate of FhG-IST (with the demands exceeding the production capacity by far) and the expensive large-area production systems needed for the development work. These systems are however suited for fabrication of full-size detectors after completion of the development phase.

In the Russian institute the full production process was in the hand of a small group. When a first series of MSGC plates was fabricated the clean room conditions were insufficient. These were however improved for a second series of prototype MSGC plates. In comparison to the design pursuit at FhG-IST and IMT, the design used in collaboration with IPM RAS differed in several respects, using, for instance, for the insulating layers a stack of polyimide/TaO₂ layers instead of SiO₂/Si₃N₄/SiO₂ layers.

Subtask 1.2.4 with the two items

“Construction of full-size MSGC module using foil converter. Laboratory tests.”

For the development of full-scale (28.5 by 28.5 cm) low-pressure MSGC detectors the following R&D work must be completed:

Final Report

1. Modelling, optimisation and CAD of full-size MSGC detectors

This task was already performed at the beginning of the project also for full-size detectors.

2. Development of the composite Gd/CsI converter in full scale

The large-area UHV chamber mentioned above allows producing full-size composite converters. This chamber replaced the existing high vacuum apparatus of 450 mm diameter at HMI (see above); its functions are described in more detail in the next sub-section.

3. Development of the MSGC multi-layer technology in full scale

As stated above, the MSGC plate development had been started first for prototype and full-size plates in collaborations with the German Fraunhofer Institute for Surface Engineering and Thin Films FhG-IST and with the Swiss firm IMT, which is expert in thin-film lithography. However, due to the need to use the large expensive inline plant at FhG-IST, the development of the MSGC multi-layer system proved too time-consuming and costly and was interrupted with incomplete results for financial reasons.

Thereafter MSGC plates of prototype size were fabricated in collaboration with IPM RAS financed partly by BMBF-funding within the German–JINR Dubna projects and with JINR Dubna, as third partner. Unfortunately, IPM RAS decided thereafter not to make the necessary investments for production of full-size plates.

Therefore, the necessary large-area physical vapor deposition (PVD) chamber for full-size plate fabrication was constructed at HMI. This was retarded due to its complicated design requiring very detailed finite-element calculations and due to the expertise and high-grade stainless steel needed for its fabrication. It was completed in the second half of year 4 by the German firm NTG (New Technologies Gelnhausen). This UHV chamber has quadratic cross section (of 90 cm square) and a two-dimensional travel and transfer system with vacuum locks connecting the PVD chamber to an in-situ analysis chamber with secondary electron spectrometer and to a glove box for further handling of the sensitive devices in an inert gas atmosphere. The UHV chamber is installed in a clean room belonging to the project laboratory. For achieving the necessary homogeneity in the deposition processes the size of the PVD chamber allows travelling the full-size plates across a central flange of 45 cm inner diameter mounted on the chamber's bottom plate, which is equipped with a complete set of sources. The installation of the full set of necessary process technologies is still in progress presently. Clean vacuum conditions as obtained in this UHV apparatus are in particular necessary for making resistive Cr/SiO_x cermet layers for producing MΩ resistors with reproducible resistivity. These resistors are integrated in the multi-layer setup on the MSGC plates together with integrated capacitors, insulating layers, micro-patterned Ti/Au conductive strip layers and a high-resistivity (N-doped a-SiCN:H or AlN) layer of $\sim 10^{14}$ Ω/square surface resistance, which is undercoating the upper micro-strip layer.

In the new chamber, all deposition processes necessary for the fabrication of full-size multi-layer MSGC plates can be performed in laboratory scale, i.e. for a limited number of samples, except (i) polyimide spinning, which shall be done at Fraunhofer institute FhG-IZM in Berlin, and (ii) the micro-patterning of the two metal layers on the MSGC plates, which will be continued in collaboration with the Swiss lithography firm IMT. IPM RAS supports the transfer of process technology developed in prototype scale. The fabrication of a first series of full-size MSGC plates shall be achieved within about one year after the end of TECHN1.

Full scale testing of foil converter MSGC module including data acquisition

For the completion and testing of the MSGC modules the following R&D tasks were completed:

Development of sub-divided multi-hit delay line and time-of-flight readout technology

The front-end readout boards for the MSGC were fabricated and successfully tested. They include for each readout node an impedance matching amplifier, which decouples the delay line from the strip read out and thus preserves the delay line's transmission characteristics.

Final Report

Development of the data acquisition (DAQ) system

The DAQ system comprises PCI DAQ boards (one for each stack of two full-size MSGC plates standing opposite to each other either side of the converter) in a PC. Each DAQ board hosts four dead-time-free 8-channel multihit TDCs with 120 ps LSB, fast FPGAs (field programmable gate arrays), a 256 MByte histogram memory and a 1 GFLOP DSP (digital signal processor). These unique boards were developed in collaboration with JINR Dubna, Russia. Two prototype DAQ boards were fabricated and tested at HMI. With the present firmware and software the maximum data throughput per board amounts to 1.7 Mevents/s. An improved even faster design with separate front-end boards (with TDCs and FPGAs) and commercial PCI boards in the PC (with histogram memory and DSPs) was completed and is presently in preparation for fabrication.

Spin-off by-product

In addition, as a spin-off by-product for multi-wire proportional chamber (MWPC) detectors with delay line readout a simplified DAQ board version was developed with the same technology, too, and fabricated in three versions. The up to now final version was fabricated in series with 12 pieces and tested with MWPC neutron detectors at the HMI reactor.

However, the testing of the MSGC boards could not be performed yet since the full-size MSGC plates could not be completed yet (see above).

Subtask 1.2.9 with the item

“Full scale intercomparison of detectors developed under sub-tasks 1.1, 1.2”

This subtask could not be performed yet due to the still missing full-size MSGC plates (see above).

LLB: Task 1

It appears that GEM detectors with high pressure gas present a overall gain too low to be competitive with MSGC detectors for that reason we did not performed a comparison between GEM and MSGC detectors.

The best high resolution detectors we have tested on our spectrometers are scintillation detectors built in Jülich.

On the same experiment, a reflection on a silver layer and a reflection on a Giant Magnetoresistive Thin Film, we have performed a simultaneous test of a MSGC detector built in Saclay and a Scintillation detector built in Jülich.

TU Delft: Task 1

Several lines of research have been followed:

- (a) An experimental setup has been built that can handle gas pressures up to 10 bar.
- (b) Extensive research has been performed on single and cascade GEM configurations of different dimensions (hole size) using a variety of gas mixtures at normal and elevated pressures. The conclusion has been drawn that small holes of ~50 microm diameter at a pitch of ~100 microm, i.e. a value smaller than the currently used pitch of 140 microm, would be optimal.
- (c) As for the gas mixtures we focused on He-CF₄, He-C₃F₈, He-C₃H₈ and He-Xe-TMA. We demonstrated that the Penning mixture Xe-TMA is an excellent stopping gas. Employing ~ 6 keV x-rays, gas gains of >100 can be realized in efficient, 1mm-position-resolution neutron detection mixtures, such as 6 bar helium with 4 bar Xe- ~100 mbar TMA. These gains could not be realized in He-CF₄, He-C₃H₈ or He-C₃F₈ mixtures at pressures corresponding to 1 mm resolution. In these mixtures discharge started before the required voltage could be applied across the GEM.

Final Report

- (d) In a thermal-neutron beam of the Delft nuclear reactor, we realized a gain of 90 using a 3 bar Xe – 100 mbar TMA – 7 bar $^3\text{He}/^4\text{He}$ mixture. It should be noted that in the pulse height spectrum the full energy line at 764 keV is significantly broadened (resolution ~ 40%). As for gamma-ray sensitivity, the probability is very small that an energetic electron resulting from gamma-ray interaction in the gas or other detector elements will deposit an energy above the threshold for neutron detection of ~ 100 keV in the neutron-absorption gap. Yet, would this happen, the signal on a ~ 1mm size pixel employed for 1 mm position resolution would be very small, i.e. well below threshold. So He-Xe-TMA is also applicable in a high-gamma-ray-intensity environment. An observation that needs attention is gain variation. This is generally observed in GEM studies. It is attributed to polarization in the GEM substratum and surface charge effects inside the holes.
- (e) For electronic readout, the charge collection time on the anode of a neutron event in the detector has been measured to be of the order of 400 ns. Instead of using front-ends of the MSGC detector, we collaborated with INFN to use their electronics for the read-out of a GEM based detector. This electronics uses the IDE VA(75ns)-TAN chips. These chips can be trimmed to deal with pulses with charge collection times of 400 ns. Using He-Xe-TMA, the size of the signal is sufficiently large to operate well above the noise level. All studies on gas mixtures were performed using one large ($3 \times 3 \text{ cm}^2$) electrode. Due to delays, for a position sensitive detector electrode fabrication was limited to pc-board and kapton foil structures. There was not enough time to construct a position sensitive GEM detector with electronic readout.
- (f) In a collaboration with the University of Coimbra, Portugal, light response of GEMs was studied. It was found that the track of a single charged particle can be well observed with a CCD camera. The gas mixture He-CF₄ has a high light yield. Xe-TMA has less intense (~ 20%) light emission in the UV. This requires some instrumental adaptation (quantum efficiency CCD). The Xe-TMA light yield per secondary electron (after gas amplification) is almost independent of the Xe-TMA pressure in the region 1-5 bar. The effect of admixture of helium at high pressure remains to be studied.

Concluding, in the electronic readout mode (fast mode, ~1 microsecond time resolution) the GEM can be efficiently employed for position-sensitive neutron detection (1 mm resolution) using the new He-Xe-TMA mixture. In the light detection mode (slow mode, > 1 ms) the GEM can be efficiently employed to observe tracks resulting from neutron interaction using He-CF₄, and appears to be promising for position sensitive detection using He-Xe-TMA.

The gains of GEMs over other technology are 1) amplification stage and readout electrode structure are uncoupled; 2) multi-GEM structures and combinations GEM-other structures (MSCC, MGC, etc.) possible, resulting in higher gains; 3) light detection possible. These techniques can not only be applied to thermal-neutron detection, but also for x-ray and synchrotron-radiation detection.

ILL: Task 2

The new charge amplifier has been studied and tested with a PSPC of 1 inch diameter. It was immediately observed that a good spatial resolution could only be obtained at a high gas amplification gain, which is at the limit of the proportional mode of the detector: the degradation of the energy resolution, for the measurement of the charge deposited after interaction of neutrons, required a sharp optimisation of the amplifier gain to find the best compromise between gamma sensitivity, position resolution, and detection efficiency. This compromise could only be defined for the final version of the D22 PSPC.

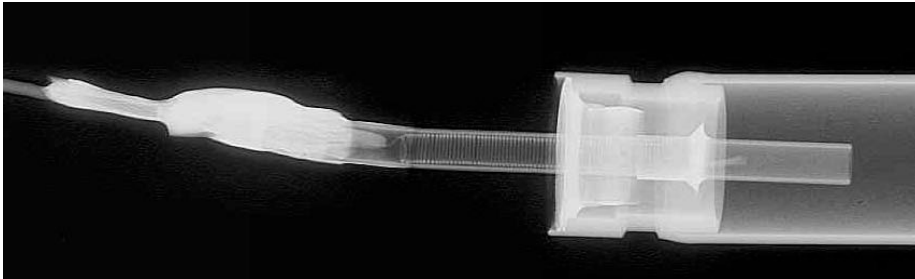
We received the first D22 PSPC prototypes from the General Electric Reuter Stokes (GE-RS) Company in October 2001. Two other series of prototypes were received during Y2 and Y3, with modified parameters: the ^3He pressure was increased from 10 to 15 bars; the anode electrical resistance has been increased to improve the signal/noise ratio of the electronics; the sensitive length was increased from 100 to 104 cm to guaranty good uniformity over at least 100 cm.

During Y3, a prototype of D22 made of 16 PSPCs revealed that anode wires must be maintained at the centre of the tube all along their length with an accuracy of the order of 0.4-0.5mm. A larger displacement induces electrostatic instabilities and sparks which, in some cases results in the destruction of the anode wires. Due to

Final Report

the small thickness of the tube, the PSPC is very flexible mechanically and must be mounted with great care on its support to avoid a bad centring of the anode wire. Therefore, a control with a 3D mechanical probe has to be performed after mounting of the tubes. Another factor which may affect the mechanical precision is the mounting of the anode wire inside the tube. As it results from the manufacturing, we could only control the tubes by X-rays radiography to measure the position of the anode wires on both ends.

The 128 PSPCs have been received during Y4. They were tested by GE-RS at 1600 Volts, 50 Volts above the working HV, and radiographed by X-Ray in Grenoble to check their mechanical precision. Only one PSPC had to be rejected.



Example of a mechanical defect: the spring guide and the detector tube are not concentric

To ease the maintenance of the detector, a data base programme, accessible through the Intranet was developed (a skeleton of it is accessible on the following Internet page: http://www.ill.fr/DPT/LD/d22_millennium/accueilD22.html)

We initiated a campaign of measurements on D22 with a Germanium detector to characterize the gamma environment in terms of energy and flux. The results were compared with those measured with an Am-Be neutron source thermalized with polyethylene. The Am-Be source was considered as much more severe than the D22 in terms of neutron/gamma ratio, and subsequently used as a reference for measuring the gamma sensitivity of the PSPC.

When under HV, the PSPCs are fragile, and can not stand any movement acceleration. For many experiments on the D22 instrument, it is foreseen that the detector is moving inside the vacuum tube to change its distance to sample. In order to guaranty a safe operation of the detector, we developed an automatic control system which allows movements only when the HV power supply is switch off, and when decoupling capacitors are discharged.

In November 2003, the 7 "Tombac" (vacuum-tight stainless steel tubes) have been mounted inside the D22 instrument vacuum tube; 3 of them were filled with 288 LEMO cables connected to the processing electronics inside the control room. In the mean time, the HV decoupling cards were mounted on a bank in order to test the capacitors under high voltage during 4 weeks. The mechanics parts of the detector arrived at the ILL beginning of December; the mounting of the PSPCs and analogue electronics started immediately afterward.

Final Report



Front view of the detector showing the 128 PSPC mounted on their frame.



View of the electronics at the rear side of the detector



The detector being moved into the D22 instrument



Cabling of the 7 tombacks

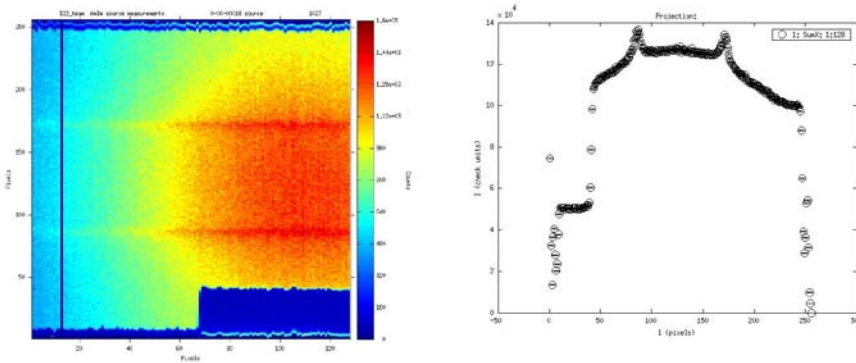
The localization method was defined as following: each of the 2 charge signals measured on a PSPC is digitalized with a precision of 11 bits at a time corresponding to the peak of the sum signal. The 2 digitalized pulse heights ADC1 and ADC2 are converted into a position address X coded on 8 bits with an EPROM programmed as following: $X = 256 \cdot \text{ADC1} / (\text{ADC1} + \text{ADC2})$. This basic position calculation algorithm has

Final Report

been improved to correct quantification errors induced by the limited resolution of the ADCs: in the calculation of $X=F(\text{ADC1},\text{ADC2})$, X is first encoded on 9 bits, before bins $2N+1$ and $2N+2$ are summed. A second improvement is the correction of the offset induced by the driver amplifiers: ADC1 and ADC2 are replaced by ADC1-Offset and ADC2-Offset, the value of Offset being determined as the average value for all the driver amplifiers. A third correction was introduced in the algorithm to take into account the non-linearity of the driver amplifiers above 2V. For ease of maintenance, this position calculation algorithm has been programmed the same for all EPROMs. It follows a negligible degradation of the spatial resolution, due to the offset approximation. The resulting image has to be corrected by the acquisition system to convert the measured position (in channels) into a real position (in cm), and to correct the non-uniform detection efficiency induced by variations between PSPCs (conversion probability and electronics response).

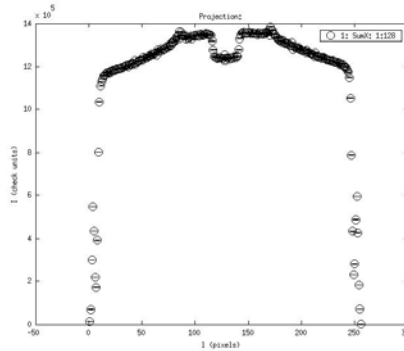
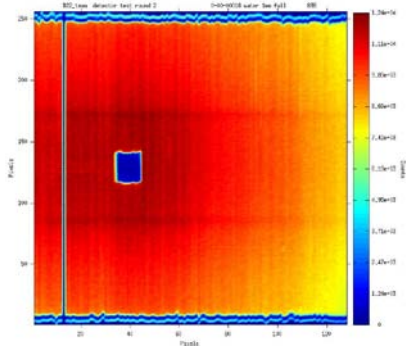
A simple method has been implemented to calculate the real position: the 2 borders of the X distribution spectrum correspond to the limits of the detection area, which is defined by a cadmium shielding. By knowing the length (100 cm) of the detection area, and the number of channels to which it corresponds, we can make the conversion in cm, and apply a re-binning, with an interpolating method, in order to present images with square pixels of 8mm x 8mm. This conversion is performed on-line by the VME acquisition system.

Preliminary tests with an Am-Be source revealed a non-expected effect in the image: we observe two horizontal areas, 5 cm wide, corresponding to an over-counting of roughly 8% of the background. Location of these areas coincide with the 2 hooking pieces glued on the rear side of each tube, and mounted on the frame. This effect has been studied on the D22 instrument with a water sample, and the following observations have been made: the relative intensity of these lines do not depend on the background level neither on the counting rate, but they decrease in intensity at longer wavelengths. The lines disappear with a Cadmium sheet in front of the detector, showing that they are induced by neutrons, not gammas. The most probable is that neutrons passing through the dead zone between 2 tubes are reflected by the hooking pieces, but further investigations are needed to confirm this explanation. The uniformity off-line correction along the tube will correct most of this effect.



Flood image (left) obtained by irradiating the detector with an Am-Be source surrounded by polyethylene (thermal neutrons). The lower right area is covered with a B4C mask to measure gamma sensitivity. One black line on the left side corresponds to a dead PSPC. Projection of this image (right) shows the intensity of the 2 parasitic lines.

Final Report

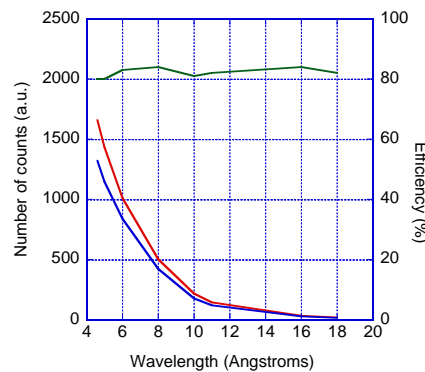
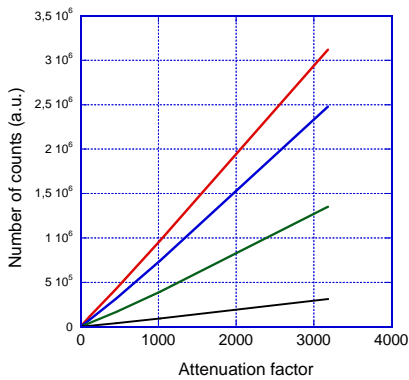


Flood image obtained with a water sample irradiated with a 0.45 nm neutron beam, and projection. The distance between the detector and the sample is 1.4m. The black square in the middle of the image corresponds to the beam-stop. The intensity of the lines is decreased at longer wavelengths.

Considering the Gaussian shape of the analogue signals, and the time required converting the maxima into an 8 bits position address (600 nsec), the dead time is of the order of 1 μ sec per event and per PSPC. This value allows counting rate of 100 KHz per tube at 10% dead time correction. For a uniform irradiation of the whole detector, the intrinsic maximum counting rate imposed by the localization electronics is 12 MHz. This value is similar to the limit of the acquisition system, but superior to the maximum rate achievable on the D22 instrument.

Measurements performed with a water sample with different attenuators, and for different wavelengths, defined by the velocity selector, showed that the “measured versus true counting rate” is very linear up to 3 MHz. On D22, it was not possible to approach the limit of the detector.

Detection efficiency has been measured by comparing the new detector with a 1” diameter proportional counter tube. Results are shown in the figure below. They confirm previous results obtained with the prototype.



counting versus attenuation curves for counting rate measured on the 1” detector (red), different wavelength; 0.6 nm (red), 0.8 nm (blue), 1 nm (green), 1.5 nm (black). in comparison with the D22 detector. The ratio between the 2 curves (in green) confirms the expected detection efficiency of around 80%.

Final Report

TU Delft: Task 3

A large series of storage phosphor materials of the type $M_2B_5O_9X:Ce^{3+},R^+$ has been studied, with $M = Sr, Ca$; $X = Br, Cl$; $R = Na, K$ or no extra dopant. Also doping with Eu^{2+} instead of Ce^{3+} was studied. All these materials have a much lower gamma-ray sensitivity than the traditional $BaFBr:Eu$ mixed with Gd_2O_3 .

Storage properties such as yield of Photon Stimulated Luminescence (PSL) and Thermo Luminescence (TL), stimulation efficiency and fading were measured, among others with various neutron sources at TU Delft and ILL, Grenoble. In addition, EPR measurements at 4K have been performed for a better understanding of the mechanisms involved. It became clear that $Sr_2B_5O_9Br:Ce^{3+}$, $Ca_2B_5O_9Br:Ce^{3+}$ and $Ca_2B_5O_9Cl:Ce^{3+},Na^+$ are promising neutron storage phosphor candidates.

Furthermore, we studied the borates SrB_4O_7 , SrB_6O_{10} , $Sr_2B_2O_5$ doped with Ce^{3+} . These materials show a PSL intensity, which is too low for application as storage phosphor.

The haloborates appeared to be very promising materials for use in neutron imaging, provided that read-out parameters are optimized, i.e. the wavelength of stimulation is ~ 400 nm instead of 630 nm in the ILL set-up and filters are adapted. Storage occurs because electrons are trapped at intrinsic impurities and the holes are trapped on the luminescence centre Ce^{3+} . The compounds showing the best properties have been selected for further optimization, and have been synthesized with enriched ^{10}B content: $Sr_2B_5O_9Br:Ce,K$; $Sr_2B_5O_9Cl:Ce,Na$; $Sr_2B_5O_9Br:Ce$, $Ca_2B_5O_9Cl:Ce,Na$; $Ca_2B_5O_9Br:Ce,Na$. In Table 1 the properties of a few materials are compared with mixed $BaFBr:Eu^{2+}/Gd_2O_3$, the standard neutron storage phosphor.

Table 1

Measured PSL yields (S_n and S_γ) of a few materials. The yields are normalized to those of $BaFBr:Eu^{2+}/Gd_2O_3$. Samples were measured under the same conditions.

	$Sr_2^{nat}B_5O_9Br:Ce(1\%)$	$Ca_2^{10}B_5O_9Cl:Ce,Na(1\%)$	$BaFBr:Eu^{2+}/Gd_2O_3$
$S_n(1.8 \text{ \AA})$	3.2	6	100
$S_\gamma(662 \text{ keV})$	0.26	0.14	18
S_n/S_γ	12	43	5.5

We notice that S_n/S_γ of $Ca_2^{10}B_5O_9Cl:Ce,Na(1\%)$ is significantly better than of $BaFBr:Eu^{2+}/Gd_2O_3$. However, the neutron sensitivity of the latter is much better. This is mainly due to the fact that a relatively thick storage phosphor layer is required at 1.8 \AA in employing ^{10}B compared with gadolinium. At longer neutron wavelength the efficiency will go up and $Ca_2^{10}B_5O_9Cl:Ce,Na(1\%)$ will become even better. Furthermore, we entered a new direction of thermal neutron storage phosphor research, using 6Li to render neutron sensitivity, i.e. we studied $LiLuSiO_4:Ce^{3+},Sm^{3+}$ and $LiYSiO_4:Ce^{3+},Sm^{3+}$. Again Ce^{3+} is the hole trap and luminescence center, but the electron trap is now controlled by means of the Sm^{3+} co-doping. Combinations with other electron trapping lanthanides were also explored. Good storage properties were demonstrated for $LiYSiO_4:Ce^{3+},Sm^{3+}$. The fundamental mechanisms of charge trapping and charge recombination are subject of study. Employing beta rays the PSL yield of these materials is ~ 30 times smaller than that of $BaFBr:Eu^{2+}$. As the neutron capture cross section of 6Li is ~ 4 times smaller than that of ^{10}B it is expected that results will not be better than for the haloborates. More work has to be done.

KCL / EMBL: Task 3

Two lines of research were developed:

- The examination of the γ -sensitivity of Eu^{2+} doped $BaFBr$ and $BaSrFBr$ phosphors ($BaSrFBr$ has a higher PSL response than $BaFBr$) phosphors containing varying quantities of Gd_2O_3 as neutron converter.

Final Report

Samples of phosphor with differing proportions of Gd₂O₃ and BaSrFBr were exposed to known neutron and Fe K X-ray fluxes, and the PSL levels measured on the LADI image plate scanner or a Molecular Dynamics 'Storm' scanner (both with $\lambda=635\text{nm}$) at ILL Grenoble. It was found that while the neutron sensitivity of the plates has a broad maximum between 40/60 and a 60/40 mixture of Gd₂O₃ and BaSrFBr, the γ -sensitivity reduced monotonically with increased Gd₂O₃ content to zero for 100% Gd₂O₃. In this system it is therefore preferable to use a 60/40 or a 70/30 ratio of Gd₂O₃ to BaSrFBr to significantly reduce γ -sensitivity while keeping a relatively high neutron DQE.

b) Investigation of the thermo-luminescent yield of various inorganic borate storage phosphors which are intrinsically neutron sensitive and contain few atoms of high atomic number, thereby having a lower γ -sensitivity.

Measurements of the X-ray induced scintillation yields of inorganic borates were made in collaboration with TU Delft. A large series of storage phosphor materials of the type M₂B₅O₉X:Ce³⁺,R⁺ were studied, with M = Sr, Ca; X = Br, Cl; R = Na, K or no extra dopant. These materials were found to have a much lower gamma-ray sensitivity than the traditional BaSrFBr:Eu mixed with Gd₂O₃, and the most promising phosphor, Sr₂B₅O₉Br:Ce³⁺, was found to give more PSL counts per incident neutron than Gd₂O₃ doped BaSrFBr. The absorption coefficient for this material is, however, significantly less than for BaSrFBr:Eu / Gd₂O₃ and requires a thick phosphor layer to absorb the neutrons. Unfortunately, this has the effect of reducing the neutron DQE, as the PSL emitted from deep within the phosphor is unable to reach the detector.

It was therefore decided to produce large image plates using a 70/30 ratio of BaSrFBr:Eu /Gd₂O₃ as the storage phosphor. Using a spraying technique for the phosphor/converter, plates of 400mm x 800 mm have been made and used for neutron diffraction studies of the test protein systems lysozyme and glucose isomerase.

FZ Juelich: Task 3

1. A new approach to the construction of image plate detectors of medium resolution (of about 1 mm), which fits to requirements of neutron scattering, was suggested.

Different storage phosphors and neutron converters have been tested at the FZ Jülich to find an appropriate mixture for the neutron image plate with low gamma-sensitivity. It is observed for the first time that the mixture KX:Eu(2+) (X=Cl, Br) (storage phosphor) and 6LiF (neutron converter) is a very attractive detector materials to be used in a high gamma-background environment.

Calculations and measurements have been performed to optimise the image plate parameters. The main processes that affect on image plate detector performance are investigated and the mathematical model is developed.

Experimental tests for preparations of such pixelated neutron image plates, was carried out. First test experiments were performed at a neutron beam port at the reactor DIDO at the FZ Jülich. Discussions with TU Delft on Gd nano-particles resulted in a change to ⁶Li, which is much more attractive from the point of view of neutron sensitivity and gamma-ray insensitivity. It was shown, that optimal size of the absorbing ⁶Li particles is about 40 μm , the optimal size of the storage phosphor is about 10 μm . MCNP calculations have been performed to study the problem of the light propagation in the image plate aiming to find optimal conditions (reflecting walls and bottom) for high effective read-out process.

Final Report

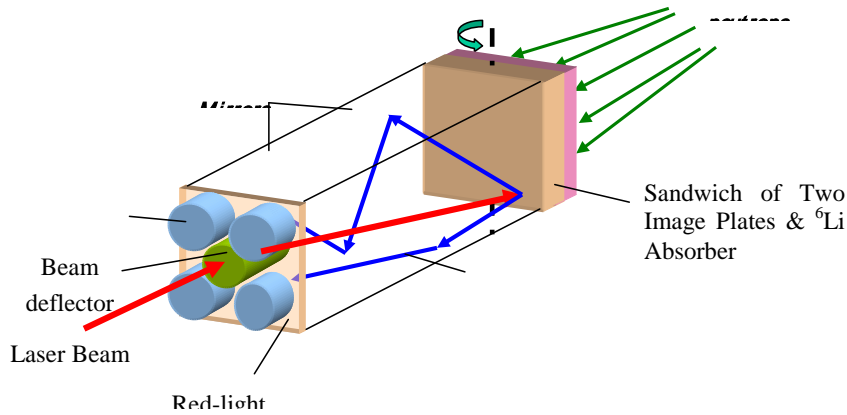


Fig. 1:

A prototype of the scanner with the high light collection efficiency was constructed & tested; the test neutron images have been scanned & parameters of the scanner have been preliminary defined

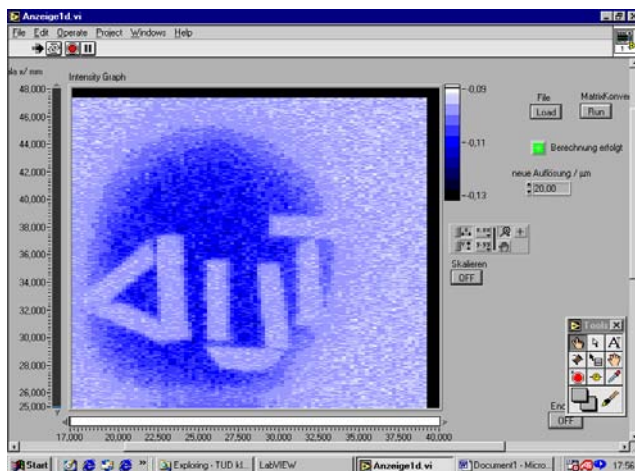


Figure 2

The layout of the image plate detector with high, more than 50% light collection, duty factor of about 100% and high-speed access.

An optimisation of parameters of the pixelated image plate was carried out. MCNP calculations have been performed to estimate the expected resolution and efficiency as a function of the pixel parameters and wall coatings. A prototype of pixelated image plate with pixel size of $1 \times 1 \text{ mm}^2$ was prepared and successfully tested at the neutron beam. The first large scale, $100 \times 100 \text{ mm}^2$, image plate was produced. The laser image

Final Report

plate scanner with the high light collection efficiency is constructed, the optical system and the control software is tested. The optical scanning system shows the resolution better than 0.03 mm that is completely satisfies our requirements (Fig. 2).

TU Delft: Task 4

In recent years, new scintillating compounds were developed and old ones were used in new kinds of applications. Detection of thermal neutrons through observation of α particles, i.e. the reaction products, in presence of γ rays is often required, e.g. at the anticipated neutron spallation facilities. Various methods employed for n- γ discrimination are based on the difference of pulse shape response. Thermal neutron response being given partly by the α particle resulting after n_{th}/Li or n_{th}/B annihilation, it is of interest to study the α - γ response of scintillating crystals. We studied a large variety of potential 6Li and ${}^{10}B$ containing inorganic thermal-neutron scintillator materials and some Gd containing compounds.

- a) Ce^{3+} activated $Li_6Gd(BO_3)_3$ material can be grown as clear single crystal suitable for small area neutron detectors. The isotopic composition of all three primary absorbers can be altered to optimize for specific neutron energy regimes. Another material, with similar chemical and crystal structure properties is $Li_6Y(BO_3)_3:Ce^{3+}$. The advantage in substituting Y for Gd arises from the much lower neutron capture cross section for naturally occurring Y. Then, to employ 6Li , depletion in ${}^{155,157}Gd$ isotopes is not necessary. The substantially higher light yield of $Li_6Gd(BO_3)_3:Ce^{3+}$ compared to that of $Li_6Y(BO_3)_3:Ce^{3+}$ (Table 2) is attributed to the efficient transport of the excitation energy/charge carriers along the one-dimensional chains of Gd^{3+} ions to the Ce^{3+} ions. The pulse shape discrimination investigation for the Ce^{3+} doped $Li_6Gd(BO_3)_3$ (depleted in high-cross section ${}^{155,157}Gd$ isotopes) does not show a good α - γ discrimination power. This implies that this crystal does not offer efficient n_{th} - γ pulse shape discrimination. In the $n_{th}+{}^6Li$ annihilation a tritium nucleus is produced in addition to the α particle. The tritium nucleus is singly charged and in the pulse shape discrimination spectrum it fills the gap between gamma and alpha response, making α - γ separation poor. For $Li_6Y(BO_3)_3:Ce^{3+}$ crystals, α - γ pulse shape discrimination appeared not to be possible either.
- b) Several Ce^{3+} doped $LiMF_4$ crystals, with $M = Y$ or Lu , have been studied. Good discrimination (optimum gate widths $t_g=600ns$ and $t_i=8\mu s$) has been obtained between 5.1 MeV α particles from ${}^{241}Am$ and 662 keV gamma rays from ${}^{137}Cs$. The very long integration time ($t_i = 8\mu s$) used to match the results (light yields) of discrimination studies with the ones obtained from pulse height measurements, make us believe that there exists a very slow component in the γ scintillation decay. It gives a large difference between the light yields derived from CW X-ray measurements and gamma ray induced pulse-height spectra. Photoelectron yields of $L_\alpha \cong 27$ phe/MeV for α particles and $L_\gamma \cong 120$ phe/MeV for γ rays were determined (Table 2). High internal α activity can be observed in $LiLuF_4:Ce^{3+}$ crystals, presumably due to ${}^{232}Th$ isotope. For $LiYF_4:Ce^{3+}$ crystals, decay times of about 70 ns, 200 ns and 8 μs were found for γ rays. For $LiYF_4:Ce^{3+}$ crystals we obtained good α/γ discrimination. The photoelectron yields are $L_\alpha \cong 40$ phe/MeV for α particles and $L_\gamma \cong 283$ phe/MeV for γ rays.
- c) Alpha- γ scintillation and discrimination studies were also made on pure and Ce^{3+} doped LaB_3O_6 , K_2LiGaF_6 , KBF_4 , $NaBF_4$, $Ca_4GdO(BO_3)_3$, $(Lu_xGd_{1-x})_3Al_5O_{12}$, Yb doped SrB_4O_7 and Mg doped $Li_2B_4O_7$ crystals. Good discrimination was obtained in a number of cases (Table 2). However, for most samples the light yield is too low for a practicable thermal neutron detector.

It appears that $Li_6Gd(BO_3)_3:Ce^{3+}$ is the best scintillator studied so far. Though n- γ discrimination by pulse shape discrimination is poor it is the only material with a sufficiently high light yield. This material is available in a form suitable for application by CCLRC in a neutron instrument. In the meantime research continued to find new scintillators with more favourable specifications.

Final Report

Table 2.

The studied scintillation properties of few ^6Li and ^{10}B and ^{157}Gd containing inorganic scintillators.

Compound	Pulse shape Discr	L.Y.			Decay time (ns)	
		α (phe/MeV)	γ (phe/MeV)	X/ γ -ray (ph/MeV)	γ	α
K_2LiGaF_6	Yes	-?	-?	450	1.5; 4.5	2; 50
$(\text{Lu}_x\text{Gd}_{1-x})_3\text{Al}_5\text{O}_{12}:\text{Ce}^{3+}$	Yes	130	180	5300	1; 3	3.2; 100
$\text{Li}_6\text{Gd}(\text{BO}_3)_3:\text{Ce}^{3+}$	Bad	850	4870	-	-	-
$\text{Li}_6\text{Y}(\text{BO}_3)_3:\text{Ce}^{3+}$	No	95	1050	-	-	-
$\text{LiLuF}_4:\text{Ce}^{3+}$	Yes	27	120	-	3; 24	70
$\text{LiYF}_4:\text{Ce}^{3+}$	Yes	40	280	-	8	5; 48
$\text{LaB}_3\text{O}_6:\text{Ce}^{3+}$	Yes	2	42	-	2	36
$\text{Li}_2\text{B}_4\text{O}_7:\text{Mg}$	Yes	-	25	-	-	-
$\text{Ca}_4\text{GdO}(\text{BO}_3)_3$	Yes	-	-	1490	-	-
$\text{SrB}_4\text{O}_7:\text{Yb}$	Yes	-	-	-	-	-
$\text{KBF}_4:\text{Ce}^{3+}$?	3	10	200	-	-
$\text{NaBF}_4:\text{Ce}^{3+}$?	2	10	290	-	-
$\text{Li}_3\text{YCl}_6:\text{Ce}^{3+}$				3,300		
$\text{Li}_2\text{CaSiO}_4:\text{Ce}^{3+}$				8,000		
$\text{LiCaPO}_4:\text{Ce}^{3+}$				5,800		
$\text{CaBPO}_5:\text{Ce}^{3+}$				1,300		
$\text{Cs}_2\text{LiYCl}_6:\text{Ce}^{3+}$	Yes	70,000 ph/n		22,000	3/1000	1000
$\text{Cs}_2\text{LiYBr}_6:\text{Ce}^{3+}$	No	88,000 ph/n		23,000	89/2500	

- d) Various other new Li/B-based, Ce^{3+} doped potential neutron-scintillator compounds were studied. Single crystals of Li_3YCl_6 , $\text{Cs}_2\text{LiYCl}_6$, $\text{Cs}_2\text{LiYBr}_6$ and powder samples of $\text{Li}_2\text{CaSiO}_4$, LiCaPO_4 , and CaBPO_5 were synthesized and studied. Particularly $\text{Cs}_2\text{LiYCl}_6:\text{Ce}^{3+}$ and $\text{Cs}_2\text{LiYBr}_6:\text{Ce}^{3+}$ show excellent neutron detection properties. The former shows core-valence luminescence (CVL), self-trapped exciton (STE) luminescence and Ce luminescence. The total light yield is in the order of 22,000 photons per MeV under X-ray absorption. Under neutron irradiation we observe 70,000 photons. CVL offers the possibility of reliable neutron/gamma discrimination, analogous to the case of $\text{LiBaF}_3:\text{Ce},\text{Rb}$. $\text{Cs}_2\text{LiYBr}_6:\text{Ce}^{3+}$ has an even higher light yield under neutron irradiation: 88,000 photons per neutron. The gamma-ray response is 23,000 photons per MeV. This material does not show CVL. However, pulse height discrimination is well possible. These new materials are very competitive with existing thermal neutron scintillators. The next step has to be the production of material in a shape that can be used in a detector (large crystals or powder-binder slabs).

Final Report

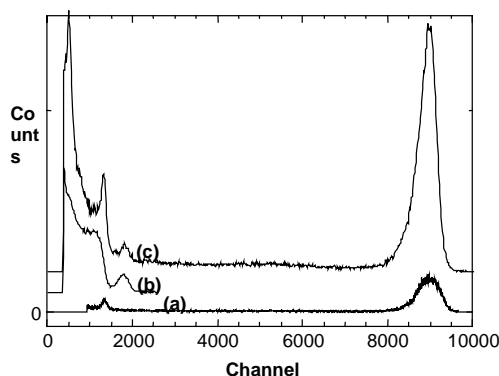


Fig. 2.

Pulse-height spectra of $\text{Cs}_2\text{LiYCl}_6:0.1\%\text{Ce}$ for (a) a thermal neutron beam (peak at channel 9000), (b) a ^{137}Cs source, (c), a combined radiation field. The peak at channel 1300 is due to ^{10}B in shielding.

INFN: Milano-Bicocca & Roma Tor Vergata Task 5

New perspectives for epithermal neutron spectroscopy are being opened by the development of the resonant detector (RD) and its use on inverse geometry time of flight spectrometers at spallation sources. The RD was first proposed in the eighties and was recently brought to a performance level exceeding conventional neutron-sensitive Li-glass scintillator detectors. It features a photon counter coupled to a neutron analyzer foil. Resonant neutron absorption in the foil results in the emission of prompt gamma rays that are detected in the photon counter. The dimensions of the RD set the spatial resolution that can be achieved, ranging from a fraction of a cm to several cm. It can thus be tailored to the construction of detector arrays of different geometry.

The main results of the research on this kind of detector are reported leading to the present optimized RD design based on a combination of YAP scintillation photon counter and uranium or gold analyzer foils. This detector has already been selected for application in the upgrade of the VESUVIO spectrometer on ISIS. A special application is the Very Low Angle Detector (VLAD) bank, which will extend the kinematical region for neutron scattering to low momentum transfer ($< 10 \text{ \AA}^{-1}$) whilst still keeping energy transfer $> 1 \text{ eV}$, thus allowing new experimental studies in condensed matter systems. The first results of tests made with prototype VLAD detectors are presented, confirming the usefulness of the RD for measurements at scattering angles as low as 2° - 5° .

Introduction

The development of new instrumentation for epithermal neutron detection is motivated by the need to extend the kinematical region that can be accessed by today's neutron scattering experiments [1]. In particular, to access the kinematical region of both high and low momentum transfers coupled to high energy-transfers one requires detection of neutrons of energy in the range 1 eV - 100 eV [2]. The Resonance Detector (RD) has been developed for experiments at such high neutron energies in inverse geometry time of flight spectrometers at pulsed sources. In the RD configuration the neutron detection is performed in a two-step process: i) an analyzer foil (^AX) strongly absorbs, over a narrow energy interval, the scattered neutrons with energies close to the resonance energy E_R ; ii) the compound nucleus (^{A+1}X), left in an excited state, radiatively decays to the ground state, generating a prompt γ -ray cascade, which covers a wide energy spectrum, ranging from tens of keV up to the multi-MeV value of the neutron binding energy in the specific absorbing nuclide; there is also a significant emission of X-ray radiation from de-excitation of the absorbing atoms. Coupled to the analyzer foil is a photon detector, which tags the arrival time of the absorbed neutron

Final Report

by detecting the photon cascade. In this way the kinematics of the scattering event can be reconstructed through the time-of-flight technique.

First investigated in the eighties [3-7], the RD was not fully developed at the time because of excessive sensitivity to background radiation [6] which favored the use of the alternative neutron detection technique called Filter Difference (FD) [8]. In the FD, Li-glass scintillators detect the scattered neutrons that are transmitted through an analyzer foil. The resulting transmission spectrum shows characteristic resonant absorption dips. By taking appropriate combinations of measurements with and without the foil, the scattering time of flight spectrum is determined [9] with a neutron energy resolution ultimately limited by the Breit-Wigner resonance width.

The FD technique works well for neutron energies E_n in the eV range. At higher energies, say above 10 eV, the $1/\sqrt{E_n}$ dependence of the neutron capture cross-section in ${}^6\text{Li}$ makes the FD technique unpractical. This led us to reconsider the RD. After a few years of prototype development, RD detectors with adequate performance have been produced and are now ready to be used for the construction of position sensitive arrays with a growing range of applications.

RD prototype development on VESUVIO

Prototype development tests were made on the VESUVIO inverse geometry time of flight spectrometer [10] at ISIS. This has been upgraded over the years and is shown schematically in Fig.1 in its latest configuration which includes an extension to the main vacuum tank enabling measurements at scattering angles as low as 2° (see below). The scattering sample is placed in the neutron beam at a distance (primary flight path) $L_0 \approx 11.05$ m from a water moderator at room temperature. The beam is undermoderated, resulting in a neutron energy spectrum in the epithermal range scaling as $1/E_n$ [11]. Most of the measurements were taken with the prototype detector at forward scattering angles (30 - 90°) at a distance between sample and analyzer foil (secondary flight path) of typically $L_1 \approx 0.3$ - 0.5 m. At this position the detector is exposed to the (signal) neutrons scattered from the sample and to an admixture of other (background) neutrons and photons. The latter originate mainly from neutron capture in the neutron dump and other material structures in the bunker surrounding the sample tank. There is also a background contribution from the analyzer foil if this is naturally or artificially radioactive.

The response of the RD to scattered neutrons and background radiation depends on the choice of analyzer foil and photon detector. The ideal RD should have a good efficiency for detecting scattered neutrons of well-defined energy while being insensitive to other radiation. This can be expressed in terms of an achieved signal/background ratio and by a statistical figure of merit [12]. Essential for achieving a good signal is the use of an analyzer foil with few, widely spaced, narrow, strong absorption resonances. Few isotopes satisfy these criteria [13], the main one being ${}^{238}\text{U}$. The resonance properties of ${}^{238}\text{U}$ are listed in Tables 1 and 2 [14]. Strong resonances mean that typical foil thicknesses used can be as low as 25 - 80 μm , which also ensures low self-absorption of the emitted photons except for the lowest photon energies. Actually the photon cascade following neutron absorption extends from as little as $E_\gamma=12$ keV up to $E_\gamma=4.060$ MeV and the photon detector should in principle detect the emitted photons efficiently while being insensitive to background radiation. It should also have a relatively fast response and, most important, be suitable for use as part of a detector array. Photon detection is the area where most research effort was put in order to achieve a performing RD.

The first explorative tests [15] were performed with a sodium iodide (NaI) scintillator (length=diameter= 8 cm), which offered good efficiency over a broad photon energy range but was strongly sensitive to neutrons. A massive shielding consisting of an inner shell of lead bricks and an outer shell of borated wax was needed in order to prevent the detector from being swamped by background radiation. Even so, an acceptable signal/background ratio was only achieved by raising the pulse height discrimination threshold to a equivalent photon energy of about 800 keV and by placing a polythene slab between the ${}^{238}\text{U}$ foil and the detector. This arrangement, while being not dissimilar from earlier attempts [4-7] and providing results of some significance, was clearly inadequate for development of detector arrays and was abandoned in favor of more compact detector solutions.

More successful was the test of cadmium-zinc-telluride (CZT) semiconductor detectors. Commercially the ternary semiconductor compound $\text{Cd}_{1-x}\text{Zn}_x\text{Te}$ has a blending fraction x of CdTe in ZnTe [16] ranging

Final Report

between 5% and 13%. This corresponds to an energy gap of 1.53 eV and 1.48 eV, respectively. The high band-gap values determine a low leakage-current level, thus allowing room temperature operation [17]. Available CZT detectors are extremely compact being typically 5x5 mm wide and 2-5 mm thick. They feature good energy resolution (3 %-5% at $E_\gamma=100$ keV) at room temperature combined with good efficiency in the 20 keV-200 keV photon energy range; the efficiency decays rapidly at higher photon energies. Interestingly, in the energy region below 700 keV, the predicted γ emission spectra following thermal neutron absorption in ^{238}U are dominated by the low-energy lines at 12 keV, 48 keV and 133.8 keV [18]. These are within the energy range where CZT has good efficiency; this range was therefore explored in detail by biparametric measurements of neutron time of flight and photon energy [19, 20]. Following [21], one of the aims of the biparametric measurements was to assess the possibility of improving the signal/background ratio of the time of flight measurements by energy discrimination, i.e. by selecting appropriate pulse height windows.

The results with the CZT detector were quite encouraging. First of all, the CZT measurements could be performed without any shielding, making the apparatus extremely simple and suitable for future development of detector arrays. A limitation encountered in the measurements was the low count rate achievable due to the small size of the detector. This did not prevent a detailed biparametric measurement of the photon emission from neutron absorption in ^{238}U [20]. Analysis of the relative intensity of the photon pulse-height spectra, performed at four neutron resonances, showed no statistically appreciable differences, suggesting that the γ -emission spectrum is mostly independent of the absorbed neutron energy. Comparative analysis of the γ pulse height spectra associated with resonant and non-resonant neutron absorption showed that the observed signal was made-up of three main components: (i) X-ray emission, (ii) radiative capture γ emission and (iii) Compton continuum in the high energy part of the spectrum. The component (i) was the most intense one and was present for both resonant and non-resonant neutron absorption, thus preventing its use for improving the signal to background ratio of the measurement via energy discrimination. Component (ii) was a clear signature of the resonant neutron absorption, but it represented only a small fraction of the overall observed signal. The component (iii), induced by radiative prompt γ s not fully absorbed in the detector, contained a significant fraction of the overall resonance signal. Both (ii) and (iii) can be used for energy discrimination to increase the signal to background ratio of the measurements, as shown in Fig.2.

Even without energy selection and without the use of shielding, the CZT measurements provided better signal/background ratios than conventional FD detectors [19]. Energy selection improved it further but at a huge cost in terms of signal intensity. This was judged unpractical, at least on present generation neutron sources.

The quality of the CZT results was surprisingly good also in view of the expected neutron sensitivity of the CZT material. This, however, turned out to be a negligible contribution to the background events thanks to the time separation between thermal and epithermal neutrons. The sensitivity to thermal neutrons (up to the cadmium cut-off at about 0.4 eV) is only manifested in the range of times of flight above 2 ms where characteristic diffraction peaks from the scattering sample can be observed [19]. This dual function as detector of thermal neutrons as well as photons is a unique feature of the CZT detector with potential applications. The main limitation in the use of CZT detectors is their small size, which would require a large number of detectors (and associated readout electronics channels) for typical applications such as epithermal neutron spectroscopy studies or studies of residual stress fields in materials using thermal neutrons.

Other photon detector tests were performed with a 0.5 mm thick Si photo-diode [22] that was cooled to -30 °C to improve its energy resolution. It was used to explore the very low photon energy region $E_\gamma < 50$ keV including the line at 12 keV, which is reported in the public databases [18] to be the most intense for absorption of thermal neutrons. The results, however, were not encouraging partly due to the high self-absorption of the ^{238}U foil at low E_γ values, which effectively meant weak signal and unfavorable signal/background ratio.

The optimised RD

The CZT results indicated that a photon detector with good efficiency in the range 20-200 keV was a good candidate for use as part of an RD regardless of its pulse height resolution. Other detection materials offering poorer energy resolution could therefore be considered provided they had a relatively large Z value, were

Final Report

insensitive to epithermal neutrons and could be easily grown in larger sizes than CZT. The choice fell on YAP (YAlO₃), a scintillator commonly employed in photon spectroscopy in different fields [23]. YAP:Ce is a short name for Yttrium Aluminium Perovskite (YAlO₃) doped with Cerium and is a fast, mechanically and chemically resistant scintillating material. Its mechanical properties enable precise machining to many different shapes. The inorganic scintillator is non-hygroscopic, glasslike, with a high density (5.55 g/cm³) but a relatively low effective atomic number ($Z=36$). The main characteristics of this scintillation material are a good light yield ($\approx 18,000$ photons/MeV) and a short decay time ($\tau=27$ ns) at a wavelength of maximum emission of 350 nm [24]. The material does not show neutron resonances in the epithermal energy range.

A YAP-based prototype RD was built [12] from a YAP crystal of cylindrical shape (35 mm diameter by 6.4 mm thickness) coupled to a standard 51-mm photomultiplier tube. The crystal's thickness was chosen so as to match the efficiency curve of the previously used CZT detectors. Above $E_\gamma=100$ keV the YAP efficiency gradually drops and is dominated by Compton interactions which give a significant absorption probability (about 10%) up to several MeV. Attached to the YAP detector's front face was a ²³⁸U analyzer foil of 2.4x3.5 cm² area and 60 μ m thickness. This provided us with a RD detector of high counting efficiency (in proportion to the foil area).

The detector performance was assessed by biparametric measurements on a reference polycrystalline Pb sample (1 mm thick and 2.5 x 3.5 cm² of area). The detector was positioned at a scattering angle of 90° and at a distance $L_1=0.30$ m from the sample position, which provided high counting rates. The initial detector (electronics) settings, chosen on the basis of previous experience with CZT detectors, confirmed the data quality achieved with the CZT. However an important observation was made which is illustrated in Fig.3. Comparison of the broadband pulse height spectrum recorded at resonance and off-resonance showed remarkable differences. In the energy range up to 400 keV the spectra have slightly different features that are not resolved due to the poor energy resolution ($>25\%$ at $E_\gamma=100$ keV). Above 400 keV the spectrum at resonance is systematically higher than the one off-resonance, except for the large peak around 500 keV, which is due to boron γ s (boron is used in the neutron dump and collimator and generally in shielding materials) and provides a convenient normalization point. Note that a significant fraction of events below 400 keV is also due to boron γ s. From the comparative shape of the two spectra it is clear that a substantial improvement in signal/background can be achieved by selecting events with pulse height above 600 keV; indeed a factor of 10 improvement was observed by increasing the threshold from 40keV to 600 keV. The other option would be to reduce the boron γ flux at the detector, either by shielding or by removing boron from the neutron dump and bunker. This option is unpractical at present but should be considered when constructing new facilities, where lithium could replace boron as a neutron-absorbing element.

Time of flight spectra of good quality have been collected on VESUVIO using the YAP RD prototype with an energy threshold of about 600 keV. An example can be seen in Fig.4, which shows the time of flight spectrum from a water sample in an Al cell. The data are of high quality and physical analysis of the hydrogen peaks will be published soon [25]. Note that, in addition to the ambient background, the RD detector records a background due to "natural" radiation from the ²³⁸U foil. As these events are not neutron driven this background has a flat time spectrum and can be measured from the asymptotic behaviour of the spectrum at long times. A detailed assessment of the RD prototype performance will be published elsewhere [12]. Here we just point out that the RD performance has exceeded the competitor FD even at neutron energies below 10 eV.

There is an apparent inconsistency in the YAP detector design: the YAP detector is set with an energy threshold of 600 keV and yet its thickness was optimised for detecting photons below 200 keV. This is far from optimal from a γ detection point of view. However one must also consider neutron backscattering in the crystal. The backscattered neutrons can be absorbed in the analyzer foil thus creating an additional offset peak in the time of flight spectrum. This cannot be resolved from the main peak and hence represents an unwanted distortion of the peak shape (which is where the physics information lies). Neutron backscattering will be investigated by means of simulations but it can already be estimated that the present YAP thickness is a good compromise between photon detection efficiency and reduction of neutron backscattering. Substantial improvement can only occur, in principle, by replacing the YAP scintillator with a higher Z and lower neutron scattering cross section material. This may be the subject of future research.

RD applications

Final Report

Two applications of the RD can be mentioned. The first concerns the upgrade of the VESUVIO spectrometer forward angle detector bank for neutron measurements in the 1-10 eV range [10]. In this range gold foils can be used as an alternative to uranium. The RD has been tested with gold foils giving satisfactory results leading to the choice of YAP based RD as detectors for the new detector banks instead of the Li-glass competitors. Combinations of measurements with foils of different thickness will be used to improve the energy resolution and background subtraction using the existing foil-changer apparatus of VESUVIO.

A special application of the RD detector is the Very Low Angle Detector Bank (VLAD) for the VESUVIO spectrometer at ISIS. VLAD will extend the kinematical region for neutron scattering to low momentum transfer ($<10 \text{ \AA}^{-1}$) whilst still keeping energy transfer $>1 \text{ eV}$, thus allowing new experimental studies in condensed matter systems. Eventually the VLAD bank will cover the angular range 1° - 5° at a distance of about 2 meters from the scattering sample. In order for this to happen, the VESUVIO neutron beam must be narrowed and a new vacuum tank must be fitted. A detector bank prototype was built to demonstrate the feasibility of VLAD. As a first step the prototype was designed to explore the scattering range 2 - 5° with two movable detectors and two fixed ones; a new vacuum tank had to be fitted to VESUVIO as shown schematically in Fig.1. Shown in Fig.5 is a photo of the prototype detectors facing the window of the new vacuum tank. The fixed detectors were positioned at 5° . The two movable detectors could slide between 2° and 5° . Visible in Fig.5 is the aluminum casing of the detectors, which contains two adjacent trapezoidal YAP crystals. The inside is painted in white and acts as a light guide towards a standard photomultiplier tube.

Data were collected from a few scattering samples. The time of flight spectrum in Fig.6 was collected by one of the movable detectors positioned at the lowest possible scattering angle of 2° . The scattering sample was ice. The spectrum has the typical features of similar spectra obtained from hydrogenated samples at intermediate scattering angles. The three peaks correspond to the first three neutron resonances in ^{238}U . A first analysis of these and similar data [26] has shown that the prototype VLAD detector bank performs its function rather well. For a more quantitative analysis it may be necessary to collect data with better statistics especially when looking for features from excitation processes with low cross section such as the O-H stretching mode excitation energy in ice.

Conclusions

New perspectives for epithermal neutron spectroscopy have been opened by the development of the resonant detector (RD) and its use on the VESUVIO inverse geometry time of flight spectrometers at ISIS. The RD was recently brought to a performance level exceeding conventional neutron-sensitive Li-glass scintillator detectors by using a combination of YAP scintillation photon counter and uranium or gold analyzer foils.

The use of the RD will extend the range of energy and momentum transfer accessible with inverse geometry time of flight spectrometers. A special application is the Very Low Angle Detector Bank (VLAD) on VESUVIO, which will extend the kinematical region for neutron scattering to low momentum transfer ($<10 \text{ \AA}^{-1}$) whilst still keeping energy transfer $>1 \text{ eV}$, thus allowing the investigations of new experimental studies in condensed matter systems. The first results of tests made with a prototype VLAD detector confirm the applicability of the RD for measurements at scattering angles as low as 2 - 5° .

The RD has reached performance levels not far from optimum. Further development can nevertheless be considered especially what concerns neutron detection efficiency and methods for improving neutron energy resolution by multiple measurements.

Finally the construction of position sensitive RD arrays will pose issues such as detector cross-talk and multiple neutron scattering which are presently being investigated.

Acknowledgements

Work performed with financial support by the European Community-Access to Research Infrastructure action of the Improving Human Potential Program. We acknowledge Consiglio Nazionale delle Ricerche (CNR)-Italy for financial support for the experiments performed at the ISIS pulsed neutron source.

References

[1] R. J. Newport et al., Nucl. Instr.& Meth. 224(1984) 120.

Final Report

- [2] A. Pietropaolo et al, “Photon detectors for epithermal neutron scattering at high- ω and low- q ” accepted for publication on *Physica B* (2004).
- [3] D. R. Allen et al., *J. Phys. E: Sci. Instr.* 13 (1980) 639.
- [4] G. P. Felcher and J. M. Carpenter, *Nucl. Instr. & Meth.* 192 (1982) 513.
- [5] L. Cseer, N. Kroo, P. Pacher, V. G. Simlin and E. V. Vasyleva, *Nucl. Instr. & Meth.* 179 (1981) 515.
- [6] N. Watanabe, IAEA 1985 Conference Proceedings, p279.
- [7] J. M. Carpenter, N. Watanabe, S. Ikeda, Y. Masuda, S. Sato and H. Rauh, *Physica B* 120 (1983) 126.
- [8] A. L. Fielding and J. Mayers, *Nucl. Instr. & Meth.* A480 (2002) 680.
- [9] P.A.Seeger, A.D.Taylor, R.M.Brugger, *Nucl.Inst. & Meth.* A263 (1985) 427.
- [10] R. Senesi, C. Andreani, Z. Bowden, D. Colognesi, E. Degiorgi, A.L. Fielding, J. Mayers, M. Nardone, J. Norris, M. Praitano, N.J. Rhodes, W.G. Stirling, J. Tomkinson, C. Uden, *Physica B* 276-278 (2000) 200.
- [11] C.G. Windsor, *Pulsed Neutron Scattering*, Taylor & Francis LTD London, 1981.
- [12] M.Tardocchi et al, “YAP:Ce scintillator for epithermal neutron spectroscopy”, to be submitted to *Nucl. Instr. & Meth. A* (2004)
- [13] A.Pietropaolo et al, *Appl. Phys A* 74 (2002) S189.
- [14] <http://atom.kaeri.re.kr/ndfplot.shtml>
- [15] C. Andreani et al, *Nucl. Instr. & Meth. A* 481 (2002) 509.
- [16] G.F. Knoll: *Radiation Detection and Measurements* (Wiley, New York, 2000)
- [17] SPIE Conf. Hard X-ray and Gamma-ray Detector Physics and Applications, July 1998 [Proc. SPIE 3446, 1 (1998)]
- [18] National Nuclear Data Center, Brookhaven National Laboratory, <http://www.nndc.bnl.gov> and Thermal Neutron Capture Home Page, Ernest O. Lawrence Berkeley National Laboratory, <http://ie.lbl.gov/ng.html>.
- [19] C. Andreani et al., *Appl. Phys. A* (2003), DOI: 10.1007/s00339-003-2087-7.
- [20] M.Tardocchi et al, “Cadmium-Zinc-Telluride photon detector for epithermal neutron spectroscopy – pulse height response characterization”, submitted to *Nucl. Instr. and Meth. A* (2003).
- [21] R. G. Johnson, *Nucl. Instr.& Meth.* A263 (1988) 427.
- [22] M. Tardocchi et al., “Assessment of a silicon detector for pulsed neutron scattering experiments”, accepted for publication on *Nucl. Instr. & Meth A* (2004).
- [23] F. de Notaristefani et al, Proceedings of the International Conference on Inorganic Scintillators and their Applications SCINT97, Shanghai Institute of Ceramics - Chinese Academy of Sciences, People's Republic of China, 353-357, (1998); T. Malatesta, F. Vittori, F. de Notaristefani, R. Pani, *Nucl. Phys. B*, Vol. 61B, 658-665, (1998).
- [24] Data compiled by C. M. Rozsa, presented in the Bicron Brochure “Efficiency for selected scintillators”, <http://www.bicron.com>.
- [25] A.Pietropaolo et al, “Deep Inelastic neutron scattering on water employing the Resonance Detector Spectrometer configuration”, paper in preparation (2004).
- [26] E.Perelli-Cippo et al, “First results of the Very Low Angle Detector bank prototype on VESUVIO” paper in preparation (2004).

Table 1

Main resonance parameters for the first four resonances in ^{238}U . E_R is the resonance energy, σ_0 is the nuclear resonance cross section, Γ is the Breit-Wigner nuclear resonance width (FWHM), Δ is the width (standard deviation) of the Gaussian broadening due to thermal motion of the absorbing nuclei at a temperature of 295 K, and σ_{eff} is the resulting effective resonance cross section [14].

E_R [eV]	σ_0 [barn]	Γ [meV]	σ_{eff} [barn]	Δ [meV]
6.671	23564	25	7570	547
20.87	37966	34	9864	96
36.68	42228	57	13363	127

66.02	20134	48	4357	170
-------	-------	----	------	-----

Table 2

Time of flight of resonant neutrons of energy E_R travelling the primary flight path $L_0=11.055$ m. This table can be used for peak identification although time offsets can be present in the experimental data (see, e.g., Fig.2). Usually the total neutron flight time is longer in scattering experiments as it includes also the secondary flight path.

E_R [eV]	t_0 [μ s]
6.671	309.5
20.87	175.0
36.68	132.0
66.02	98.37
80.73	88.95
102.5	78.94
116.9	73.92
189.7	58.03
208.5	55.22

Figure Captions

Fig.1 Schematics of the VESUVIO inverse geometry time of flight spectrometer at ISIS. Eye symbols are used to mark the detector positions used for the tests, including the positions at low scattering angles of the VLAD prototype detector bank.

Fig.2 Time of flight spectra measured with a CZT detector and a ^{238}U foil placed in the neutron beam. The full line spectrum is inclusive of events of any pulse height above a threshold set at about 20 keV. The dashed line spectrum includes only events in a narrow energy window around the 133.8 keV line. The spectra have been normalized so that the intensity of the lowest neutron energy resonance is the same.

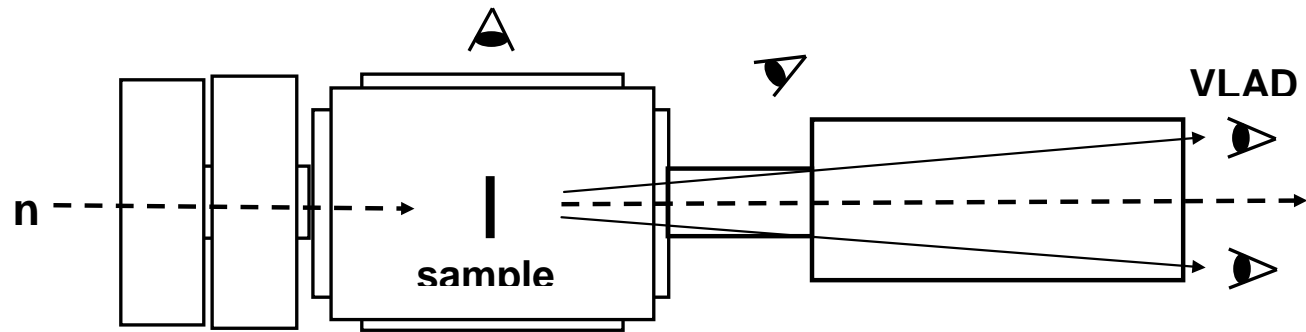
Fig. 3 Pulse height spectra measured with a YAP detector and a ^{238}U foil recording neutrons scattered from a Pb sample. The spectra are obtained from biparametric data integrated over different time intervals. Two normalized spectra are shown corresponding to a narrow time window around the neutron resonance at 6.67 eV (continuous line) and an off-resonance region (dashed line). The broad peak at about 500 keV is due to background γ s from boron.

Fig. 4 Time of flight spectrum from a water sample in an Al cell measured with a RD (^{238}U foil + YAP detector). The dashed and dot-dashed lines indicate the cell and the H_2O recoil peaks for the first three ^{238}U resonances.

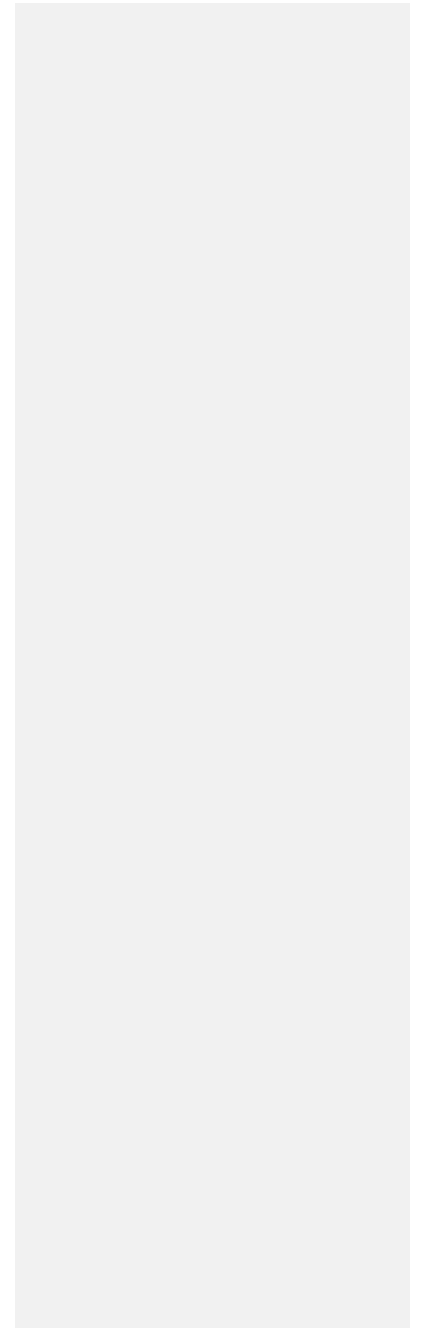
Fig.5 The VLAD prototype detector bank. Clearly visible are four detectors, each consisting of a pair of YAP scintillation crystals inside a light guide coupled to a photomultiplier tube. The detectors are close to the aluminum vacuum tank window. Also visible is a fifth (unused) detector equipped with Li-glass scintillator instead of YAP.

Fig.6 Time of flight spectrum collected by one of the movable detectors positioned at the lowest possible scattering angle of 2° in the VLAD prototype. The scattering sample was ice at 270 K. The three largest peaks correspond to the first three resonances in ^{238}U . More resonances are also visible (compare with Fig.2)

Final Report



G.Gorini Fig.1



Final Report

Fig.2

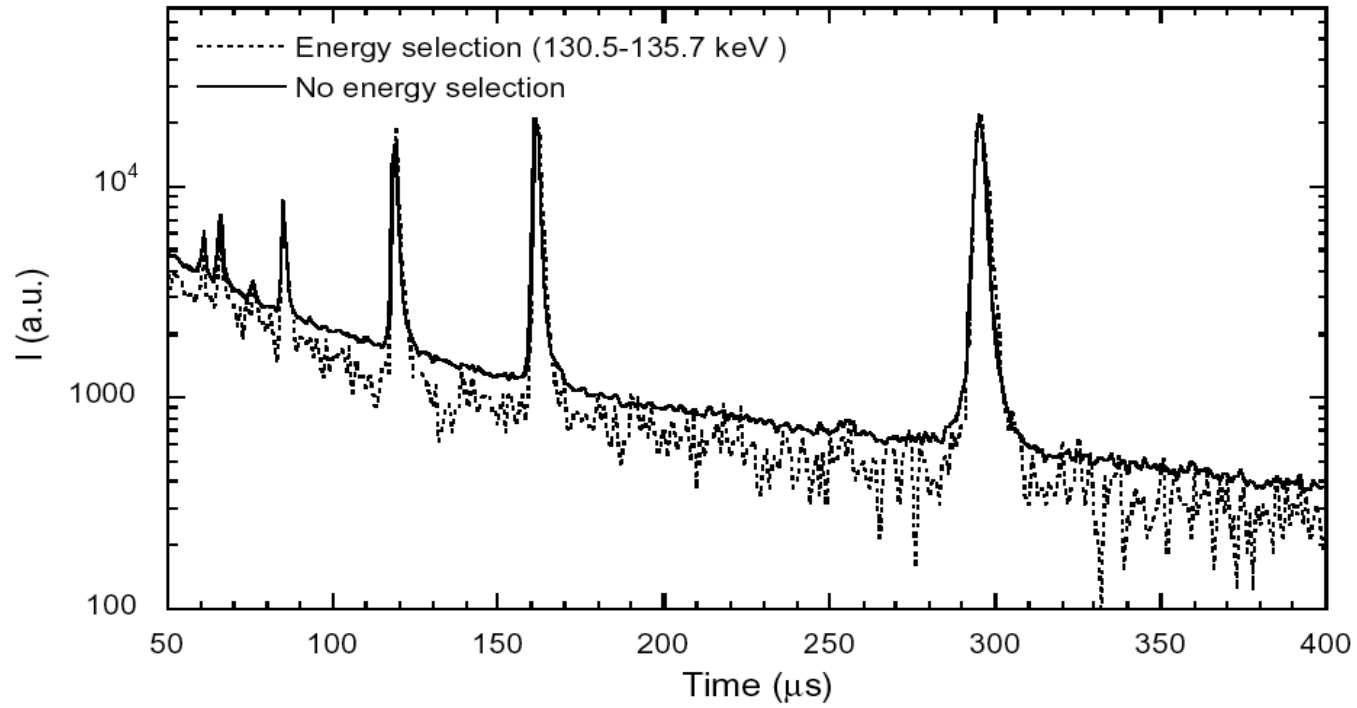
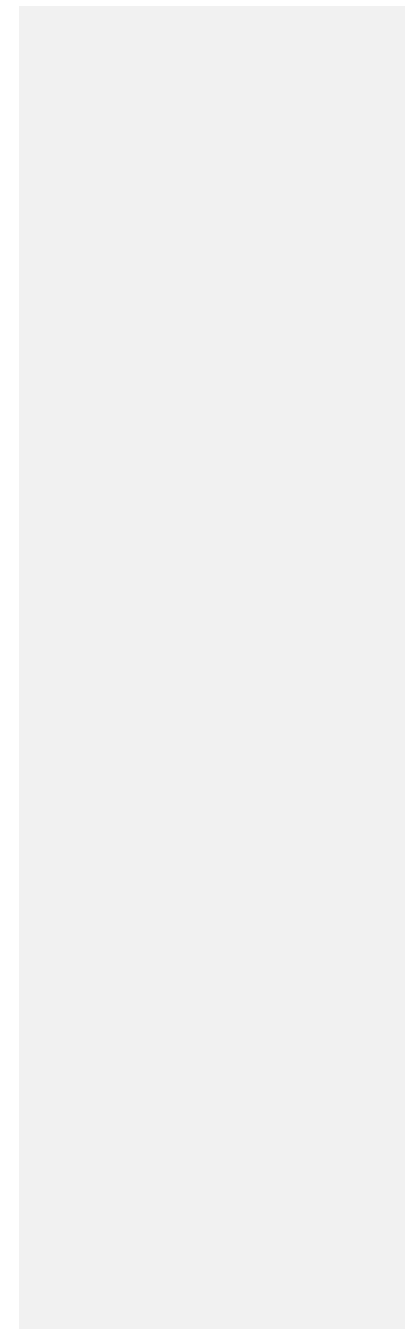
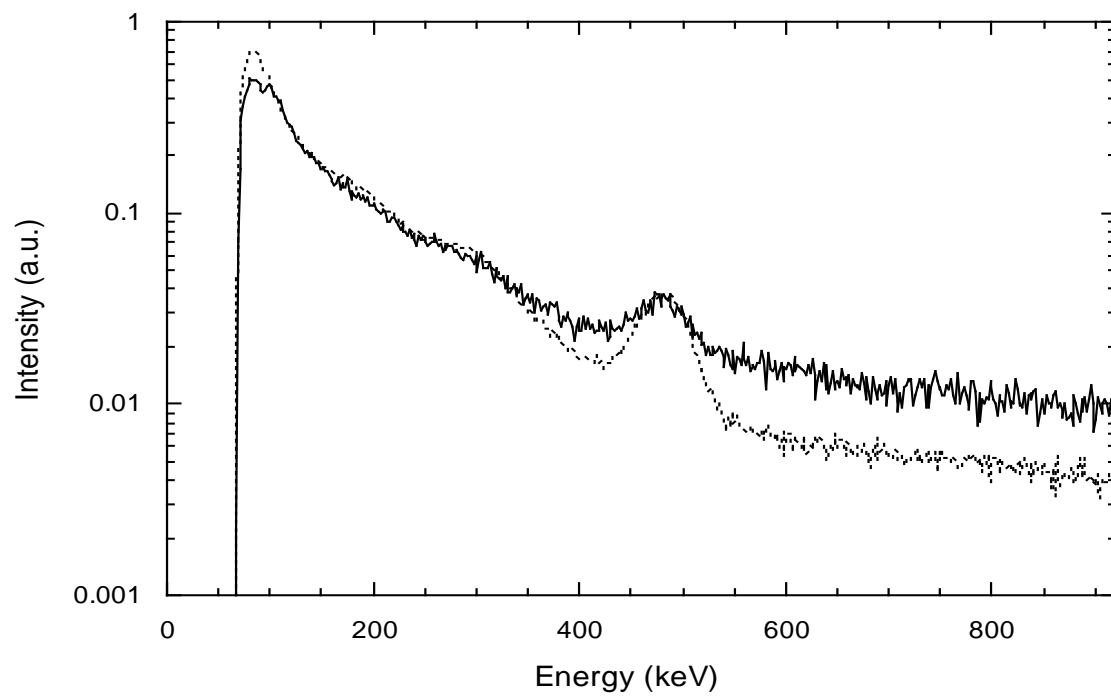
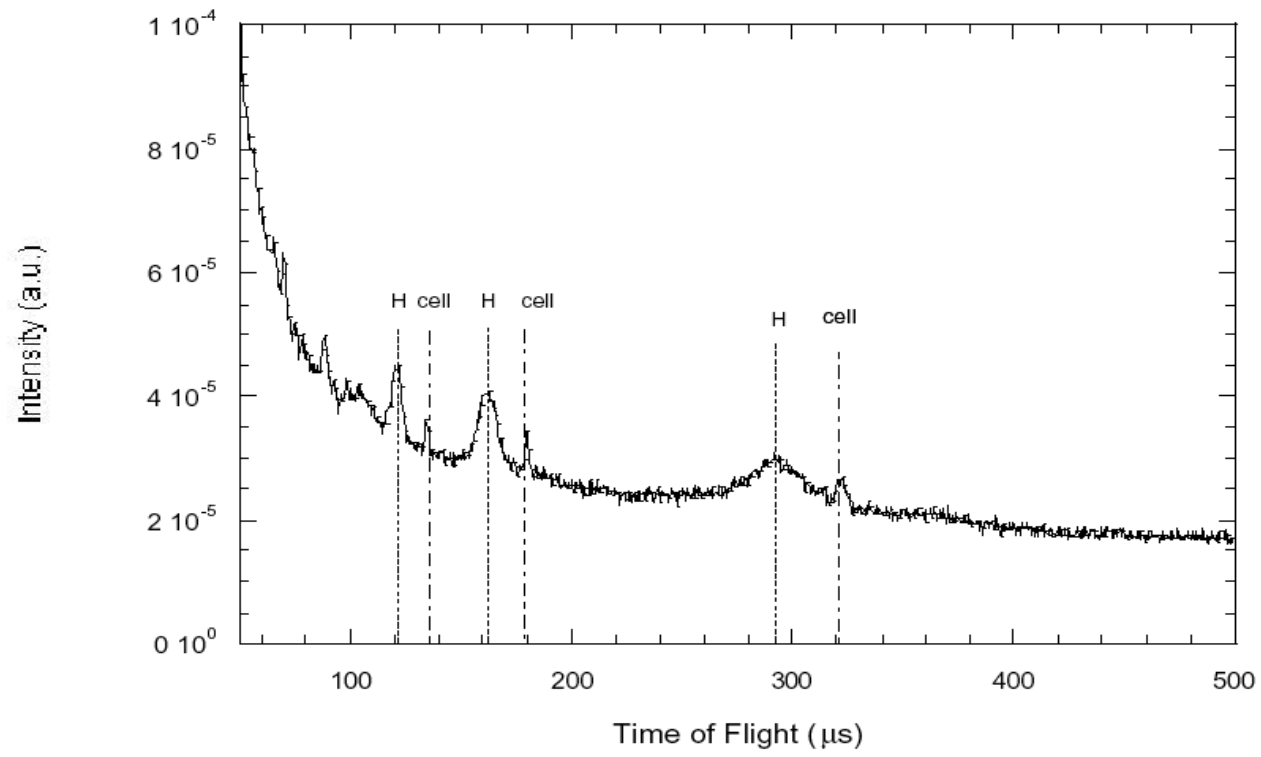


Fig.3

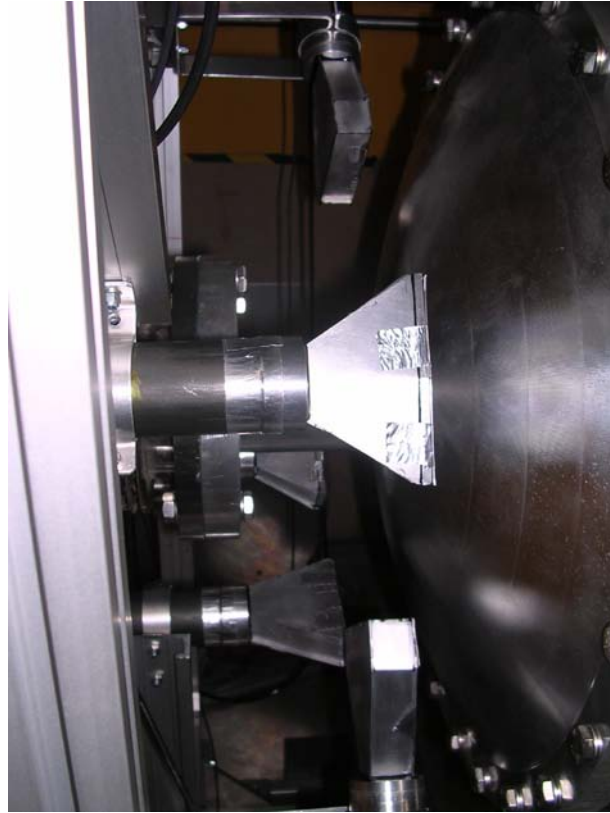


Final Report

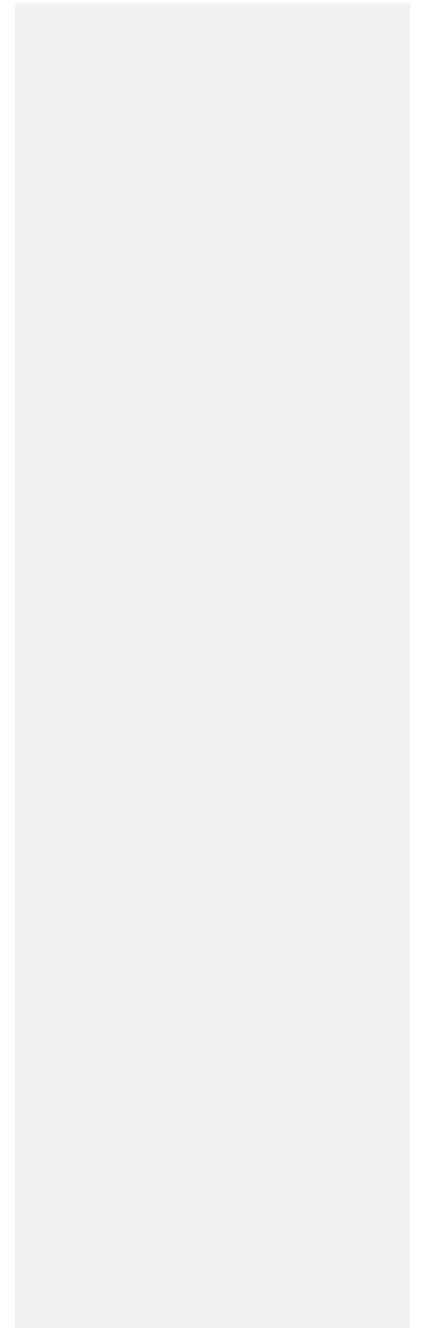
Fig.4



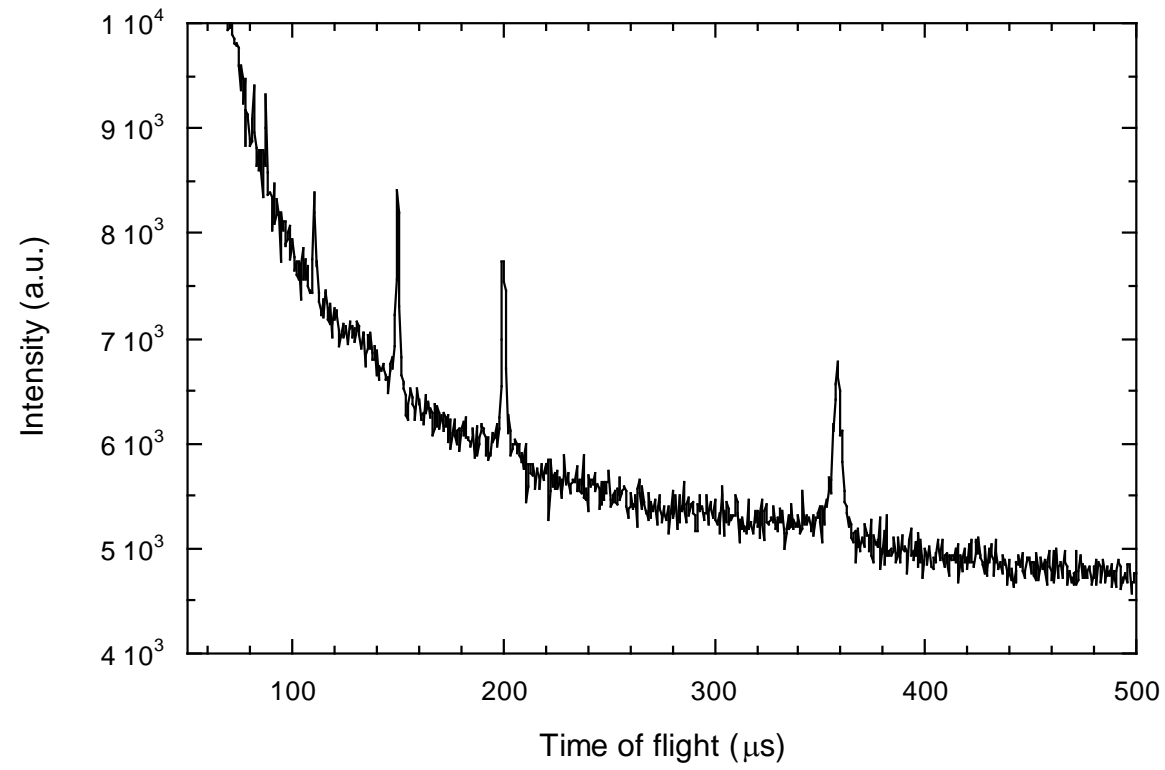
Final Report



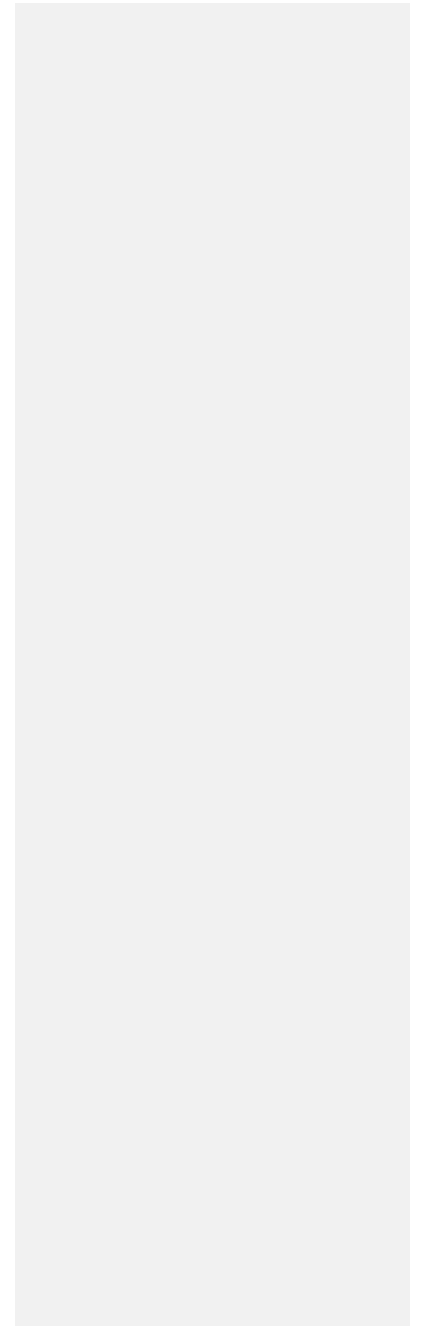
G.Gorini Fig.5



Final Report



G.Gorini Fig.6



Final Report

INFN: Milan / Perugia - Task 6

Neutron Focusing Devices

Recent innovative applications of neutron radiography and imaging have stimulated the development of novel optical devices for neutron beam focusing. Long ago, it was demonstrated that a phase reversal zone plate (ZP), that is a Fresnel lens which obeys the equation of thin lenses, can be successfully employed to focus and image a cold neutron beam ($\lambda \approx 20 \text{ \AA}$). It is only in recent time that progress achieved in nanofabrication has made possible the production of high-efficiency and high-resolution ZPs for focusing of short wavelength x-rays. Implementation of patterning techniques complementary to the electron beam lithography, such as subtractive patterning by means of ion milling and/or reactive ion etching, enabled to improve the resolution and the aspect ratio of the Fresnel zone plate. Exploiting the modern nanolithographic techniques, challenging possibilities for neutron applications, like microscopy, could be opened.

A set of neutron lens prototypes, based on the concept of the phase shifting binary zone plate, have been designed and fabricated at the TASC Laboratory & Elettra Synchrotron Light Source (Trieste, Italy). To match with the typical needs of low intensity neutron beams, and compatibly with the fabrication constraints, the devices we developed were characterized by a relatively large aperture and size of the lens, while aimed at operation at rather short focal lengths. Natural Nickel was used as phase shifter and quite high aspect ratios, typically of the order of 10 (35 has been recently obtained), characterized the devices, as a consequence of the large thickness of the phase shifter (typically in excess of 3.5 \mu m). The basic prototype was a large aperture phase reversal ZP, with 5 mm diameter, 0.4 \mu m resolution and 11 m focal length at 1.8 \AA neutron wavelength (6.9 m focal length at 3 \AA). Further details of the various binary ZP prototypes are reported in Table II and some scanning electron microscope images are shown in the Figures.

To fully exploit the potentialities of the ZP device for neutron beam applications, we investigated the possibility of a matrix arrangement of zone plates. A first mask and replica were produced enabling to obtain an array with a global size of $45 \times 45 \text{ mm}^2$, made as a 5×5 matrix of base units, each separately consisting of a 15×15 matrix ($9 \times 9 \text{ mm}^2$ size) of single zone plates (618 \mu m diameter). The fabrication parameters corresponded to a focal length of 1 m at 3 \AA neutron wavelength. However, a few technical problems prevented to complete the fabrication of this very large area matrix, for which the mask and the replica had been obtained. Therefore, a second, smaller size, square matrix, 1 cm^2 surface, consisting of 900 zone plates, 0.3 mm diameter each and 1 m focal length at 3 \AA , was fabricated. This matrix was capable of focusing the neutron beam from a point source into 900 small spots.

As a way to shorten the focal length, for practical use of the ZP at relatively short neutron wavelength, we tested a number of Fresnel zone plates stacked together. The zone plates for the first stack were fabricated with the same characteristics as the first prototype, namely 5 mm diameter and 11 m focal length at 1.8 \AA thermal neutron wavelength. A second series of ZP for a new stack was obtained from a new mask and using, again, natural Ni as phase shifter. The new ZPs had the highest presently achievable aspect ratio, namely 35, following from the fabrication parameters, that is 1 mm diameter, 0.3 \mu m outermost zone width, resist thickness from 10.5 \mu m in the outer zones to 8.5 \mu m in the innermost. Up to now, this ZP was replicated in two pieces, although having established the fabrication protocol makes the replicas of many different optics possible.

All the neutron tests on the ZP prototypes were carried out on the monochromatic beam of the TPA spectrometer at the LLB/Saclay. Specifically, we tested three types of devices: the single and large size binary ZP, the stack of several ZPs and the matrix of ZPs.

The performances of the single 5 mm diameter ZP were measured at the neutron wavelength $\lambda = 6.9 \text{ \AA}$, produced by a mechanical selector installed at the end of the neutron guide and characterized by $\Delta\lambda/\lambda \approx 0.16$. This wavelength value corresponds to a focal length of 3 m and a theoretical efficiency of $\sim 40\%$. A 1 mm pinhole was inserted at 3 m upstream the ZP, so that a parallel beam, 5 mm diameter, was expected at the neutron image plate detector, having $0.15 \times 0.15 \text{ mm}^2$ pixel size and placed at 4 m downstream the lens. The difference between the intensities collected with and without insertion of the ZP is shown in the Figure. An efficiency in excess of 20% was measured.

Final Report

A set of ZPs fabricated with the same characteristics as the 5 mm diameter prototype were stacked together using a proper mechanical system. Alignment of the ZPs in the neutron beam was accomplished by means of a mechanical system enabling three translations, and the insertion of consecutive lenses. The neutron test was performed at the neutron wavelength $\lambda = 6.60 \text{ \AA}$. A 1 mm diameter pinhole, downstream the velocity selector, was used to produce a small size neutron image. The ZP stack was mounted at a distance of 2700 mm from the pinhole and the 2-d detector was at 4700 mm from the stack. The results of the experiment clearly show that the response of the stack of zone plates obeys the same rules as those of two or more refractive lenses assembled together, familiar from the geometrical optics, with the expected concentration of the intensity. On the practical side, the tests demonstrate the effectiveness of the ZP stack for neutron beam manipulation.

The ZP matrix was characterized by a two-steps procedure. A first series of tests consisted in measuring the efficiency of an individual zone plate lens of the matrix. Since an ultra-high resolution neutron detector ($<50\mu\text{m}$) is not available yet, it was not possible to directly image the focusing spot of the lens. Thus the focusing experiment was performed in an indirect geometry: the zone plate matrix was tested at a wavelength $\lambda = 13.7 \text{ \AA}$, with a 0.8 mm pinhole placed at the image position, 23.6 cm from the lens. The incoming collimation was 0.5 mrad. In this experimental configuration, without the lens, a sharp spot is expected, corresponding to the geometrical shadow of the pinhole, whereas, with the lens, a broad spot is formed at the detector position, 4 m away from the image. In the attached Figure, the intensity map measured on the image plate detector with and without a single lens in the beam is shown. The effect of the ZP is very clear: a broadening of the beam is observed due to the “decollimation” effect induced by the focusing effect of the lens. From the measured intensities, a lens efficiency of about 30% was found, which is very close to the theoretical value of 27% expected at this wavelength.

The second series of tests consisted in characterizing the whole array. Thus the neutron detector was set-up at the image position (34 cm from the Zone Plate Matrix, at $\lambda = 9.8 \text{ \AA}$). Two experimental limitations affected the measurements, namely the incoming beam was not fully homogeneous across the whole section of the ZP matrix, and the image plate resolution, about $150\mu\text{m}$, exceeded the expected size of the individual focusing spots, about $100\mu\text{m}$ in the image plane in this configuration. Nevertheless, it was possible to image the individual focusing spots even though the detector resolution was limited.

These tests demonstrate the excellent operation of this new device, which enabled an easy focusing of the neutron beam at sub-millimeter scale.

One of the last achievements of the project was the acquirement of a quantity of ^{58}Ni to be used as a phase shifter for production of a higher efficiency device.

Table 2

Fresnel Zone Plate	ZP_0	ZP_1	ZP_2	ZP_3	SZP_1	ZP_4
Binary – Phase Shifting	Single	Single	Matrix	Matrix	Stack of ZP_1	Single & Stack
Shifter	Natural Ni 1.2 μm	Natural Ni 3.8 - 4 μm	-----	Natural Ni 5 μm	Natural Ni 4 μm	Natural Ni 10.5 μm
No. of Zone Plates	1	1	5625	900	2 – 5	2
Zone Plate diameter (mm)	5	5	0.618	0.300	5	1
Size of the array (mm^2)	19.63	19.63	45 x 45	10 x 10	19.63	0.79
Resolution (μm)	0.4	0.4	0.2	1	0.4	0.3
Aspect Ratio	3	10	11	5	10	35
Focal length (m) at $\lambda = 3 \text{ \AA}$	6.9	6.9	1	1	6.9	1

Final Report

CCLRC: Task 6

The Neutron Silicon lens (NSL) has proved to be a practical focussing device with a number of applications in the sphere of neutron instrument design. This has only become apparent during the very last phase of the TECHNI programme, when the full performance of the lens has been demonstrated.

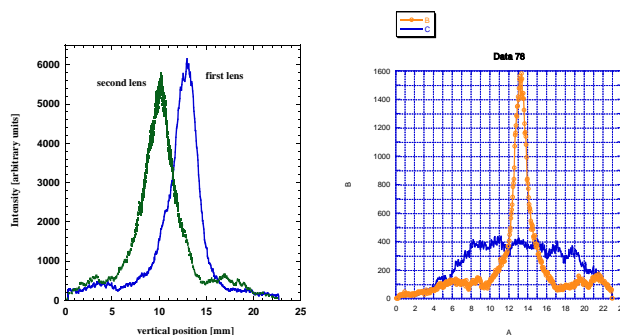
The neutron silicon lens design (NSL) was been completed during the first year of the TECHNI programme using a newly written optimisation program, and Monte Carlo simulations. This design indicated that a lens consisting of 144 mirrors would lead to a well imaged line source at 500mm from the lens. These calculations were performed at a number of wavelengths, demonstrating the expected increase in effectiveness with wavelength, up to the maximum wavelength that the lens is designed for.

This design also established two important features: that the use of a small number of stock sizes had little effect on the lens' performance, and that the ideal, elliptical shape of the mirror surfaces also has a minimal effect if the lens dimensions are chosen correctly. These conclusions and the numerical results have been published (M R Daymond & M W Johnson, NIM A485, 2002, p606).

Silicon wafers were then purchased from Virginia Semiconductor with a range of thickness from 30 to 400 microns. These wafers were then coated at the PSI with a $m=2$ supermirror coating. After careful assembly in a clean room (class 100) the lens was tested on the OSIRIS spectrometer at the ISIS facility. The results of these tests confirmed that the principle of the lens construction worked, and an image of the neutron illuminated slit was observed 500mm from the lens, as predicted. In fact sufficient measurements were taken to show that the image was at its sharpest very close to the expected focal position. However, the test also revealed that the lens was only achieving an image intensity that was approximately 25% of that theoretically achievable. An analysis of the data showed that the most likely cause was due to the non-parallel alignment of the mirror surfaces. It had been hoped that this would have been achieved naturally from the high precision wafers used in the construction (1 micron taper tolerance), and the use of clean-room conditions when building the stack. From the broadening of the image we have estimated that the wafers have an average of 15micron taper between each mirror.

In the second year detailed measurements of the wafer thickness were made, and confirmed the fact that – if the Si wafers had been in intimate contact – the lens would have been more efficient than was actually measured. Attention then turned to the possibility that trapped air is the cause of the imperfect stacking. A new lens holder was designed with a number of significant improvements. This accurate design allowed the positions of each wafer to be measured and the 'parallelism' determined more accurately during construction. Secondly the holder will enable the lens to be held in a vacuum, thereby eliminating the possibility of air pockets displacing the wafers.

In the third year a new NSL device was made in which the wafers are held under vacuum, and under compression. This device was hoped to remove the possibility that the wafers were being held apart by air trapped between the wafers. At the same time the middle section of the lens was removed (i.e. the section containing the thinnest wafers < 100 μ m) and replaced by wafers of 100 μ m in thickness. The results of the second trial lens (see figure below (a)) were a disappointment, since now significant improvement in focussing was been achieved.



a) Third year results with 2.5mm (FWHM) b) Fourth year results with 1.5mm (FWHM)

Final Report

In this final year a third trial was made with the lens. The holder was the same as that used in the third year, but on this occasion the lens was pre-heated to 200C for 2h while under vacuum. Following the vacuum-heat treatment a force of approximately 75kg was applied to the NSL wafer stack. Some initial improvement in the lens performance (about 25% increase in the peak height) was observed. However, much further increases in performances were obtained by careful adjustment of the optical parameters. These parameters were the horizontal alignment of the lens (tilt), and the primary and secondary focal lengths. By adjusting these parameters by about 10% very significant improvements in the focussing ability of the lens was observed. This is illustrated in the figure above (b), which shows the image obtained from the same 1mm slit. In this figure the effect of the lens is compared to the 'no-lens' configuration, and the effect of the lens, in deflecting neutrons into the central peak area is clearly demonstrated.

The sharpness of the image obtained (1.5mm full width at half maximum height (FWHM)) is also clearly seen and is now close to the MC simulation predictions. It has therefore been concluded that the performance of the NSL has been amply demonstrated, and can be considered for use in forthcoming instrument designs. It also indicates that, with the use of polarising neutron supermirrors on each of the NSL wafers, the device could be used to provide a focussed line of polarised neutrons.

Riso: Task 6

The RITA-2 spectrometer is a cold-neutron triple axis spectrometer with a flexible 9-blade analyzer and a position-sensitive detector (PSD). The analyzer and detector are placed in a common shielding tank (Fig. 1) to allow for maximum flexibility in the analyzer system, which has the possibility of being operated in a variety of different 3-axis modes. [1]

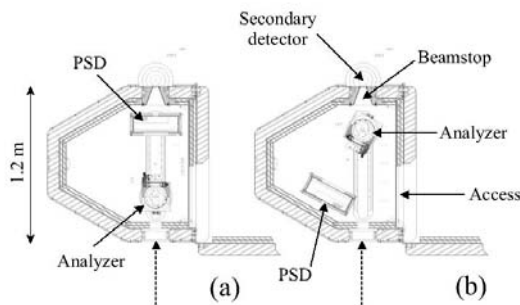


Figure 1. The RITA-2 analyzer-detector tank. (a) shows the tank with the detector in two-axis mode. (b) shows the tank in three-axis mode.

Before 2003, the RITA-1 and RITA-2 spectrometers were mostly operated in standard triple-axis mode or in the monochromatic point-to-point focusing mode, see Fig. 2(a). Only one experiment was performed that took advantage of the powerful option of collecting multiple data points simultaneously (one point in (q,ω) space for each analyzer blade) [2]. The limiting factor was a common concern that cross-talk between the signals from neighboring blades would render the measurements useless, *e.g.* in the case where one blade would detect a large elastic signal, while the neighbor blades were set to observe a weak inelastic signal.

Final Report

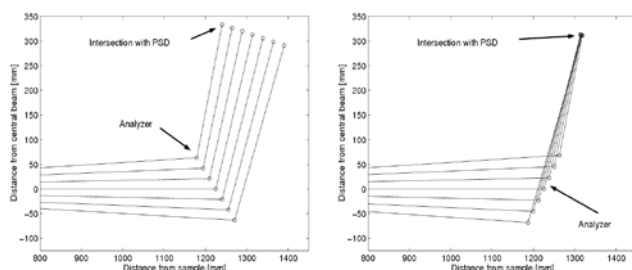


Figure 2. Monochromatic modes at $E_f=5.0$ meV (a) point-to-point focusing, (b) imaging.

The new Risø task set for the TECHNI project implied implementing a new analyzer mode, *the monochromatic imaging mode*, where all blades reflect neutrons at the same energy, but with different scattering angles. [3] A flexible collimator would then be designed and constructed so to separate the beams from each blade towards the PSD. Finally, the combination of mode and detector would be tested in a real experiment.

The specifications of the monochromatic imaging analyzer mode was derived mathematically [3]. We searched for solutions with equidistant beams spots on the PSD, spaced with the same distance as the analyzer blades on the mount (at RITA-2: 25 mm). This requirement can be fulfilled to first order for energies above 3.2 meV [3].

The monochromatic imaging mode was first tested without collimation and was found to perform as expected. Figure 3 shows the image from the PSD in one vanadium measurement at 5.0 meV, where 5 analyzer blades are used. The beams are seen to be almost equidistant, but slightly overlapping. The small (15%) variation in intensity is caused by a difference in quality of the PG analyzer crystals. This can be accounted for by a proper calibration. A triple-axis powder scattering experiment was performed, and to avoid cross-talk between signals from different blades only every second blade was used. Figure 4 shows the effect of the factor-three improvement in the resulting data.

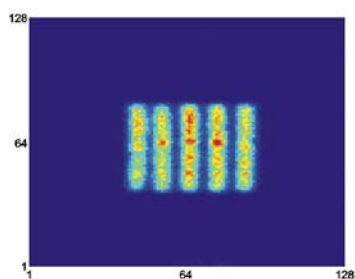


Figure 3. Counts in the PSD for an isotropic scatterer, using 5 analyzer blades in the monochromatic imaging mode without collimator.

Final Report

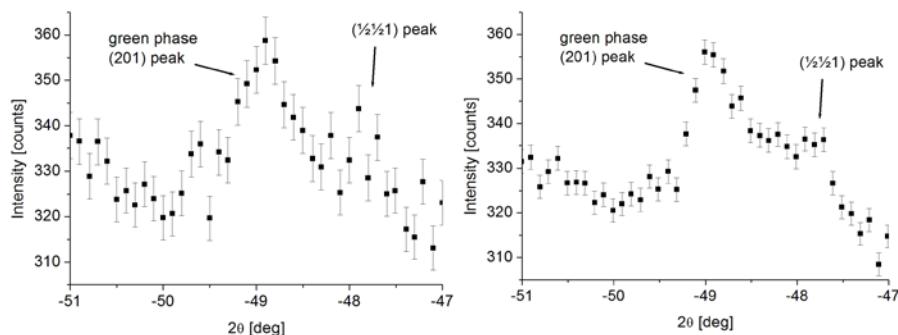


Figure 4. (left) A powder scan without collimator where only the central analyzer blade is shown. (right) the same scan where the signals from 3 blades have been normalized, shifted by a proper amount (approx. 2 degrees), and averaged.

After setting the scene for the use of (and need for) an imaging mode collimator, the actual designing and construction work began. The main requirement is that the collimator must constitute a set of vanes, guiding each beam from the analyzer blade to its respective position at the PSD. To allow for operation at different energies, the vanes must be flexible, since the spatial position of the analyzer blades will vary. The collimator was designed so that each of the 10 blades are hinged on the side closest to the PSD with a spacing of 25 mm, while two motors each drive 5 blades with different gearings, scaled 1:3:5:7:9, respectively. The collimator is shown in Figure 5, the blade height is 250 mm.

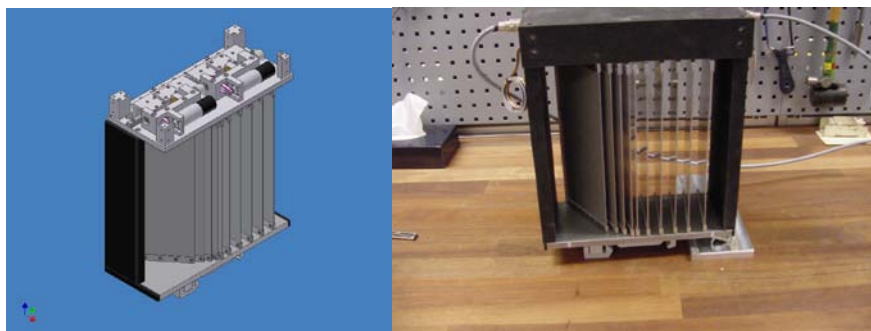


Figure 5. (left) drawing of the flexible radial collimator, (right) photograph of the collimator

After 3 prototype versions, the collimator was found to be mechanically acceptable, and a full-scale collimator was produced. The mechanical tests showed good reproducibility in the positioning of the blades, and the electronic interface to the control software worked well.

In November 2003, the first tests were performed in real operation mode at RITA-2 at PSI with a collimator with 100 mm long blades. It was found that the spectrometer movements would cause the collimator blades, especially the outer ones, to wobble up to 3 mm. This problem was solved temporarily in order to perform

Final Report

the neutron tests. It was first found that the collimator blades did indeed define the required vanes with simultaneous line-of-sight from all 7 used analyzer blades to the correct parts of the PSD.

The cross-talk was measured in two ways having only the middle analyzer blade in reflection at 5.0 meV. First, a powder scan on a calibration sample was performed, resulting in a strong peak in the part of the PSD, belonging to the middle blade. The part of the PSD corresponding to the neighbor blade showed a signal that was roughly 1.0% the value of the main signal. This is the elastic cross-talk value. Secondly, incoherent scattering from vanadium was used to perform an inelastic scan. In the neighbor window this scan peaks at an energy transfer of around 0.2 meV with a peak value of around 2.0% of the main signal. This is the inelastic cross-talk value.

As a final test, we performed a measurement of phonons in a lead crystal at room temperature, repeating the experiment by Brockhouse et al [4]. We used the monochromatic imaging mode with 7 analyzer blades to obtain two-dimensional scattering maps for constant energy transfers. The results were remarkably detailed, taking into account that each map was produced in the course of just 7 hours, see Fig. 6

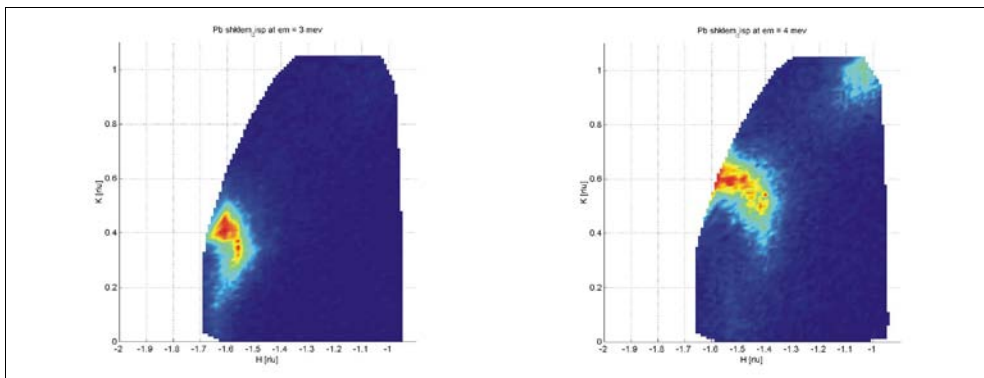


Figure 6. Detailed measurement of phonons in lead in the $(h,k,0)$ plane at two energy transfers (left) 3.0 meV, and (right) 4.0 meV, taken at RITA-2. The measurements used the monochromatic imaging mode with 7 blades and the flexible collimator. The curved edge of the data range shows movement limits of the spectrometer due to the neutron guide after RITA-2. Each setting counted for 25 seconds, and 772 settings were used per picture, yielding 5404 data point. The data taking lasted in total 7 hours per picture.

References

- [1] K. Lefmann, D. F. McMorrow, H. M. Rønnow, K. Nielsen, K. N. Clausen, B. Lake & G. Aeppli. *Physica B* **283**, 343 (2000)
- [2] P. Zetterström, A. Chahid & R. L. McGreevy. *Physica B* **266**, 115 (1999)
- [3] C. R. H. Bahl, P. Andersen, S. N. Klausen & K. Lefmann. Submitted to *Nucl. Instr. Meth. B* (2004)
- [4] B. N. Brockhouse, K. R. Rao, A. D. B. Woods, G. Caglioti & T. Arase. *Phys. Rev.* **128**, 1099 (1962)
- [5] A. Abrahamsen, C. H. R. Bahl, S. N. Klausen, T. B. S. Jensen, and K. Lefmann (in preparation)

Final Report

PSI: Task 7

The characteristic parameters of the SM polarisers we achieved to produce are not extraordinary if taken on their own. It is their combination, which allows for new applications. The main effort was to reduce the in-plane stress while keeping or even improving the remanence. Stress causes the wanted magnetic properties via magnetostriction, but it restricts the total layer thickness and thus the upper limit for m .

At the beginning of the project remanent supermirrors based on Fe/Si reached $m=2.2$, only, while the polarising efficiency was below 93% and the coercitive field below 20 Oe.

Within this project we developed and tested magnetically remanent Fe/Si supermirror polarisers with $m=2.5$ and $m=3$ with coercitive fields up to 40 Oe. The $m=2.5$ polarisers show a polarisation efficiency of more than 96% in zero-field in transmission geometry. These supermirrors were used to build a white beam transmission polariser for the SANS at SINQ, Switzerland. The $m=3$ polariser shows a slightly lower efficiency in transmission, but it has an efficiency of about 98% in reflection mode in zero-field.

CCLRC: Task 8

High Resolution Scintillator Detector for ENGIN-X

ENGIN-X requirements

ENGIN-X is a new diffractometer for engineering studies at ISIS. Design of the ENGIN-X detector array called for 2 banks of 5 detector modules centred at a 90° scattering angle. Each detector module required 240 individual detector elements 3 mm wide and 195 mm high. The entire ENGIN-X detector array therefore needs 2400 detector elements covering an area of 1.4 m^2 .

ISIS uses ZnS^{60}Li scintillation detectors for most of its powder diffraction instruments. In these detectors the strips of scintillators are coupled by coded fibre optic arrays to sets of photomultiplier tubes. To maximise neutron detection efficiency the neutron path length through the scintillator has been increased by forming the scintillators into V shapes, with the apex of the V pointing at the sample. At the start of TECHNICAL scintillator size, thickness, reflector geometry and fibre optic readout have all been optimised to give arrays of linear detectors with a position resolution of 5 mm. In designing ENGIN-X, there was a clear requirement for a linear detector with an improved position resolution of 3 mm.

Detector design concepts for ENGIN-X

The main issues considered during the development of the ENGIN-X detector design are:

- The scintillator has to be tilted, to elongate the neutron path length and thereby increase the neutron detection efficiency.
- Light collection from both sides of the scintillator is required to maximise light collection efficiency.
- A good optical isolation between the scintillator elements is required to prevent cross talk.
- The scintillator and fibre geometry has to be chosen so that a neutron generates enough light in at least two adjacent fibres to identify a neutron by a coincidence signal from two photomultiplier tubes.
- Variations in detector performance from element-to-element reproducibility should be minimised.
- The assembly should be simple to reduce production time and costs.

Final Report

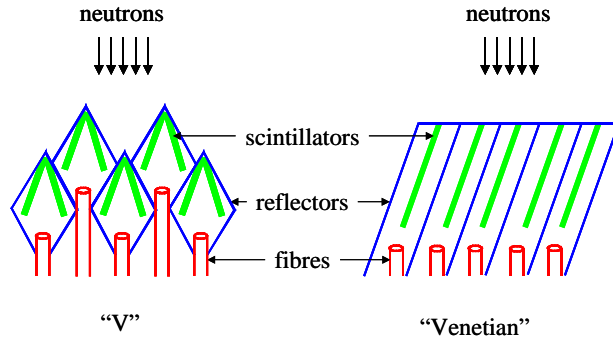


Figure 1: Schematic diagram of the front-end of two possible scintillator arrangements, the so-called “V” geometry on the left and the “Venetian” geometry on the right.

Monte Carlo simulations identified two candidate scintillator / reflector geometries. Both geometries, the so-called “V” geometry and “Venetian” geometry, are schematically shown in Figure 1. The “Venetian” geometry owed its name to the scintillator arrangement, which looks like a Venetian blind. Measurements with prototype detectors and constructional considerations were used to decide which of these two geometries could be used for the ENGIN-X detector.

Monte Carlo simulations

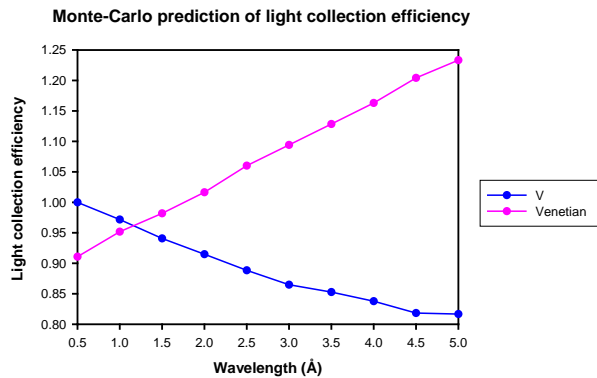


Figure 2: Light collection efficiency of the “V” and “Venetian” geometries as a function of neutron wavelength, calculated with Monte Carlo simulations. The curves are normalised to the light collection efficiency of the “V” geometry at a neutron wavelength of 0.5 Å.

Monte Carlo simulations have been extensively used to optimise design parameters and compare the performance of the two geometries. Figure 2 shows the results of the simulation of the light collection efficiency of the optical fibres as a function of neutron wavelength. Clearly for increasing neutron wavelength, the light collection efficiency of the “V” geometry is decreasing while the light collection efficiency of the “Venetian” geometry is increasing. This trend can be understood by realising that long wavelength neutrons are predominantly absorbed at the top surface of the scintillator, see Figure 1. Since ZnS is an opaque scintillator, most of the light resulting from long wavelength neutron absorption will escape from the top surface of the scintillator. Collection of this light in the “V” geometry is relatively poor because of the small distance between the scintillator and reflector. The light collection efficiency of the “V” geometry is therefore decreasing with increasing neutron wavelength. In contrast, the “Venetian” geometry has a good light collection from the top surface of the scintillator. Light collection efficiency is improving

Final Report

for longer wavelengths because the average path length of light in the scintillator will be shorter and the self-absorption of the scintillator will be less.

Prototype evaluation

To provide a means of determining detector characteristics from the two different detector geometries and to explore the mechanical problems associated with detector manufacture, two 15 channel prototype detectors have been constructed; one with a “V” geometry and one with a “Venetian” geometry. Pictures of the front end of these prototype detectors are shown in Figure 3. These two detectors have been extensively tested, both on the Am-Be neutron source of the neutron detector group and on the ROTAX beam-line at ISIS.



Figure 3: Pictures of the front end of the prototype detectors with the so-called “V” geometry on the left and the “Venetian” geometry on the right.

The uniformity of neutron detection efficiency gives an indication of the reproducibility and quality of the assembly. Figure 4 shows the count rate for both the “V” and “Venetian” geometry prototype detectors, as measured on the Am-Be neutron source. The “Venetian” type prototype detector did not have a scintillator fitted for detector element 8 during this measurement, hence the gap in the data. The spectrum of the “V”-geometry shows an up down variation of $\pm 10\%$ in count rate. This feature is partly due to the highly diverging radiation from the Am-Be source and partly due to some overlap of scintillators in the top and bottom row, see Figure 1. Apart from this effect, the neutron count rate is uniform to within $\pm 5\%$. In contrast, the spectrum of the “Venetian” prototype does not show an up-down structure and the total variation in count rate is $\pm 5\%$. The fact that this good uniformity is achieved without fine-tuning the high voltage on the PMTs and discriminator settings of the electronics shows that the quality of the assembly is high for both prototypes.

Final Report

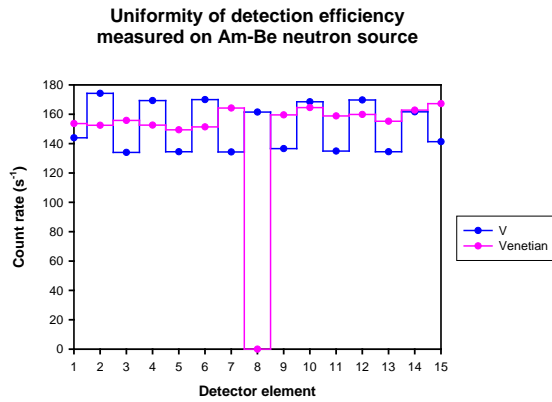


Figure 4: Uniformity of detection efficiency of 15 detector elements, measured with the “V” and “Venetian” prototype detectors on an Am-Be neutron source.

The measurements shown in Figure 4 demonstrate that the detection efficiency, on an Am-Be neutron source, is the same for both geometries. Figure 5 shows the average ratio of the neutron detection efficiency of a prototype detector as a function of neutron wavelength, as measured on the ROTAX beam line with a vanadium sample. The efficiency of both prototypes is similar for thermal and epithermal neutrons, though the “Venetian” prototype is ~10% more efficient for low energy neutrons. This is in agreement with the results of the Monte Carlo simulation of the light collection efficiency shown in Figure 2. Since the neutron detection efficiency is proportional to the light collection efficiency, a “Venetian” type detector is expected to be more efficient for long wavelength neutrons than a “V” type detector.

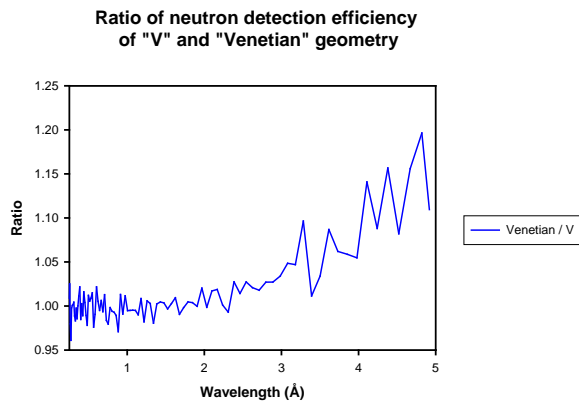


Figure 5: Neutron detection efficiency of the “Venetian” geometry divided by that of the “V” geometry, measured as a function of neutron wavelength.

The optical fibers in a “Venetian” type detector are molded in a black B₄C block. For the “Venetian” geometry, 85% of the active area of the fiber block is black and thus absorbing the scintillation light. Monte Carlo simulations predict that the light collection efficiency of the fibers could be enhanced by 20% when the surface of the fiber block is coated with a white reflector. To evaluate the improvement in neutron detection efficiency for such a white painted fiber block, two 27 element detectors with the “Venetian” geometry have been produced. One detector has an unpainted black fiber block whereas the other detector

Final Report

has a white painted fiber block; all other parts are identical. Figure 6 shows the result of an evaluation of both prototype detectors on an Am-Be neutron source. This result reveals that the measured difference in neutron detection efficiency is only 6%. Since the white painted fiber block is significantly more expensive to produce, this option proved to be unattractive.

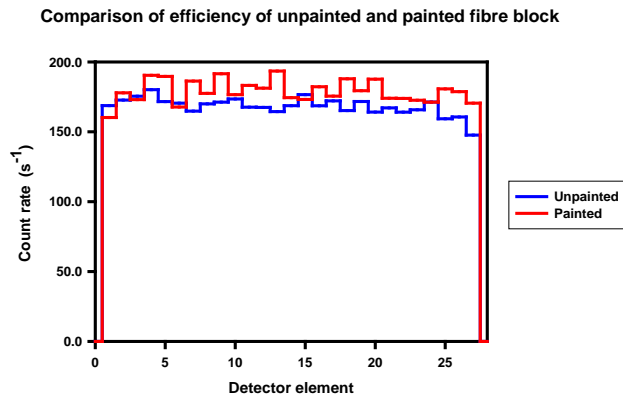


Figure 6: Comparison of the neutron detection efficiency of two 3 mm linear detector prototypes, one with a black unpainted and one with a white painted fibre block.

Detector realisation

The measurements with the prototype detectors, described in section 0, did not reveal a significant difference in performance of the “V” and “Venetian” type scintillator geometry. The detection efficiency, gamma sensitivity and intrinsic detector background measured with both prototype detectors are similar and within the specifications for the ENGIN-X detectors. Hence, both a “V” and “Venetian” type of detector will meet all the specifications for the ENGIN-X detectors. However, it is more cost effective to produce the Venetian detector geometry. This feature, combined with the improved performance of the Venetian detector at longer wavelengths led to the “Venetian” geometry being chosen for the ENGIN-X detector design.

A full size ENGIN-X module contains 240 individual detector elements, each 196 mm high and 3 mm wide. The elements are viewed by optical fibre arrays coded into two sets of 16 photomultiplier tubes, one set on the left and one set on the right hand side of the detector. A photograph of an almost completely assembled detector module is shown in Figure 7. The whole ENGIN-X detector array requires 10 of these modules.

Final Report

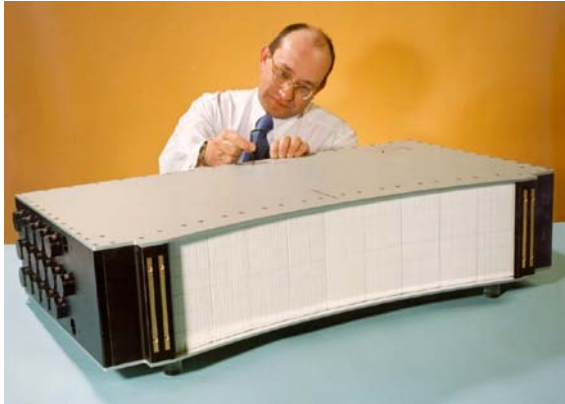


Figure 7: *Photograph of a full size ENGIN-X detector module. The front reflectors, front cover and PMT assembly has not yet been fitted.*

Evaluation of the full size ENGIN-X detector modules on an Am-Be source

Before installation on ENGIN-X, the uniformity of neutron detection efficiency of all 10 detector modules has been evaluated on an Am-Be neutron source. Figure 8 shows the result of this evaluation for one of the detector modules. The lower number of counts at the edges of the detector module is caused by a non-uniform neutron flux and not by a reduction in neutron detection efficiency. The uniformity of neutron detection efficiency for a typical detector module is very good, with a standard deviation of 5%. This result shows that full size detector modules can be produced with a good uniformity. During the evaluation, all discriminator electronics channels have been set up identically and the photomultiplier tubes are set to specifications given by the manufacturer. That this level of uniformity has been obtained without fine-tuning the settings of individual channels illustrates the fact that these scintillation detectors are easy to set up.

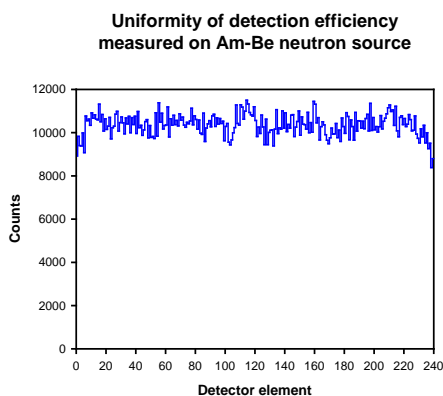


Figure 8: *Uniformity of detection efficiency of a full size ENGIN-X detector module, measured with an Am-Be neutron source. The lower number of counts at the edges of the detector module is caused by a non-uniform neutron flux.*

Evaluation of the detector modules on ENGIN-X

Ten of these full size detector modules have now been produced and installed on the ENGIN-X beam line. These 10 detector modules have been made by industry, and no problems have been encountered during

Final Report

construction. A photograph of 5 detector modules, installed on one of the two detector banks of the ENGIN-X beam line, is shown in Figure 9.



Figure 9: Photograph of 5 detector modules installed on the south bank of ENGIN-X.

Uniformity of neutron detection efficiency of the detectors as installed on the ENGIN-X beam line has been evaluated. Figure 10 shows the neutron count distribution over the 5 detectors in the south bank of ENGIN-X, using a vanadium sample. The measured uniformity of $\pm 20\%$ is considerably worse than the $\pm 10\%$ uniformity of an ENGIN-X detector measured on an Am-Be source before installation. Beam line components, like jaws and collimators, can significantly contribute to the inhomogeneity of neutron flux distribution onto the detectors, affecting the evaluation of the neutron detection efficiency. A good fraction of the difference in uniformity between the ENGIN-X beam line and the Am-Be source measurements is therefore believed to be caused by other beam line components.

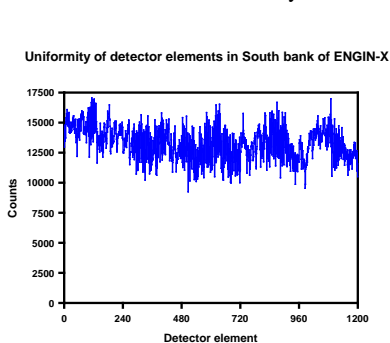


Figure 10: Uniformity of neutron counts of all 1200 detector elements in the ENGIN-X South bank, using a vanadium sample.

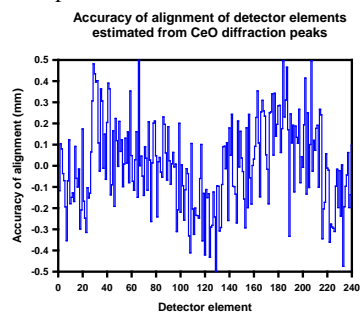


Figure 11: Estimated accuracy of the alignment of the 240 detector elements in an ENGIN-X detector module.

Powder diffraction provides a convenient means to evaluate the accuracy of the alignment of the detector elements. Using Bragg's law it is possible to relate the time of flight (TOF) of a diffraction peak to the scattering angle and therefore to the actual position of a detector element. The alignment is determined from the difference between the actual position and theoretical position of a detector element. The result of this evaluation for a single detector module on the ENGIN-X beam line, using a CeO powder, is shown in Figure

Final Report

11. The majority of the element-to-element variation is due to the statistical error in the determination of the TOF of the diffraction peaks. The estimated alignment for all detector elements is better than ± 0.5 mm, while the alignment of the elements for the majority of the detector is better than ± 0.3 mm. This result shows that a very accurate positioning of the scintillators has been achieved.

To illustrate the benefit of the new geometry with a 3 mm position resolution over the standard detectors with a 5 mm position resolution, the effect of the position resolution of the detector on the TOF resolution has been assessed on ENGIN-X. Figure 12 shows the main diffraction peak using a cerium oxide powder sample, measured for two neighbouring detector elements within a module. The peak shift in TOF is 39 ms, whereas the FWHM of the peaks is 125 ms. The peak shift is therefore 30% of the peak width. The width of the detector elements is thus affecting the TOF resolution and ENGIN-X benefits from the higher position resolution offered by the newly developed detector geometry.

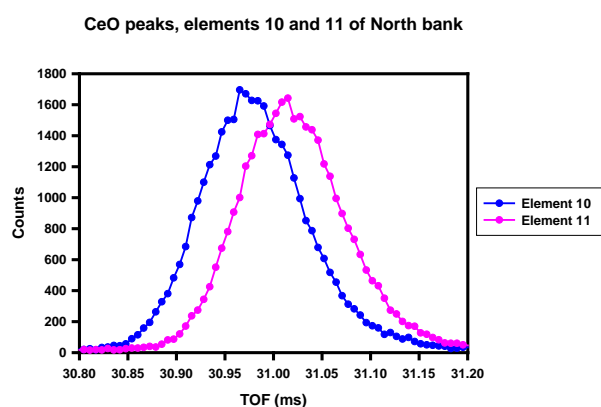


Figure 12: Diffraction spectra of a cerium oxide powder measured with two neighbouring detector elements on the ENGIN-X beam line.

Evaluation of the potential of the new high efficiency ZnS geometry

The Venetian concept extended to two dimensions

Neutron scintillation detectors for single crystal applications at ISIS currently utilise single sheets of 0.4 mm thick ZnS scintillator on top of a reflector grid, as shown in 13. These detectors have an active area of 200 mm x 200 mm and two-dimensional position sensitivity with a resolution of 3 mm. Such detectors do not suffer significantly from parallax errors, even at sample to detector distances as short as 250 mm. However, neutron detector efficiency is $\sim 20\%$ at 1 Å, which is relatively low.

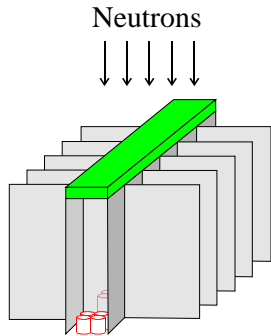


Figure 13: Schematic representation of the existing 3 mm pixel detector geometry with a flat scintillator on top of a reflector grid.

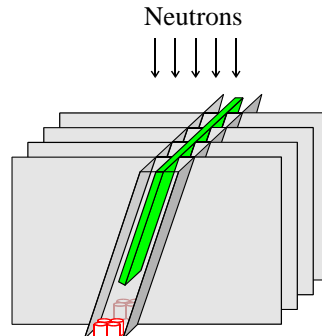


Figure 14: Schematic representation of a pixel detector with a 3 mm resolution, based on the 3 mm strip detector geometry of the ENGIN-X detectors.

The possibility of making a high efficiency pixel detector with a 3 mm resolution, using ZnS scintillator and a reflector geometry based on the 3 mm strip detector design, has been studied. A schematic drawing of such a detector is shown in Figure . A detector with this geometry will have approximately 2.5 times higher detection efficiency for 1Å neutrons than the current single crystal detectors used at ISIS. The design challenge of this geometry is to minimise degradation of position resolution due to parallax effects, whilst realising enhanced neutron detection efficiency.

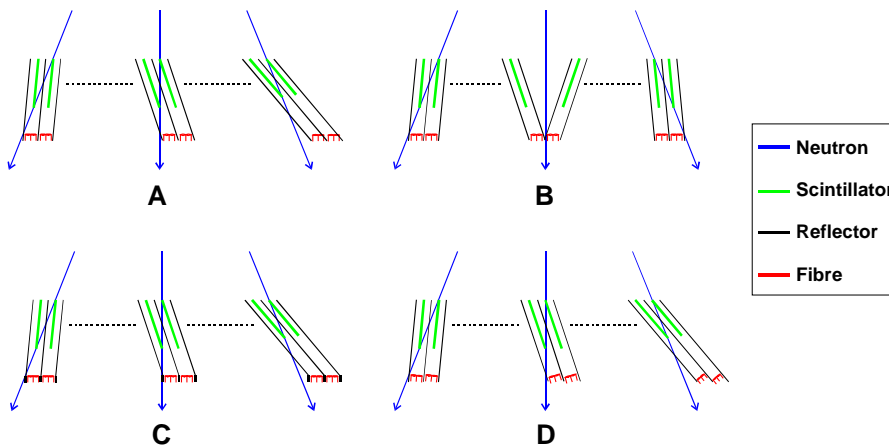


Figure 15: Parallax free high efficiency ZnS scintillator and reflector geometries, designed for pixel detectors with a 3 mm position resolution.

Figure 15 shows a number of parallax free designs. Design A is not feasible as the fibres are obstructed by the reflectors. Design B does not suffer from obstructed fibres, but it has a 6 mm region in the centre of the detector without scintillators. This is a serious disadvantage for a single crystal diffraction detector. Raising the angled reflectors above the fibres and adding another reflector grid between the fibres, as shown in design C, has been considered as a means to avoid obstructed fibres. Aligning both sets of reflectors will nevertheless be difficult, increasing the probability of optical cross talk between pixels. Design D has angled fibres and suffers from neither parallax problems nor obstructed fibres. As the existing single crystal

Final Report

detectors do not have angled fibres, there is no possibility of incorporating this design into these detectors. Nevertheless, design D provides a promising design for future high efficiency ZnS detectors where the concept of angled fibres can be incorporated into these detectors at the design stage.

Higher resolution linear position sensitive detectors

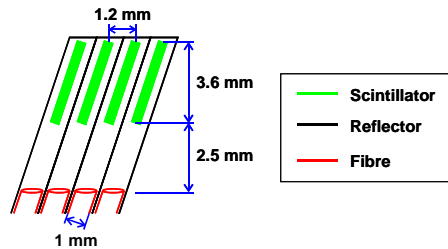


Figure 16: Schematic diagram of the preferred fibre, scintillator and reflector geometry for a high efficiency ZnS scintillator strip detector with a 1.2 mm position resolution.

The scintillator and reflector geometry of the 3 mm strip detector has the potential of being adapted for detectors with an even better position resolution. Monte-Carlo simulations have been carried out to study the feasibility of such a higher resolution detector. These simulations show that, with a carefully optimised geometry, it should be possible to build one-dimensional position sensitive detectors with a position resolution of 1 to 2 mm. Optimisations procedures have resulted in the geometry chosen in Figure 16.

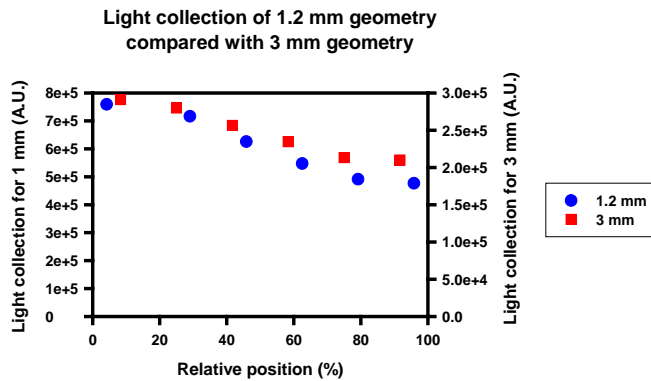


Figure 17: Comparison of the light collection efficiency of a 1.2 mm and 3 mm linear position sensitive detector, calculated as a function of the position of neutron absorption along the width of the strip. Results are estimated with a Monte-Carlo simulation.

Figure 17 shows that Monte-Carlo simulations predict that the light collection efficiency of this 1.2 mm geometry could be circa 2.5 times better than that of the 3 mm ENGIN-X geometry. As a result of the simulations carried out under TECHNI a prototype detector based on this geometry is now under construction. This detector consists of 240 individual detector elements, each 50 mm in length. Pictures of the B₄C fibre block, scintillator grid and detector casing are shown in Figure 18, Figure 19 and Figure 20,

Final Report

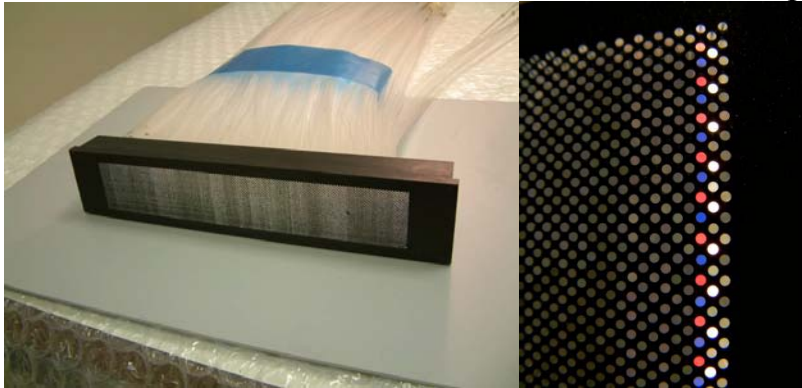


Figure 18: Two photographs of the fibre block of the 1.2 mm prototype detector. The photograph on the left shows the B₄C block with the 6000 optical fibres. A close up of the fibre block, demonstrating the fibre arrangement, is shown on the right.

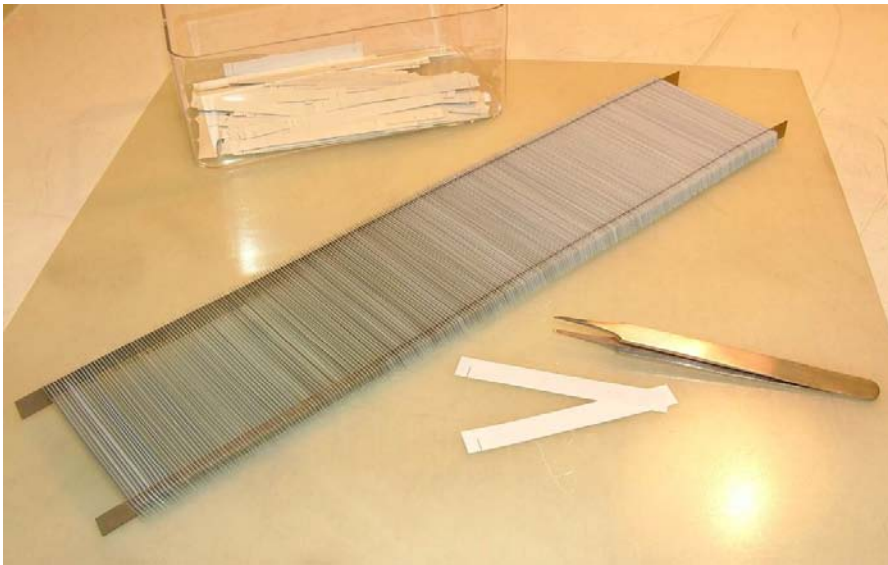


Figure 19: Photograph of the partly finished stainless steel reflector grid assembly of the 240 element prototype detector with a 1.2 mm position resolution.

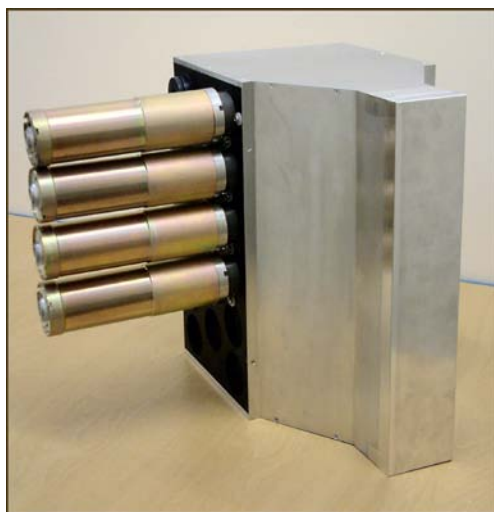


Figure 20: Photograph showing the casing of the 1.2 mm prototype detector complete with 4 of the 32 PMT assemblies.

Evaluation of new scintillator materials

Choice of scintillator material

Over half the neutron detectors at ISIS are based on scintillation detectors. The properties of these detectors have been exploited to meet particular demands of different instruments. Most of these scintillation detectors utilise $\text{ZnS}/^6\text{Li}$ scintillator read out by encoded fibre optic light guides. Whilst many of the properties of the scintillation detectors are exploited to great advantage with these systems, the light emission from $\text{ZnS}/^6\text{Li}$ scintillator has some long decay time components. This results in a rate limitation for some applications.

Under research task 4.2 TU-Delft has shown that many scintillators having faster decay times can be made neutron sensitive. In general the total light emission from such scintillators is low and they cannot easily be read out by fibre optic encoded systems of the type developed at ISIS. The TU-Delft work has shown that in terms of fast decay constant and high light output, the most promising new scintillator for use with this type of readout system is $^6\text{Li}_6\text{Gd}(\text{BO}_3)_3:\text{Ce}^{3+}$ scintillator, (LGBO).

LGBO scintillator in pixel detectors for single crystal diffraction

LGBO scintillator has been evaluated using a pixel detector with two-dimensional position sensitivity, of the type utilized for single crystal diffraction at ISIS. As the existing detectors are close to saturation and have a neutron detection efficiency of only 20% at 1 \AA , this type of detector will derive the most benefit from the use of the new scintillator.

A 1 cm by 1 cm sheet of LGBO has been placed on top of the reflector grid of a two-dimensional position sensitive detector with 3 mm pixels. This detector has the same geometry as the standard fibre optic encoded ZnS pixel detector configuration shown in Figure . Encoding of the optical fibre array is shown in Figure 21, where the green square represents the LGBO scintillator. Fibres indicated with the same colour are grouped into the same bundle. The fibres shown in light and dark blue will collect light from all pixels covered by the scintillator, whereas the pink and red fibres will only collect light from a single row or column of pixels. In the remainder of this section, the bundle of fibres indicated in dark blue will be referred to as the dark blue fibre bundle, etc.

Final Report

Tests showed that the light output of LGBO is sufficient for such an encoded fibre optic readout. To illustrate this result, pulse height distributions measured with four fibre bundles are shown in Figure 22. The light blue and dark blue graphs, recorded with fibre bundles that fully cover the scintillator area, have a similar shape to results obtained with an LGBO scintillator in direct contact with the window of a photomultiplier tube.

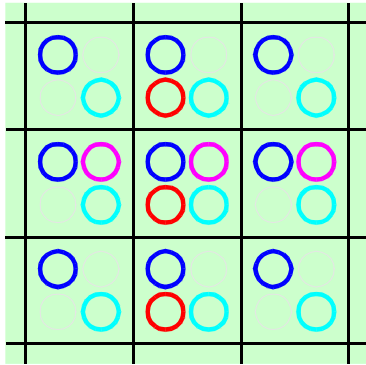


Figure 21: Fibre encoding scheme of pixel scintillation detectors. Fibres indicated with the same colour are grouped into the same bundle.

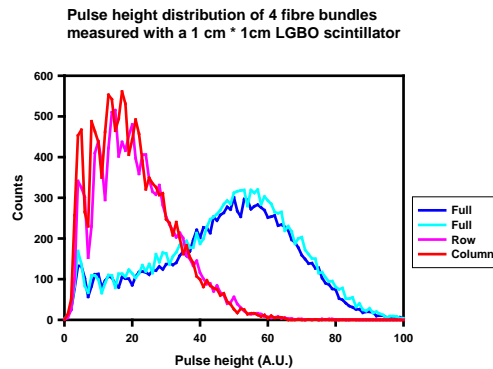


Figure 22: Pulse height distributions measured with 4 fibre bundles. The colour of the graphs corresponds to the colour of the fibres shown in Figure.

Figure 22 also illustrates that, in the scintillator / reflector geometry used for this evaluation, the scintillation light was shared between many pixels. As can be seen in Figure 22, the peak of the pulse height distribution of the light and dark blue graphs is three times higher in pulse height than the peak of the pink and red graphs. Per neutron, the light and dark blue fibre bundles therefore have collected circa three times as much light as the pink and red fibre bundles. From Figure 21 it can be seen that the light and dark blue fibre bundles cover three times as large an area as the pink and red fibres bundles. Hence, the light collection per unit area is the same for the light and dark blue fibre bundles as for the pink and red fibre bundles. This indicates that the light is being uniformly distributed over the pixels, making the determination of the position of neutron absorption unsuccessful.

A solution to this problem is to form the active volume of the scintillator from individual detector pixels that are optically isolated from each other. To date finding such a method that is cost effective and compatible with single crystal diffraction requirements remains a challenge. Notwithstanding these short-term obstacles, LGBO remains a very interesting new scintillator because of the fast decay time and the high light emission. This work has shown that the light emission is high enough for use in a fibre optic encoded pixel detector.

LGBO scintillator in linear position sensitive detectors

Another potentially very beneficial application of LGBO scintillator is in a one-dimensional position sensitive detector for reflectometer instruments. Highly reflective samples studied at these instruments could reflect almost the full beam onto the detector so that a fast scintillator is required. Due to the small detector area of these instruments, the relatively high cost of LGBO is of less importance. All linear position sensitive ZnS scintillation detectors at ISIS are built with optically isolated detector elements. Hence, producing a linear position sensitive LGBO scintillation detector without optical cross talk is relatively straightforward.

As a first step towards a very high resolution linear detector for reflectometer instruments, detector mechanics and electronics have been manufactured for testing the LGBO scintillator in a linear detector with a 3 mm position resolution. Twenty seven LGBO strips have been purchased and final assembly and testing of this prototype detector will commence once the scintillator has been delivered.

Final Report



Figure 23: *Photograph of the detector mechanics that has been constructed for evaluating the LGBO scintillator in a 27 element linear detector with a 3 mm position resolution*

Conclusion

A linear position sensitive neutron scintillation detector with 3 mm position resolution has been developed for the new engineering diffractometer, ENGIN-X. This detector is based on a $\text{ZnS}/^6\text{Li}$ scintillator and a coded fibre optic readout system. To achieve the required position resolution two new scintillator / reflector geometries have been designed, the so-called “V” and “Venetian” geometries. Results from prototype detectors have shown that detector characteristics are similar to the 5 mm “V” type detectors already operating on some of the ISIS instruments. Detectors based on either the “V” or the “Venetian” geometry could meet the ENGIN-X detector specifications. The “Venetian” geometry was selected since it is cheaper to produce and has a higher neutron detection efficiency at longer wavelengths.

Ten full size detector modules for ENGIN-X, based on the “Venetian” geometry, have been successfully manufactured by industry. These detector modules have been economic to produce and easy to install. The 10 detector modules comprise a total of 2400 individual detector elements, each 3 mm wide and 196 mm long, and cover a total active area of 1.4 m². Evaluation of this large area detector array has confirmed its excellent performance. ENGIN-X is now fully commissioned and represents a major addition to the ISIS instrument suite for engineering science.

The “Venetian” geometry offers significant potential for further development. Based on the “Venetian” design, a high efficiency two-dimensional position sensitive detector for single crystal diffraction has been designed. Monte-Carlo simulations have shown that further improvement of the position resolution of an ENGIN-X type detector is feasible. This work has led to the design and construction of a 240 element linear detector with a 1.2 mm position resolution.

$\text{ZnS}/^6\text{Li}$ scintillator, used in the “Venetian” type designs, has a long decay time and new faster scintillator materials are required to fully exploit the advantages of scintillation detectors for some applications. TU-Delft research has shown that the most promising new scintillator compatible with use in a coded fibre optic readout system is $^6\text{Li}_0\text{Gd}(\text{BO}_3)_3\text{Ce}^{3+}$ scintillator, (LGBO). LGBO is particularly attractive for use in two dimensional position sensitive detectors for single crystal diffraction. Evaluation of LGBO has confirmed that light emission of the scintillator is high enough for use in this type of detector and has highlighted the necessity of optical isolation of the detector elements. Linear position sensitive detectors for reflectometer

Final Report

beam lines will also greatly benefit from the higher count rate capability of LGBO. The potential of LGBO in a linear position sensitive detector with a 3 mm position resolution is therefore now under investigation.

In summary, this has been a very successful research task that has resulted in the ability to produce large area one-dimensional position sensitive detectors with a 3 mm position resolution. This work has underpinned the detector development of ENGIN-X, a major new diffractometer for engineering science. The detector geometry developed for this project is immediately available for use on instruments at ISIS and other neutron scattering centres. Furthermore, the work has stimulated the development of higher resolution ZnS and

FZ Juelich: Task 9

Currently the resolution of neutron spin-echo spectrometers is mainly limited by the ability to achieve very high homogeneity of the magnetic field integrals within a beam, i.e. a bundle of paths. Especially if a large solid angle for sample illumination and in particular also for detection of the scattered neutrons shall be covered. In principle the combined effect of different lengths and variations of magnetic fields from a set of cylindrical coils can be "homogenized" by three correction elements. The correction elements represent radial current distributions in the neutron beam. They have to carry high current densities up to 150A/mm for the next generation instruments and at the same time must be transparent to neutrons. In addition their position and geometry must be accurately defined and stable. The concept we decided to follow bases on the devices that are in use at the FZJ-NSE spectrometer, i.e. concentric rings with a thickness modulation to interpolate the current distribution function within the rings, however, with limited accuracy in the current realization. To hold the required current density outer thickness of 20-30mm are required. The first question that has been solved within TECHNI was: how does the thickness modulation and the large outer thickness influences the performance respectively the radial current function?

For this purpose a module to calculate the magnetic field contribution of a thick correction element at all points including the path sections crossing the inside of the elements has been implemented into the software to compute the coefficients for the shape functions and to assess the performance. The results obtained are the following: 1) the shapes with finite thickness shown no deterioration of the ability to correct for inhomogeneity (compared to the previous model with infinite thin coils), 2) the shape coefficients, however, are somewhat different from the previously determined shape coefficients, 3) the corresponding coefficient can now be computed routinely. In addition calculations show that by carefully choosing the positions of the two outer corrections the middle one can be made very weak (which means less current, less accuracy required). With these new parameters a full set of elements for the FZJ-NSE has been specified and will be made by the ZAT of the FZ-Jülich for a neutron test.

The second big problem is to achieve the mechanical accuracy of the correction coils, which after cutting the "spiral" become very floppy. A first test production of a device was performed to assess a method to fix the windings (after cutting a semicircle) with wax. Since this proved not effective it has been abandoned and a new concept is being about to be tested: gluing a semicircular back-plate onto the spirals after cutting on one semicircle and then proceed with the other half. The electrical isolation between "spiral coil" and back-plate is effected by a thin Al-oxide layer (Al being the material of back-plate and coil). The gluing is done with a very thin layer of epoxy, the neutron transmission of it being better than 98%.

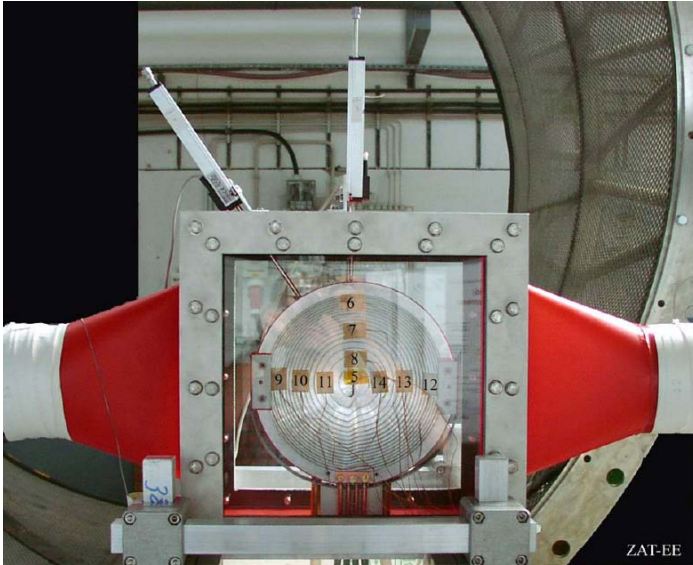


Figure 3

The instrumental setup of the test stand with thermoelements, position sensors and gas and water flow cooling.

Finally – especially, the next generation instruments with their high current densities pose severe conditions on the heat removal due to the current flow. To investigate this problem a test piece with a water-cooled back-plate inside a chamber that allows for a controlled air-flow has been installed and equipped with thermocouples, respectively has been monitored by an infrared imaging thermocamera. First test show that at a current of 300A (for 2mm outer zone width) a temperature rise of about 25 to 30K was observed from outside at $\sim 20^{\circ}\text{C}$ to the middle, with conduction cooling through the end plate and some airflow. However, the innermost zone still had not enough contact with the back-plate and exhibited a hot spot beyond 100°C . This showed which improvements are needed (namely better coverage of the inner zone) for the next test piece. The cooling results, however, are very reassuring that the current densities needed for a new instrument with at least 5-fold increased resolution can be realized with reasonable cooling measures.

Final Report



Figure 4

Latest version of the prototype of the planoconcave correction element.

Next steps comprise the making of the full set of coils for the FZJ-NSE to test part of the new concept. Further improvement of the calculation procedure to include the effect of the current finger leading current to the center of the coils. Further tests of the manufacturing method and the exact shape and assembly of the back-plate with the corresponding assessment of cooling issues. Part of these activities will reach beyond the end of TECHNI.

An extensive Monte-Carlo simulations of a NSE spectrometer based upon rotating magnetic fields were carried out. For these purposes a special computing module was written, thoroughly tested and finally included in the VITESS simulation package. The possibility of a manifold increase in the resolution of such spectrometer by the bootstrap method was shown. The robustness of the spectrometer against non-zero tolerances of the magnetic field areas were shown. Applications of this technique for purposes of neutron reflectometry and small angle scattering were demonstrated.

Final Report

1.3. Comparison of Planned & Actual Work

CCLRC Rutherford Appleton Laboratory

With the successful development of both the 3mm linear scintillator PSD and the novel neutron silicon lens, both of CCLRC's major technical contributions (tasks 4 and 6) to the TECHNI project have been well met, and no significant deviation from the planned programme has occurred.

INFN: Milan/Perugia

The general objectives of the programme on both the neutron detectors and lenses were met and the prototypes listed in Tables I and II were fabricated and tested, and can be delivered on request. Specific remarks concern:

- a) a delayed production of the 2-d version of the Si/Gd microstrip detector, which was due to both limitations in the commercially available readout chips and the matchless high cost of designing and production of a limited series of new ASICS
- b) faster progress than originally planned in designing and production of ZP-based neutron focusing devices, which resulted in fabrication of several optimized new masks and prototypes and new protocols for producing ZPs with isotopic Ni as phase shifter.

INFN: HEND-BICOCCA & HEND-TOV

Work has been accomplished according to expectations. No major deviation needs to be reported.

RISO

The monochromatic imaging mode works nicely together with the produced flexible collimator, resulting in an increase of data taking rate of (in the best case) a factor 7. This is in agreement with the modified activity plan for Risø.

The collimator is, however, not yet in its final form. Improvement is going on, the most important issue is longer blades (150 mm) in order to make the vanes as far as possible to reduce the cross talk value to (estimated) 0.2%. Another important factor is to reduce the error uncertainty in the blade position. The improvements will be finished during the spring of 2004 and will subsequently be tested and installed permanently at RITA-2.

PSI

With respect to the design of improved SM polarisers the initial aims are fulfilled: 2 devices based on the new knowledge are already in use, some more are in construction. We failed to get self-supporting films.

KCL / EMBL

The objectives of the research: to identify, characterise and produce neutron-sensitive image plates that have reduced gamma sensitivity while retaining their neutron DQE have been met.

Juelich

The main part of the work planned for the period covered by this report has been done. A new approach to the construction of image plate detectors of medium resolution (of about 1 mm), which fits to requirements of neutron scattering, was successfully realized. A prototype of pixelated image plate with pixel size of 1 x 1 mm² was prepared and successfully tested at the neutron beam. The first large scale, 100 x 100 mm², image plate was produced. The laser scanner for a large area, neutron pixelated image plate detector was constructed. Technology for production of correction elements, for a new generation NSE spectrometers was developed. Multiple measurements of parameters of these elements were carried out and requirements to the accuracy of their positioning were defined.

Delft - Task 1

All planned activities on fundamental aspects of thermal-neutron detection employing the GEM were realized. New approaches were introduced, viz use of the He-Xe-TMA mixture and the optical observation

Final Report

of the tracks of the reaction products using He-CF₄. So D1.5 was realized. We developed GEM readout electrode structures (D1.9), and selected and studied readout electronics. However due to poor GEM foils, polluted counting gases and problems with electric contacts, a significant delay occurred. Consequently we were not able to realize a position-sensitive detector read-out electronically.

Delft - Task 3

Optimisation storage phosphors and deliverables D3.1, D3.3 and D3.6 realized. Discussions with FZ Juelich on Gd nano-particles resulted in a change to ⁶Li, which is much more attractive from the point of view of neutron sensitivity and gamma-ray insensitivity. This new line is only in its initial phase.

Delft - Task 4

Planned activities well realized. Best scintillator after two years selected and available at CCLRC (Li₆Gd(BO₃)₃:Ce³⁺). Yet, even better scintillators discovered in year(s) three (/four) (Cs₂LiYCl₆:Ce³⁺ and Cs₂LiYBr₆:Ce³⁺). These need further development.

ILL

The new fast SANS detector was installed on D22 and became operational in the first week of the first reactor cycle of 2004. It was able to count water scattering at a rate of 3 MHz at the end of that week. Until today, only three detector tubes were lost, of which one was not operational from the beginning, the second gave up after a few hours at high tension (1550 V, i.e. less than the guaranteed 1600 V), both before installation. The third tube stopped counting after a few days. In the following time, several hundred runs were registered serving to characterize the detector, e.g. its linearity, tube dead-times, limiting count rates, optimal operating conditions (voltage and thresholds), etc. Some of these measurements have yet to be evaluated. A procedure for the re-bining of the raw charge-division data into the standard D22 format was developed and is being applied to allow users to continue with all standard data treatment procedures. After only three weeks, the instrument has accommodated its first visitors, collecting data at high precision and partially with count rates never achieved so far. Following the first four scheduled experiments, there will be a further commissioning period of about a week and another round of scheduled experiment. Although it is reasonable to draw final conclusions only after the last cycle of this year, it appears that the fast detector is performing up to expectations, and quite probably it will be possible to reach even higher count rates by using yet faster processors in the acquisition card.

HMI

Task 1.2.4 and in consequence **Task 1.2.9** could not be completed yet, since:

- FhG-IST could not deliver full-size multi-layer MSGC plates (as quoted before beginning of the project), and
- IPM RAS decided later not to fabricate full-size MSGC plates in contrast to earlier offers, but to support the transfer of process technology to HMI developed for prototype fabrication.

Consequently,

- The further MSGC plate fabrication was concentrated at HMI. This necessitated the construction of a dedicated large-area UHV process chamber. The delivery of this device was delayed up to the second half of year 4. Therefore, the implementation of the specific process technology into this chamber is still going on.
- Using this process chamber, at HMI the size of composite Gd/CsI converters, which were developed there in the necessary quality in prototype scale, will also be upgraded to full scale.

Independently, the development of the MSGC front-end electronics as well as of the dedicated data acquisition (DAQ) system was accomplished, and in addition – as a spin-off by-product – unique DAQ boards for multi-wire chambers with delay line readout based on the same technology were developed up to series production.

Final Report

3. LIST OF DELIVERABLES

Table 3.1, below, lists the major tasks the achievements made by the TECHNI programme. This may be compared to the initial objectives laid out in table 1.1.

	Research Task	Technical Objectives (Deliverables) - Achieved
1	Millimetre and Sub-Millimetre Detectors	The construction of a second-generation Si microstrip has been accomplished, but the final delivery of the advanced design of microstrip gas detectors (MSGC), using ¹⁵⁷ Gd converter has run somewhat slower than planned. nevertheless this task has made enormous strides in solving a number of the key design problems in this challenging detector. Nevertheless, alternative approaches to sub-millimetre neutron detection have been pursued, and these have demonstrated that a resolution of 0.8mm (GMSD) or less (using optical methods). The applicability of GEM technology to different MSGC designs has been established, and the three detector types have been compared.
2	> 3 MHz count rate Area PSD	The demonstration of a large area multi-wire neutron PSD detector able to operate at sustained count rates in excess of 3 MHz has been achieved, and incorporated into new ILL instrumentation.
3	Image Plate Detectors	The second generation of neutron image plates with an improved quantum efficiency, gamma rejection and scanning technology has been demonstrated.
4	3mm scintillator strip detector	A linear scintillator position sensitive detector with >50% efficiency at 1Å, high γ rejection (< E-6), and having a spatial resolution 3mm has been built and incorporated into a new ISIS instrument for measuring engineering stresses, ENGINX. In addition the technique has been extended to a detector resolution of 1.2mm – significantly beyond that originally proposed.
5	>10eV Energy Neutron detector	A new type of resonant neutron detector capable of efficiently detecting neutrons in the 100 eV energy range has been designed and tested. The new design has proved to be a very significant improvement over previous designs.
6	Neutron Focussing Devices	New Neutron Zone plates (NZP) and neutron Silicon Lens (NSL) focussing devices have been built and their characteristics measured.
7	Neutron Polarisation	The next generation of remanent neutron supermirror polarisers which have a divergence suitable for use with thermal (i.e. $\lambda > 1\text{\AA}$) neutron beams have been made.
8	Neutron Energy Selection Devices	An optimised neutron optical grating for neutron energy analysis has been built.
9	NSE Radial Correction Coils	A new design of NSE radial correction coils has been designed.

Table 3.1

Final Report

4. EXPLOITATION & DISSEMINATION OF RESULTS

Publications, Oral Presentations & Seminars

CCLRC, Rutherford Appleton Laboratory

M W Johnson & M R Daymond

The Neutron Silicon Lens: a new design for thermal neutrons

Physica (2000) 308 – 313

M W Johnson & M R Daymond

The Neutron Silicon Lens: an update of the thermal neutron lens results

15th Meeting of the International Collaboration on Advanced Neutron Sources, November 6-9, 2000, Tskuba, Japan.

M R Daymond & M W Johnson

An Experimental test of a neutron silicon lens

Nuclear Instruments and Methods A 485 (2002) 606-614

M W Johnson, S Manolopoulos, N J Rhodes, E M Schooneveld, R Turchetta, CC Wilson, J Penfold & M R Daymond

Silicon Active Pixel Sensor Detectors for Neutron Scattering

Presented at VERTEX 2001, Accepted for publication in Nuclear Instruments & Methods (2002)

E.M. Schooneveld, J.B. Czirr, T.K. McKnight, N.J. Rhodes and R.M Ibberson.

Evaluation of a position sensitive neutron detector based on $Li_6Gd(BO_3)_3$ scintillator.

Proceedings of SPIE 7-8 July 2002 Seattle, Washington, USA Volume 4785 243

M W Johnson, S Manolopoulos, N J Rhodes, E M Schoenfeld, R Turchetta & M R Daymond

Silicon APS detectors for Neutron Scattering, NIM A 501 (2003) 72 -79

TU Delft

T.L. van Vuure, C.W.E. van Eijk, F.A.F. Fraga, R.W. Hollander & L. Margato

High- pressure GEM operation aiming at thermal neutron detection.

IEEE Trans. Nucl. Sci. 48 (2001) 1092-1094

T.L. van Vuure, C.W.E. van Eijk, F. Fraga, R.W. Hollander, R. Kreuger & L.M.S. Margato

GEM neutron detector development

Presented at International workshop on Position Sensitive Neutron Detectors, Hahn-Meitner Institut, Berlin, 28-30 June 2001

T.L. van Vuure, A.J.J. Bos, C.W.E. van Eijk, M. Farahmand, S.T.G. Fetal, F.A.F. Fraga, R.W. Hollander, R. Kreuger, L.M.S. Margato & J.M. Schippers.

GEM applications in neutron detection, dosimetry and proton therapy

Presented at International workshop on Position Sensitive Neutron Detectors, Hahn-Meitner Institut, Berlin, 28-30 June 2001

R. Kreuger, C.W.E. van Eijk, F.A.F. Fraga, M.M. Fraga, S.T.G. Fetal, R.W. Hollander, L.M.S. Margato & T.L. van Vuure

Performance of high pressure Xe/TMA in GEMs for neutron & X-ray detection

Conference Record of IEEE 2001 Nuclear Science Symposium & Medical Image Conference, San Diego, California, November 4 – 10, 2001, CD, N13_2

Final Report

A.V. Sidorenko, A.J.J. Bos, P. Dorenbos, N.J.M. Le Masson, P.A. Rodnyi, C.W.E. van Eijk, I.V. Berezovskaya & V.P. Dotsenko.

Storage phosphors for thermal neutron detection

Presented at SCINT 2001, 6th International Conference on Inorganic Scintillators & their use in Scientific & Industrial Applications, Sep. 16-21, 2001, Chammonix France.

V.P. Dotsenko, I.V. Berezovskaya, N.P. Efryushina, A.S. Voloshinovskii, P. Dorenbos & C.W.E. van Eijk.

Luminescence of Ce³⁺ ions in strontium haloborates

Journal of Luminescence 93 (2001) 137-145.

C.P. Allier, R.W. Hollander, C.W.E. van Eijk, P.M. Sarro, P.M. de Boer, M. Czirr, J.B. Chaminade & J.P. Fouassier.

Thin photodiodes for a neutron scintillator-silicon well detector IEEE Trans.

Nucl. Sci. 48 (2001) 1154-1157

C.W.E. van Eijk

Inorganic Scintillators and Storage Phosphors for Position-Sensitive Neutron Detection

Presented at International Workshop on Position Sensitive Neutron Detectors, Hahn-Meitner Institut, Berlin, 28-30 June 2001

L.E. Dinca, P. Dorenbos, J.T.M. de Haas, V.R. Bom & C.W.E. van Eijk

Alpha-gamma pulse shape discrimination in CsI:Tl, CsI:Na and BaF₂ scintillators

Presented at SCINT 2001, 6th International Conference on Inorganic Scintillators & their use in Scientific & Industrial Applications, Sep. 16-21, 2001, Chammonix France.

C.W.E. van Eijk

Neutron PSDs for the next generation of spallation neutron sources

Nucl. Instr. Meth. A 477 (2002) 383-390

L.E. Dinca, P. Dorenbos, J.T.M. Haas, V.R. Bom & C.W.E. van Eijk

Alpha-gamma pulse shape discrimination in CsI:Tl, CsI:Na and BaF₂ scintillators

Nucl. Instr. Meth. A 486 (2002) 141-145

E. van Loef, P. Dorenbos, C.W.E. van Eijk, K.W. Kramer & H.U. Gudel

Scintillation and spectroscopy of the pure and Ce³⁺-doped elpasolites: Cs₂LiYX₆ (X=Cl,Br)

Journal of Physics, Condensed Matter Volume 14 (2002) 8481 – 8496

F.A.F. Fraga, L.M.S. Margato, S.T.G. Fetal, M.M.F.R. Fraga, R. Ferreira Marques,

A.J.P.L. Policarpo, B. Guérard, A. Oed, G. Manzini & T.L. van Vuure

CCD readout of GEM based neutron detectors

Nucl. Instr. & Meth. A478 (2002) 357-361

P. Dorenbos, L. Pierron, L. Dinca, C.W.E. van Eijk, A. Kahn-Harari & B. Viana

4f-5d spectroscopy of Ce³⁺ in CaBPO₅, LiCaPO₄ & Li₂CaSiO₄

Journal of Physics, Condensed Matter Volume 15 (2003) 511 – 520

V.P. Dotsenko, I.V. Berezovskaya, P.V. Pyrogenko, N.P. Efryushina, P.A. Rodnyi, C.W.E. van Eijk & A.V. Sidorenko

Valence States & Luminescence Properties of Ytterbium ions in Strontium Haloborates

Journal of Solid State Chemistry 166 (2002) 271-276

A. Sidorenko, A.J.J. Bos, P. Dorenbos, N.J.M. Le Masson, P.A. Rodnyi, C.W.E. van Eijk, I.V. Berezovskaya & V.P. Dotsenko

Storage phosphors for thermal neutron detection

Nucl. Instr. and Meth. A 486 (2002) 160-163

Final Report

T. L. van Vuure, F. D. van den Berg, C. W. E. van Eijk & R. W. Hollander

Limits to proportionality in the double GEM detector

Nuclear Instruments & Methods in Physics Research Section A: Accelerators, Spectrometers, Detectors & Associated Equipment, Volume 477, Issues 1-3, 21 January 2002.

R. Kreuger, C.W.E. van Eijk, F.A.F. Fraga, M.M. Fraga, S.T.G. Fetal, R.W. Hollander, L.M.S. Margato & T.L. van Vuure

Gem neutron detector development (Poster)

ESS European Conference Bonn, 16-17 May 2002

R.Kreuger, C.W.E. Van Eijk, S.T.G. Fetal, F.A.F. Fraga, M.M.R.F. Fraga, R.W. Hollander,

L.M.S. Margato, P.J.B. Mendes & T.L. Van Vuure

GEM based ^3He filled position sensitive detectors (Poster)

ESS European Conference Bonn, 16-17 May 2002

R. Kreuger, C.W.E. van Eijk, S.T.G. Fetalb, F.A.F. Fraga, R.W. Hollander, L.M.S. Margato & T.L van Vuure

A GEM based neutron detector (Presentation)

PSD6 Conference, Leicester, 9-13 September 2002

T.L. van Vuure, R. Kreuger, C.W.E. van Eijk and R.W. Hollander, L. M. S. Margato, F. A. F. Fraga,

M. M. F. R. Fraga, S. T. G. Fetal, R. Ferreira Marques & A. J. P. L. Policarpo

Applications of the GEM at high pressure for neutrons and X-rays (presentation)

IWORD Conference Amsterdam, 9-13 September 2002

R. Kreuger, C.W.E. van Eijk, R.W. Hollander & T.L van Vuure

A GEM based neutron detector (presentation)

6th TECHNI Meeting, Saclay, 17-18 October 2002

HMI

Gebauer, B.

Novel microstrip detectors & data acquisition strategies for thermal neutron imaging at the next generation pulsed neutron sources

Proc. Of 2nd Int. Workshop on Data Acquisition Systems for Neutron Experimental Facilities (DANEF-2000), Dubna, Russia, June 5-7, 2000, JINR E10-2001-11, pp. 28-43

Levchanovski, F.V.; Gebauer, B. & Schulz, Ch.

A PCI DAQ board for a two-dimensional high-resolution delay line detector

Proc. Of 2nd Int. Workshop on Data Acquisition Systems for Neutron Experimental Facilities (DANEF-2000), Dubna, Russia, June 5-7, 2000, JINR E10-2001-11, pp. 89-95

Gebauer, B; Schulz, Ch.; Richter, G.; Levchanovsky. F.V., Nikiforov, A.

Development of a hybrid MSGC detector for thermal neutron imaging with a MHz data acquisition & histogramming system

Nucl. Instr. & Meth. A 471 (2001), pp. 249-253

Butenko, V.; Drozdov, V.; Gebauer, B.; Levchanovski, F.; Nikiforov, A. & Prikhodko,

V. Application of DSPs in Data Acquisition Systems for Neutron Scattering Experiments at the IBR-2 Pulsed Reactor

Proc. of the Int. Conf. On Computing in High Energy and Nuclear Physics (CHEP'2001), Sept. 3-7, 2001, Beijing, China, pp. 560-561

Gebauer, B.

Development of high-resolution and fast hybrid micropattern detectors for the next generation pulsed neutron sources

Int. Workshop on Position-Sensitive Neutron Detectors (PSND), Berlin, June 28-30, 2001, Book of Abstracts, pp. 49-51

Final Report

Gebauer, B.; Schulz, Ch.; Levchanovski, F.V.; Nikiforov, A.; Balykov, L.N.; Richter, G.; Namaschk; B.; Klimov, A.Yu.; Rogov, V.V. & Shashkin, V.I.

A large-area hybrid multi-layer micro-strip gas chamber (MSGC) detector for thermal neutron imaging
2nd German-Russian User Meeting, Dubna, April 21-25, 2001

Gebauer, B.

Very high resolution & fast large-area hybrid low-pressure MSGC detector for thermal neutron imaging
3rd TECHNI Meeting, Univ. Milano-Bicocca, Milan, Italy, May 3-4, 2001

Gebauer, B. (in collaboration with Mezei, F.; Gutberlet, Th. & Wilpert, Th.)

Int. Workshop on Position-Sensitive Neutron Detectors (PSND), Berlin, June 28-30, 2001

Schulz, Ch.; Gebauer, B.; Balykov, L.; Richter, G.; Levchanovsky, F.V. & Nikiforov A. *Development of high-resolution, large-area hybrid MSGC detectors for thermal neutron imaging*

Int. Workshop on Position-Sensitive Neutron Detectors (PSND), Berlin, June 28-30, 2001, Book of Abstracts, pp. 74-76

Organization of Conferences/ International

B. Gebauer (in collaboration with F. Mezei, Th. Gutberlet, Th. Wilpert)

Int. Workshop on Position-Sensitive Neutron Detectors (PSND), Berlin, June 28-30, 2001

Schulz, Ch.; Gebauer, B.; Levchanovski, F.V.; Nikiforov, A.; Richter, G.; Balykov, L.N.; Shashkin, V.I.; Klimov, A.Yu. & Rogov, V.V.

A novel large-area, low-pressure detector with high position & time-of-flight resolution for thermal neutron imaging

Int. Conf. on Neutron Scattering (ICNS 2001), München, Sept. 9-13, 2001; Book of Abstracts, p. 30 (T-98)

Gebauer, B.

Development of very high resolution and fast hybrid 2D-micro-strip gas chamber detectors for the next generation pulsed neutron sources

4th TECHNI Meeting, Paul Scherrer Institut, Villigen, Switzerland, October 18-19, 2001

Gebauer, B.

Development of very high resolution & fast hybrid 2D-micro-strip gas chamber detectors for ESS

5th TECHNI Meeting & European Conference ESS, Alter Bundestag, Bonn, Germany, May 15-17, 2002

B. Gebauer, Ch. Schulz, B. Wang, B. Namaschk, G. Richter, Th. Wilpert, L.N. Balykov,

F.V. Levchanovsky, A. Nikiforov, A.Yu. Klimov, V.V. Rogov & V.I. Shashkin

Development of fast high-resolution microstrip detectors with thin neutron converter foils for ESS

European Conference ESS, Alter Bundestag, Bonn, Germany, May 16-17, 2002

B. Gebauer, Ch. Schulz, B. Wang, B. Namaschk, G. Richter, Th. Wilpert, L.N. Balykov, F.V. Levchanovsky & A. Nikiforov

Very-high resolution hybrid MSGC detectors,

European Conference ESS, Alter Bundestag, Bonn, Germany, May 16-17, 2002

Detector requirements for the European spallation neutron source ESS

Invited Talk, Proc. of SPIE's 47th Annual Meeting, Seattle, USA, July 7-11, 2002, ISBN 0-8194-4552-5, Vol. 4785, pp. 182-196

Ch. Schulz, B. Gebauer, G. Richter, B. Namaschk, L.N. Balykov, F.V. Levchanovski, A. Nikiforov, V.I. Shashkin, A.Yu. Klimov & V.V. Rogov

Development of hybrid MSGC detectors with high position & time-of-flight resolution for neutron scattering experiments at ESS.

Proc. of SPIE's 47th Annual Meeting, Seattle, USA, July 7-11, 2002, ISBN 0-8194-4552-5, Vol. 4785, pp. 203-213

Final Report

Gebauer, B.

Development of very high resolution & fast hybrid 2D-micro-strip gas chamber detectors for ESS

6th TECHNI Meeting, Orsay, France, October 17-18, 2002

Refereed Publications

B. Gebauer,

Detector requirements for the European spallation neutron source ESS,

Invited Talk, Proc. of SPIE's 47th Annual Meeting, Seattle, USA, July 7-11, 2002, ISBN 0-8194-4552-5, Vol. 4785, pp. 182-196

Ch. Schulz, B. Gebauer, G. Richter, B. Namaschk, L.N. Balykov, F.V. Levchanovski, A. Nikiforov, V.I. Shashkin, A.Yu. Klimov and V.V. Rogov,

Development of hybrid MSGC detectors with high position and time-of-flight resolution for neutron scattering experiments at ESS,

Proc. of SPIE's 47th Annual Meeting, Seattle, USA, July 7-11, 2002, ISBN 0-8194-4552-5, Vol. 4785, pp. 203-213

B. Gebauer, Ch. Schulz, G. Richter, F.V. Levchanovski, A. Nikiforov

Development of a hybrid MSGC detector for thermal neutron imaging with a MHz data acquisition and histogramming system

Nucl. Instr. and Meth. A 471 (2001), pp. 249-253

Further Publications

B. Gebauer

Novel microstrip detectors and data acquisition strategies for thermal neutron imaging at the next generation pulsed neutron sources

Proc. of the 2nd Int. Workshop on Data Acquisition Systems for Neutron Experimental Facilities (DANEF-2000), Dubna, Russia, June 5-7, 2000, JINR E10-2001-11, pp. 28-43

F.V. Levchanovski, B. Gebauer, Ch. Schulz

A PCI DAQ board for a two-dimensional high-resolution delay line detector

Proc. of the 2nd Int. Workshop on Data Acquisition Systems for Neutron Experimental Facilities (DANEF-2000), Dubna, Russia, June 5-7, 2000, JINR E10-2001-11, pp. 89-95

V. Butenko, V. Drozdov, B. Gebauer, F.V. Levchanovski, A. Nikiforov, V. Prikhodko

Application of DSPs in Data Acquisition Systems for Neutron Scattering Experiments at the IBR-2 Pulsed Reactor

Proc. of the Int. Conf. on Computing in High Energy and Nuclear Physics (CHEP'2001), Sept. 3-7, 2001, Beijing, China, pp. 560-561

Invited Conference Talks / International

B. Gebauer

Novel micro-strip detectors and data acquisition strategies for thermal neutron imaging at the next generation pulsed neutron sources

2nd Int. Workshop on Data Acquisition Systems for Neutron Experimental Facilities (DANEF-2000), Dubna, Russia, June 5-7, 2000

F.V. Levchanovski, B. Gebauer, Ch. Schulz

A PCI DAQ board for a two-dimensional high-resolution delay line detector

Int. Workshop on Data Acquisition Systems for Neutron Experimental Facilities (DANEF-2000), Dubna, Russia, June 5-7, 2000

B. Gebauer

Development of high-resolution and fast hybrid micro-pattern detectors for the next generation pulsed neutron sources

Int. Workshop on Position-Sensitive Neutron Detectors (PSND), Berlin, June 28-30, 2001, Book of Abstracts, pp. 49-51

Final Report

B. Gebauer

Towards detectors for next generation spallation neutron sources

Invited Review Talk, The Xth Vienna Conference on Instrumentation (VCI 2004), Vienna, Austria, February 16-21, 2004; to be published in Nucl. Instr. and Meth. A

B. Gebauer, S.S. Alimov, A.Yu. Klimov, F.V. Levchanovski, E.I. Litvinenko, A.S. Nikiforov, V.I. Prikhodko, G. Richter, V.V. Rogov, Ch. Schulz, V.I. Shashkin, M. Wilhelm, Th. Wilpert

Development of hybrid low-pressure MSGC neutron detectors

Invited Talk, Third Int. Workshop on Position-Sensitive Neutron Detectors (PSND 2004), Tokyo, Japan, January 12-16, 2004; accepted for publication in Nucl. Instr. and Meth. A

Further Conference Talks / International

F.V. Levchanovski, B. Gebauer, E.I. Litvinenko, A.S. Nikiforov, V.I. Prikhodko, Ch. Schulz, Th. Wilpert

A PCI DAQ board for MWPC detectors with high-rate 2D delay line position readout

Third Int. Workshop on Position-Sensitive Neutron Detectors (PSND 2004), Tokyo, Japan, January 12-16, 2004; accepted for publication in Nucl. Instr. and Meth. A

B. Gebauer, Ch. Schulz, F.V. Levchanovsky, E.I. Litvinenko, A.S. Nikiforov, S.S. Alimov, Th. Wilpert

Cross-fertilization between spallation neutron source and third generation synchrotron radiation detectors

Proc. of Eighth Int. Conf. on Synchrotron Radiation Instrumentation (SRI 2003), San Francisco, USA, August 25-29, 2003; accepted for publication by American Institute of Physics

B. Gebauer, Ch. Schulz, G. Richter, F.V. Levchanovsky, A. Nikiforov

Development of a hybrid MSGC detector for thermal neutron imaging with a MHz data acquisition and histogramming system

Int. Conf. Imaging 2000, Stockholm, Sweden, June 28 – July 1, 2000

B. Gebauer, Ch. Schulz, F.V. Levchanovski, A. Nikiforov, L.N. Balykov, G. Richter, B. Namaschk, A.Yu. Klimov, V.V. Rogov, V.I. Shashkin

A large-area hybrid multi-layer micro-strip gas chamber (MSGC) detector for thermal neutron imaging

2nd German-Russian User Meeting, Dubna, April 21-25, 2001

Ch. Schulz, B. Gebauer, F.V. Levchanovski, A. Nikiforov, G. Richter, L.N. Balykov, V.I. Shashkin, A.Yu. Klimov, V.V. Rogov

A novel large-area, low-pressure detector with high position and time-of-flight resolution for thermal neutron imaging

Int. Conf. on Neutron Scattering (ICNS 2001), München, Sept. 9-13, 2001; Book of Abstracts, p. 30 (T-98)

Further Conference Talks / National

B. Gebauer

Entwicklung eines hochauflösenden Niederdruck-Mikrostreifen-Neutronendetektors mit Folienkonverter für ESS

Herbsttagung der deutschen Studiengruppe für elektronische Instrumentierung, Berlin, 25.-27. September 2000

Poster Contributions / International

B. Gebauer, Ch. Schulz, B. Wang, B. Namaschk, G. Richter, Th. Wilpert, L.N. Balykov, F.V. Levchanovsky, A. Nikiforov, A.Yu. Klimov, V.V. Rogov, V.I. Shashkin,

Development of fast high-resolution microstrip detectors with thin neutron converter foils for ESS

European Conference ESS, Alter Bundestag, Bonn, Germany, May 16-17, 2002

B. Gebauer, Ch. Schulz, B. Wang, B. Namaschk, G. Richter, Th. Wilpert, L.N. Balykov, F.V. Levchanovsky, A. Nikiforov,

Very-high resolution hybrid MSGC detectors,

European Conference ESS, Alter Bundestag, Bonn, Germany, May 16-17, 2002

Final Report

Ch. Schulz, B. Gebauer, L.N. Balykov, G. Richter, F.V. Levchanovsky, A. Nikiforov
Development of high-resolution, large-area hybrid MSGC detectors for thermal neutron imaging
Int. Workshop on Position-Sensitive Neutron Detectors (PSND), Berlin, June 28-30, 2001, Book of Abstracts, pp. 74-76

Invited Talks at other Institutes

B. Gebauer

Novel hybrid low-pressure microstrip gas chamber detectors for high-resolution thermal neutron imaging
Institute for Physics of Microstructures, Russian Academy of Sciences, Nizhny Novgorod, Russia, June 13, 2000

B. Gebauer

Entwicklung eines hochauflösenden Niederdruck-Mikrostreifen-Gas-Neutronendetektors mit Folienkonverter für ESS
Zentrallabor für Elektronik, Forschungszentrum Jülich, 11. Dezember 2000

Further Talks

B. Gebauer:

Very-high resolution large-area MSGC detectors
1st TECHN Meeting, Abingdon, U.K., March 30-31, 2000

B. Gebauer:

Very-high resolution large-area MSGC detectors
2nd TECHN Meeting, Grenoble, France, October 12-13, 2000

B. Gebauer:

Very high resolution and fast large-area hybrid low-pressure MSGC detector for thermal neutron imaging
3rd TECHN Meeting, Univ. Milano-Bicocca, Milan, Italy, May 3-4, 2001

B. Gebauer:

Development of very high resolution and fast hybrid 2D-micro-strip gas chamber detectors for the next generation pulsed neutron sources
4th TECHN Meeting, Paul Scherrer Institut, Villigen, Switzerland, October 18-19, 2001

B. Gebauer:

Development of very high resolution and fast hybrid 2D-micro-strip gas chamber detectors for ESS
5th TECHN Meeting and European Conference ESS, Alter Bundestag, Bonn, Germany, May 15-17, 2002

B. Gebauer:

Development of very-high resolution and fast hybrid 2D micro-strip detectors (MSGC & Si-MSD)
6th TECHN Meeting, Orsay, France, October 17-18, 2002

B. Gebauer:

Development of very-high resolution and fast hybrid 2D micro-strip detectors (MSGC & Si-MSD)
7th TECHN Meeting, Coimbra, Portugal, May 5-6, 2003

B. Gebauer

Development of very high resolution and fast hybrid 2D micro-strip detectors (MSGC & Si-MSD)
8th TECHN Meeting, Trieste, Italy, October 9-10, 2003

B. Gebauer

High-resolution and fast hybrid 2D MSGC detector developments
9th TECHN Meeting, Abingdon, U.K., February 26, 2004

Final Report

Contacts with potential users

The spin-off (i.e. MWPC) version of the novel DAQ board has immediately found interest. Except at HMI and Dubna, which has bought 5 boards, firm interest in buying boards has been expressed so far by groups of HASYLAB (DESY, Germany), GKSS (Geesthacht, Germany), ELETTRA (Italy), Princeton (USA) and KAERI (Korea). For selling boards a portable package of the DAQ software must be completed incl. licence; this is planned for June/July 2004.

INFM (HEND-BICOCCA and HEND-TOV)

A.Pietropaolo & M.Tardocchi

"Electron-volt spectroscopy at a pulsed neutron source using a resonance detector technique"

Notiziario Neutroni e Luce di Sincrotrone Vol. 6, n. 1 (2001) .

A. Pietropaolo, C. Andreani, A. D'Angelo, R. Senesi, G. Gorini, S. Imberti, M. Tardocchi,
N. Rhodes & E.S. Schooneveld

" \square Detectors for deep inelastic neutron scattering in the 1-100 eV"

To appear on Appl. Phys. A 74 in Vol 3-4 (2002).

C.Andreani, A.Pietropaolo, R.Senesi, G.Gorini, M.Tardocchi, A.Bracco, N.Rhodes & E.Schooneveld

"Electron-volt spectroscopy at a pulsed neutron source using a resonance detector technique"

Nucl Instr and Meth in Phys Res A 481 (2002) 509

M. Tardocchi, A. Pietropaolo, R. Senesi, C. Andreani & G. Gorini

"Development of resonant detectors for epithermal neutron spectroscopy at pulsed neutron sources"

Nucl. Instr. and Meth. A, 518/1-2 (2003) p. 259-260

A. Pietropaolo, R. Senesi, M. Tardocchi, C. Andreani & G. Gorini

"Photon detectors for epithermal neutron scattering at high- \square and low-q"

To be published on Physica B, proceedings of the 3rd European Conference on Neutron Scattering
Montpellier, 3-6 September 2003

M. Tardocchi, C. Arnaboldi, G. Gorini, S. Imberti, G. Pessina, E. Previtali, C. Andreani,
A. Pietropaolo & R. Senesi

"Assessment of a silicon detector for pulsed neutron scattering experiments"

To be published on Physica B, proceedings of the 3rd European Conference on Neutron Scattering
Montpellier, 3-6 September 2003

C. Andreani, A. D'Angelo, G. Gorini, S. Imberti, A.Pietropaolo, N. J. Rhodes, E. M. Schooneveld,
R. Senesi & M. Tardocchi

"CdZnTe gamma detector for Deep Inelastic Neutron Scattering studies on the VESUVIO spectrometer"

Accepted for publication in Appl. Phys. A (2004)

Conference Presentations

A. Pietropaolo, C. Andreani, A. D'Angelo, R. Senesi, G. Gorini, S. Imberti, M. Tardocchi,
E. Schooneveld & N. Rhodes

Poster presentation at the International Conference on Neutron Scattering 2001

9.-13. September 2001, Munich, German Technische Universität München

M. Tardocchi, C. Andreani, A. D'Angelo, A. Pietropaolo, R. Senesi, G. Gorini, S. Imberti,
E. Schooneveld & N. Rhodes

*Oral contribution to the XII nation annual meeting of SISN (Società Italiana di Spettroscopia Neutronica),
Milazzo 8-10 November 2001*

Final Report

A. Pietropaolo, C. Andreani, A. D'Angelo, M. Tardocchi, R. Senesi, G. Gorini, S. Imberti, E. Schooneveld & N. Rhodes
Oral contribution to the XIII national annual meeting of SISN (società italiana di Spettroscopia neutronica), Bonn 16-17 May 2002.

A. Pietropaolo, C. Andreani, A. D'Angelo, M. Tardocchi, R. Senesi, G. Gorini, S. Imberti, E. Schooneveld & N. Rhodes
Oral contribution to the Eleventh International Symposium on Capture Gamma-Ray Spectroscopy and Related Topics, Pruhonice, 2-6 September 2002.

A. Pietropaolo, C. Andreani, A. D'Angelo, G. Gorini, S. Imberti, M. Tardocchi, N. Rhodes, E.M. Schooneveld & R. Senesi
"The Resonance Detector Spectrometer for neutron spectroscopy in the eV energy region", Published on Proceedings of "Eleventh International Symposium on Capture Gamma-Ray spectroscopy and related Topics", World Scientific 2003, pg. 555.

A. Pietropaolo, M. Tardocchi, R. Senesi, C. Andreani & G. Gorini
Oral contribution to the 16th Meeting of the International Collaboration on Advanced Neutron Sources Dusseldorf-Neuss, Germany 12-15 May 2003

A. Pietropaolo, M. Tardocchi, R. Senesi, C. Andreani & G. Gorini
"New perspectives for electron Volt neutron spectroscopy on inverse geometry instruments at pulsed sources"
Published on the proceedings of the 16th Meeting of the International Collaboration on Advanced Neutron Sources", Dusseldorf-Neuss, Germany 12-15 May 2003.

Technical reports

C. Andreani, A. Pietropaolo, R. Senesi, G. Gorini, M. Tardocchi, A. Bracco, N. Rhodes & E Schooneveld
"Electron-volt spectroscopy at a pulsed neutron source using a resonance detector technique" Technical Report RAL-TR-2002-015, ISSN 1358-6254, Rutherford Appleton Laboratory, Chilton, UK (2002).

G. Gorini, C. Andreani, A. D'Angelo, S. Imberti, E. Perelli-Cippo, G. Pessina, A. Pietropaolo, E. Previtali, R. Senesi, M. Tardocchi, A. Bracco, N. Rhodes & E Schooneveld
"The resonant detector and its application to epithermal neutron spectroscopy", Technical Report RAL-TR-2004-XXX, ISSN 1358-6254, Rutherford Appleton Laboratory, Chilton, UK (2004).

INFN (Milan/Perugia)

Contacts with Los Alamos National Laboratory under the SNS project.

Collaboration with the department of Electronic Engineering of Politecnico di Milano.

Presentation of the achievements to the Italian Neutron Scattering School (Palau, September 2002) and to the Annual Meetings of the Italian Neutron Scattering Society.

Thesis for achievement of Laurea in Ingegneria Nucleare – 5 years course – Politecnico di Milano.

Ph.D. in Physics of the Politecnico di Milano for designing of new detectors for thermal neutrons.

Ph.D. in Physics of the Politecnico di Milano for fabrication and test of zone plates for cold and thermal neutrons.

Final Report

Ph.D. in Electronics of the Politecnico di Milano for designing Si detectors and ASICs for x-rays and thermal neutrons.

Collaboration with TU-Delft, that was provided with the test PCB, originally designed for the TEC_2 detector, equipped with VA32/TAN chips and the necessary software for programming the ASICs.

Invited talk *Fresnel Zone Plates as neutron optical elements* to NOP2004, Joint Meeting on Neutron Optics and Detectors, Tokyo, January 2004.

Contribution *Zone Plate for thermal neutron focusing: design, fabrication and first experimental tests* to the International Conference on Micro and Nano Engineering, Cambridge, September 2003.

Contribution *Fresnel Zone Plates as neutron optical elements for neutron imaging* to the European Conference on Neutron Scattering, Montpellier, September 2003.

Publications

Si/Gd 1-d microstrip neutron detector - SG-1d-128 - INFM Technical Report accompanying the TEC_0 detector delivered to Los Alamos.

ISIS Experimental Report - RB11670 - 16-Oct-2000.

A coincidence experiment of two coherent beams of thermal neutrons

M. Iannuzzi, V. Merlo, A. Paciaroni, C. Petrillo & F. Sacchetti
Foundations of Physics Letters **13**, 1 (2000).

An inverse geometry neutron scattering spectrometer with graphite venetian blind crystal analyser and a para-hydrogen filter

C. Petrillo, F. Sacchetti, M. Celli, M. Zoppi & C. A. Checchi
Nuclear Instruments and Methods **A 441**, 494 (2000).

The double focussing monochromator of IN4C

G. Cicognani, H. Mutka, D. Weddle, F. Sacchetti, C. Petrillo & E. Babucci
Physica B **276**, 85 (2000).

A honeycomb collimator for the neutron Brillouin scattering spectrometer BRISP

C. Petrillo, E. Guarini, F. Formisano, F. Sacchetti, E. Babucci & C. Campeggi,
Nuclear Instruments and Methods **A 489**, 304 (2002).

Fresnel Zone Plates for imaging and focusing of thermal and cold neutrons

F. Sacchetti, M. Altissimo, C. Petrillo, E. Di Fabrizio, S. Colleoni & F. Ott,
Neutron News Vol. **14**, No. 2, 37 (2003).

Fresnel Zone Plates as neutron optical elements for neutron imaging

F. Sacchetti, M. Altissimo, C. Petrillo, E. Di Fabrizio, S. Colleoni & F. Ott
to be published in Physica B (2004).

Zone Plate for thermal neutron focusing: design, fabrication and first experimental tests

M. Altissimo, C. Petrillo, F. Sacchetti, F. Ott & E. di Fabrizio
to be published in Micro Electronic Engineering (2004).

Fresnel Zone Plates as neutron optical elements

M. Altissimo, E. Di Fabrizio, F. Ott, C. Petrillo & F. Sacchetti
to be published in Nuclear Instrument and Methods **A** (2004).

Final Report

FZ Juelich

At the final stage of the TECHNI project, the number of contacts was established with industrial vendors to specify technological aspects of the prototypes built. Results obtained within the TECHNI project have been extensively reported at TECHNI annual workshops, at international conferences and workshops. More than 20 contributions related to the developments made within the TECHNI Projects have been published or submitted to regular journals and conference proceedings (see References).

Scientific articles

S.Masalovich, A.Ioffe, E.Kuessel, M.Schlapp, H. von Seggern, Th.Brueckel:
Applied Physics A74 (2002) 118.

M.Schlapp, H. von Seggern, S.Masalovich, A.Ioffe, H.Conrad, Th.Brueckel:
Applied Physics A74 (2002) 109.

Monkenbusch, M.? Neutron spin echo spectroscopy / ed.: F. Mezei ... - Berlin,2003
(Lecture notes in physics ; 601). - 3-540-44293-6. - S. 201 – 212

Ioffe A, Manoshine S.
Physica B 245 (2004) 235.

Ohl,M, Monkenbusch,M, Richter,D
Physica B,335 (2003),S. 153 - 156

Massalovitch,S, Ioffe,A, Küssel,E, Schlapp,M, vonSeggern,H, Brückel,Th
Appl. Physics A [Suppl.] 74, S118 (2002)

Schlapp,M, vonSeggern,H, Massalovich,S, Ioffe,A, Conrad,H, Brueckel,T
Appl. Phys. A 74 [Suppl.], 109-111 (2002)

Conference contributions

Schlapp,M. "Entwicklung hocheffizienter, gamma-insensitiver Detektormaterialien und Bildplatten für Neutronen", Darmstadt, Techn. Univ., Dissertation, 2003

Ohl,M, Monkenbusch,M, Richter,D, Mezei,F, Pappas,C, Lieutenant,K, Krist,T, Zsigmond,G. Proceedings of the International Collaboration on Advanced Neutron Sources (ICANS) XVI. - 1 (2003). - S. 207 – 214

Massalovitch,S, Ioffe,A, Küssel,E, Schlapp,M, Brückel,Th. International Workshop on Position-Sensitive Neutron Detectors - Status and Perspectives, ISSN 1433-559 2, 569 (2002)

Brueckel,Th. Ioffe,A, ENSA Meeting, Creta April 2003.

Ioffe A, Monkenbusch M & Ohl M.
TECHNI Meeting Trieste, Italy. 08.10.2003 - 10.10.2003

A Ioffe, S Masalovich, E Kuessel, M Schlapp, H. von Seggern & Th.Brueckel
European Conference of Neutron Scattering Montpellier,France: 2-6.09.2003.

Ohl M & Monkenbusch M
TECHNI Meeting, Coimbra, Portugal - 06.05.2003.

A offe & Th. Brueckel
International Conference on Magnetism, Rome, August 2003

M Ohl, M Monkenbusch, W Bünten, D Richter, K Lieutenant, G Zsigmond, T Krist, C Pappas & F Mezei
Workshop at the SNS: Kick-Off Meeting '*Polarized Neutrons in Condensed Matter Investigations*'
Oak Ridge,USA: 13.10.2003 - 18.10.2003

Final Report

Ohl M, Monkenbusch M, Richter D, Lieutenant,K, Zsigmond,G, Krist,T, Pappas,C, Mezei,F.
EFAC Meeting at the SNS Oak Ridge,USA: 18.03.2003 - 24.03.2003

Ioffe A & Manoshine S.
International Workshop on polarized neutrons in condensed matter investigations
Venedig, August 2003.

Ohl M, Monkenbusch M, Richter,D, Pappas,C, Lieutenant,K, Zsigmond,G, Mezei,F. T
European Conference on Neutron Scattering, Montpellier,France: 02.09.2003 - 06.09.2003 Poster

Ohl,M, Monkenbusch,M, Richter,D, Pappas,C, Mezei,F, Lieutenant,K, Zsigmond,G.
ICANS XVI : 16th Meeting of the International Collaboration on Advanced Neutron Sources; Convention Center,Neuss: 15.05.2003

M Ohl, M Monkenbusch, Richter,D, Pappas,C, Mezei,F, Lieutenant,K, Zsigmond,G.
7th ESS-SAC Meeting Neuss: 12.05.2003

A.Ioffe.
McStas & VITESS International Workshop, Abingdon, February 2004.

S Massalovitch, A Ioffe, E Küssel, Th. Brückel, M Schlapp & H vonSeggern
ESS-Konferenz (Bonn) Poster (2002)

PSI

The knowledge obtained from the work within the TECHNI network was used to build a white beam polariser for the SANS and a switchable analyser for TOPSI, both at SINQ. The research results were presented in a talk on

5th Autumn School on X-ray scattering from surfaces and thin layers, Smolenice, Slovakia, 2001

SPIE's 47th Annual Meeting, Seattle, USA (2002)

A remanent transmission neutron polariser
J. Stahn, D. Clemens
Proceedings of SPIE **4785**-17 (2002).

A Remanent Fe/Si Supermirror Transmission Polarizer
J. Stahn, D. Clemens
Applied Physics A **75**, S1532-S1534 (2002)

A switchable white-beam neutron polariser
J. Stahn
Physica B **345**, 243-245 (2003)

The SANS polariser is discussed in detail in:
Short note on the new time-resolved and polarization option for the SANS-I instrument at SINQ
J. Kohlbrecher, J. Stahn
Swiss Neutron News **24**, 11-17 (2004)

J. Stahn & D. Clemens
A Remanent Fe/Si Supermirror Polarizer. *Applied Physics A*, accepted 11.2001

Final Report

J. Stahn & M. Christensen

Spin polarizing neutron supermirrors. Oral presentation at the 5th Autumn School on X-ray scattering from surfaces & thin layers, Smolenice, Slovakia, 09.2001

J. Stahn & D. Clemens

A Remanent Fe/Si Supermirror Polarizer, Poster at the International Conference on Neutron Scattering' (ICNS), Munich, Germany, 09.2001.

J. Stahn, M. Christensen, P. Kailbauer & D. Clemens

Improved remanent supermirror polarizers. PSI Scientific Report 2001, Vol. III, p.95.

D Clemens & J Stahn

Stress anisotropy in Fe_{0.87}Co_{0.13}/Si multilayers. PSI Scientific Report 2001, Vol. III, p.97.

J Stahn & D Clemens

A remanent transmission neutron polariser

SPIE's 47th Annual Meeting, Seattle, USA (2002) & published in *Proceedings of SPIE* 4785-17 (2002).

KCL / EMBL

Publications

Kinetics of nanocavity formation based on F-centre aggregation in thermochemically reduced MgO single crystals.

V N Kuzovkov, A. I. Popov, E A Kotormin, M A Monge, R Gonzalez & Y Chen. Phys Rev B 64, 64102 (2001).

LADI - A dedicated facility for biological crystallography.

D. Myles, F Cipriani, M Lehmann & C Wilkinson. Neutron News, 12, 3 8-43 (2001).

VIVALDI - A thermal-neutron Laue diffractometer for physics, chemistry and materials science.

C Wilkinson, J A Cowan, D A A Myles, F Cipriani, and G J McIntyre. Neutron News, 13, 37-41 (2002).

Photostimulable storage phosphors: progress in radiation imaging and material understanding. -

A.I. Popov, D.A.A. Myles, F. Dauvergne & C. Wilkinson

Progress Physics (invited/in preparation)

BaSrFBr:Eu²⁺/Gd₂O₃ storage phosphor as photostimulable storage phosphor for neutron imaging.

A.I.Popov, D.A.A. Myles, F.Dauvergne, P.Lebians & C.Wilkinson

Appl.Phys.Lett. (in preparation)

Oral presentation at conferences and scientific meetings

"PSL storage phosphors; their properties and applications"

A I Popov at Institut Laue Langevin, Grenoble (9/7/2001)

"Neutron image plate detectors for crystallography"

C Wilkinson at European Crystallographic Meeting (abstr. S6.M2.04), Krakow, Poland (26.08.2001)

"Neutron Image Plate Detectors"

C Wilkinson at Australian National Science & Technology Organisation, Lucas Heights, Australia (18.12.2001)

"The LADI Neutron Image Plate Detector at ILL"

D.A.A. Myles at International Workshop on position-sensitive neutron detectors, Hahn-Meitner-Institut, Berlin, Germany (28.6.2001)

Final Report

"Neutron diffraction: case studies at ILL"

D.A.A.Myles at Neutron Diffraction Workshop, American Crystallographic Association 2001, Los Angeles, USA (21.7.2001)

"The State of the Art and Future Prospects for Neutron Protein Crystallography"

D.A.A.Myles at the Neutron Source Development & Instrumentation at European Crystallographic Meeting 20, Krakow, Poland (26.8.2001)

"Storage phosphor and image plate development for neutron imaging"

A.I. Popov, D.A.A. Myles, F. Dauvergne & C. Wilkinson

Third International Conference of Advanced Optical Materials & Devices (abstr. p.106), Riga, Latvia (19-22.8.2002)

"Storage phosphor and image plate development for neutron imaging"

A.I. Popov, D.A.A. Myles, F. Dauvergne & C. Wilkinson

European Spallation Source Conference (abstr. p. 89), Bonn, Germany (16-17.05.2002)

"The use of storage phosphors in the measurement of neutron diffraction patterns"

C Wilkinson at Institute of Solid State Physics, University of Latvia, Riga, Latvia (14/10/2003)

Poster Presentation

"Storage Phosphor and Image Plate Development for Neutron Crystallography"

C. Wilkinson, A.I.Popov, D.A.A.Myles and F.Dauvergne at the 21st European Crystallographic Meeting, Durban, (24-28:8:2003)

Riso

The TECHNI project has resulted in one publication and another one in preparation as follows:

In Publication

C. R. H. Bahl, P. Andersen, S. N. Klausen, and K. Lefmann, submitted to Nucl. Instr. Meth. B (2004)

In Preparation

A. Abrahamsen, C. H. R. Bahl, S. N. Klausen, T. B. S. Jensen and K. Lefmann (in preparation)

The results were presented at the PSI User Meeting,; January 2004, by Christian R. H. Bahl.

ILL

"High count rate detectors for small Angle Neutron Scattering"

The ILL millennium symposium & European user meeting, proceedings, 6-7 April 2001

"Overview of the ILL's millennium programme" Annual report 2001

Fast SANS detector for D22, ILL-News #35, June 2001

D22 Stopped-Flow apparatus for real time measurements, ILL-News #35, June 2001

Etude de detecteurs de neutrons a haut taux de comptage (French), 18th Dec. 2002, Université Grenoble 1.

Laboratory prototype for commissioning of the PSPC, the mechanics, and the electronics

"Design criteria for electronics for resistive charge division in thermal neutron detection", Nuclear Instruments and Methods in Physics Research Section A: Accelerators, Spectrometers, Detectors and Associated Equipment, In Press, Corrected Proof (2004)

Final Report

5. MANAGEMENT & COORDINATION

5.1. Co-ordination

The TECHNI project was co-ordinated by Dr M W Johnson at the Rutherford Appleton Laboratory, where he is the Director of Instrumentation. The Rutherford Appleton Laboratory provided the necessary technical direction and leadership required for a project of this size, together with the secretarial support necessary to service the management meetings and information dissemination.

The project is steered and progress monitored by the *TECHNI Project Management Committee* (TPMC) with representatives from all of the participating groups in the TECHNI programme. The TPMC was chaired by the co-ordinator, Dr. M W Johnson, and met at approximately six-month intervals to set and refine objectives, define priorities and to review progress. The TPMC meetings were held at each of the member laboratories in turn, thereby encouraging further interaction, in addition to that naturally occurring through the research programmes themselves.

Each of the research tasks listed in table A1 was assigned a *task-leader*. This person was be responsible for managing the progress of the research, preparing written reports, and reporting the progress of the research to the TPMC. Detailed technical co-ordination has been achieved by meetings between the *task-leader* and the relevant partners, as appropriate.

CCLRC

The co-ordinator has been in close contact by email with all participants during the 4 year period, and successfully organised nine management meetings held during the period. Considerable technical interaction through technical meetings or correspondence has occurred with partners at the ILL, Rome, Milan and PSI. Other interactions and comments of the partners are given below.

List of TECHNI Meetings

	Date	Venue	Participants
1.	30 th & 31 st March 2000	Abingdon, UK	21
2.	12 th & 13 th October 2000	ILL, Grenoble, France	23
3.	3 ^d & 4 th May 2001	Milano-Bicocca University, Milan	22
4.	18 th & 19 th October 2001	Paul Scherrer Institut, Switzerland	20
5.	15 th May 2002	Bundeshaus, Bonn, Germany	32
6.	17 th & 18 th October 2002	Saclay, France	31
7.	5 th & 6 th May 2003	Coimbra, Portugal	25
8.	9 th & 10 th October 2003	Triest, Italy	20
9.	26 th February 2004	Abingdon, UK	23

Final Report

Table A1: Research Task by year and partner contribution

	Partner	Y1	Y2	Y3	Y4
1	<i>1.4. Millimetre and sub-millimetre resolution detector programme</i>				
1.1	<i>1.5. Si Microstrip</i>				
1.1.1	INFM	Design and development of a 1-d array of Si/Gd microstrip modules. Development and fabrication of foil converters for microstrip detectors in collaboration with HMI. D1.1: prototype Si/Gd microstrip module	Electrical test measurements on the prototype detector. (Q1) D1.6: Mid-term on prototype Si/Gd microstrip module neutron test measurements		
1.1.2	CCLRC		neutron test measurements on the prototype detector from 1.1.1 (Q2-3)		
1.1.3	INFM		Based on the results of 1.1.2 begin the design and development of a double-sided Si/Gd microstrip module. (Q4)	Complete design and development of a double-sided Si/Gd microstrip module. (Q1-Q3) D1.11: report on double sided Si/Gd microstrip module neutron test measurements	
1.1.4	CCLRC			Neutron test measurements on the prototype detector.(Q4)	
1.1.5	INFM				Participate in inter-comparison study between detectors produced by research tasks 1.1 and 1.2.

Final Report

1.2	<i>1.6. Microstrip Gas Detectors (MSGC)</i>				
1.2.1	HMI	<p>Development and fabrication of foil converters for MSGC and Si strip detectors in collaboration with INFM.</p> <p>D1.2: foil converter for MSGC and Si strip detectors</p> <p>Construction of small-scale, low pressure MSGC prototype using Gd converter design.</p> <p>D1.3: low pressure MSGC prototype</p>			
1.2.2	LLB	<p>Design of a ^3He converter based MSGC.</p> <p>D1.4: prototype electronics and mechanics of ^3He MSGC</p>			
1.2.3	TUD (DELFT),HMI	<p>Design of Gas Electron Multiplication (GEM) component for MSGC. Modelling of GEM performance.</p> <p>D1.5: report on expected performance of GEM device</p>			
1.2.4	HMI		<p>Construction of full-size MSGC module using foil converter. Laboratory tests.</p> <p>D1.7: completion of full-size MSGC module</p>	<p>Full scale testing of foil converter MSGC module including data acquisition.</p> <p>D1.12: report on foil converter MSGC neutron test measurements</p>	
1.2.5	LLB		<p>Mounting of the prototype ^3He MSGC and completion of test on a neutron beam.</p> <p>D1.8: Mid-term report of neutron tests on He3 MSGC module</p>	<p>Completion of long term stability evaluation and test of extreme conditions stability (high neutron intensity).</p> <p>D1.13: final report of neutron tests on ^3He MSGC module</p>	

Final Report

1.2.6	TUD (DELFT), HMI		Fabrication of GEM read-out electrodes (D1.9). Theoretical Evaluation of possible gains of using GEM technology in detectors produced by sub-tasks 1.2.1 and 1.2.2 D1.10: Mid-term report of neutron tests on ³He MGSC module		
1.2.7	HMI, TUD (DELFT), LLB			Collaboration on systems and component design of front-end electronics for MSGC.	
1.2.8	TUD (DELFT), HMI, LLB			From results passed by 1.2.6 produce a design incorporating GEM technology into detector type 1.2.1 and/or 1.2.2 and completion of prototype (D1.14).	
1.2.9	TUD (DELFT), HMI, LLB, CCLRC, ILL, INFM			Full scale inter-comparison of detectors developed under sub-tasks 1.1,1.2	working GEM BASED DETECTOR module(s) demonstrated in beam tests and added to the inter-comparison of mm resolution neutron detectors. D1.15: Final report of inter-comparison of neutron tests on millimetre and sub-millimetre detector systems.

2	> MHz count rate Area PSD				
2.1	ILL	Construct prototype including 10 resistive wires, 1m long, with a pitch of 5 mm(D2.1)			
2.2	CCLRC	Based on previous 3 years of design experience, prepare electronics design for use with the detector 2.1(D2.2)	Collaborate with ILL in adapting existing single detector PSD electronics to multi wire system.		

Final Report

2.3	ILL		Collaborate with CCLRC in adapting existing single detector PSD electronics to multi wire system. D2.3 Working PSD module	Laboratory tests (Q1-2) Full test on an instrument at the ILL.(Q3-Q4) D2.4 Report on the performance and characteristics of the PSD detector	Manufacture of full scale detector.
-----	-----	--	---	---	-------------------------------------

3	Image Plate Detector Development				
3.1	TUD (DELFT)	Identification of suitable new candidates for storage phosphor materials for the teams at KCL (LONDON) and JUELICH, and supply samples to these teams. D3.1 Samples of potential new phosphors	Continue with identification of suitable candidate materials for storage phosphors. D3.3 Samples of potential new phosphors	Optimisation of storage phosphor design, including collaboration with JUELICH on Gd nano-particle sensitiser. D3.6 Samples of potential new phosphors	
3.2	KCL (LONDON)	Lab. tests to characterise existing storage phosphor materials and confirm their optical and chemical properties. Prototype image plate construction. D3.2 Report on image plate performance	Lab. tests to characterise new materials chosen and confirm their optical and chemical suitability. Incorporate into prototype image plate. D3.4 Mid-term report on image plate performance	Continuing Lab. Tests to characterise the materials chosen. Preparation of large area plates.	Evaluation of image plate results. D3.7 Final report on image plate performance
3.3	JUELICH	Construction of prototype online scanner using existing storage phosphors	Complete scanner optimisation including incorporation of possible new scintillators provided by TUD (DELFT) D3.5 Mid-term report on image plate performance	Development of Gd nano-particle sensitiser in collaboration with TUD (DELFT). Incorporation into image plate and testing	Design of ceramic image plate materials. Installation of image plate detector unit on neutron spectrometer. D3.8 Final report on image plate performance
3.4	ILL		Experimental measurement of neutron and γ -ray sensitivities.	Incorporation of plates from KCL (LONDON) into working neutron diffractometer.	Continued use in working neutron diffractometer

Final Report

4	<u>3 mm Scintillator Strip Detector</u>				
4.1	CCLRC	Computer studies to evaluate the advantages of different geometrical designs. Selection of manufacturing method.	First prototype construction & testing using existing scintillator. Develop prototype design. D4.1 Mid-term report on design of 3mm scintillator strip detector	Incorporation of new scintillator produced by TUD (DELFT). Further prototype testing and evaluation.	Incorporation into working instrument at CCLRC. D4.1 Final report on performance and characteristics of 3mm scintillator strip detector
4.2	TUD (DELFT)	Identification of suitable scintillator candidates for improved scintillator material	Laboratory tests to confirm suitability of new scintillators. D4.2 New scintillator material. D4.3 Mid term report on potential new scintillator material	Optimisation to obtain best scintillator material. Best scintillator delivered to CCLRC	

5	<u>Neutron Detector for Energies over 10eV</u>				
5.1	HEND-BICOCCA, HEND-TOV	Identification of suitable candidates for the construction materials	Laboratory tests to confirm their suitability for use in the device (Q1-2)	Prototype device construction, and confirmation of principal characteristics D5.2 >10eV neutron detector prototype	D5.3 Final report on >10eV neutron detector
5.2	CCLRC		Full scale test at the ISIS neutron facility at CCLRC to demonstrate suitability in a facility environment. (Q3-4) D5.1 Mid term report on >10eV neutron detector scintillator tests.		Full test of prototype at ISIS neutron facility at CCLRC to confirm all salient characteristics

Final Report

6	Neutron Focussing Devices				
6.1	CCLRC	Complete design studies of Neutron Silicon Lenses (NSL) including Monte Carlo simulations (Q1) (D6.1) Si wafer production and coating (Q2-3) – send to the ILL for coating. (D6.2)	Assemble Lens with coatings supplied by the ILL. Test Neutron Silicon Lens at the ISIS facility at CCLRC. D6.6 Mid-term report on NSL test results Supply of second lens material to PSI for polarised coating.	Construction of a complete collimator-lens-collimator assembly designed by RISO. Test at the ISIS facility at CCLRC.	Test prototype polarising lens using PSI coatings . D6.7 Provide measurements for the inter-comparison of CRL, ZP and NSL techniques.
6.2	RISO	Design studies of sub-millimetre collimation.	Design and Monte-Carlo simulations of an integrated collimator-lens-collimator assembly for test at CCLRC using the RISO software MCSTAS. D6.7 Mid-term report on MC simulation studies.	Neutron test measurements on the binary Zone Plate ZP from INFM	Incorporation of new collimation designs into neutron instruments. D6.7 Provide measurements for the inter-comparison of CRL, ZP and NSL techniques.
6.3	ILL	Investigation of compound refractive lens (CRL) designs. D6.3 Report on CRL designs Coating of Neutron Silicon Lenses from CCLRC with m=2 SM coating(Q4) (D6.4) Monte Carlo simulation of ZP in collaboration with the INFM.	Prototype CRL device construction . Neutron test measurements of CRL devices. D6.8 Mid-term report on CRL device tests.	Neutron test measurements on the binary ZP from INFM	D6.7 Provide measurements for the inter-comparison of CRL, ZP and NSL techniques.
6.4	PSI			Provide improved SM polariser coatings for NSL from CCLRC – for task 6.1	test prototype lenses and incorporate new SM coating into PSI instrument design. D6.7 Provide measurements for the inter-comparison of CRL, ZP and NSL techniques.
6.5	INFM	Design study of a binary Zone Plate (ZP). D6.5 Report on ZP designs	Fabrication of a binary ZP and optical testing (in collaboration with LLB) of the focusing performance and optical	D6.9 Report on ZP test measurements at ILL and	D6.7 Provide measurements for the inter-comparison of CRL, ZP and NSL

Final Report

		Monte Carlo simulation in collaboration with the ILL. Evaluation of electron lithography techniques with the LLB.	efficiency. Send to the ILL for neutron testing.	RISO	techniques.
6.5	LLB	Evaluation of electron lithography techniques with the INFM.	Optical testing measurements on the binary ZP from INFM		D6.7 Provide measurements for the inter-comparison of CRL, ZP and NSL techniques.

7	Neutron Polarisation				
7.1	PSI	Investigate suitable sputtering conditions to increase stress/magnetisation anisotropy for the production of Improved SM polarisers.	Find suitable materials and combinations thereof for the production of Improved SM polarisers. Optimise layer sequences develop prototypes. D7.1 Mid-term report on improved SM polarisers Send to ILL for testing (D7.2)	Provide improved SM polariser coatings for NSL from CCLRC – for task 7.1	Incorporate new SM coating into PSI instrument design. D 7.4 Provide inter-comparison tests results on relative performance of transmission and reflection polarisation devices. Contribute to joint report.
7.2	ILL	Evaluation and test of various techniques for producing Self Supporting Multilayers (SSM):	Definition of optimum methods. First prototype SSM construction. Send to RISO for assembly into complete device including collimation components. D7.2 Mid-term report on improved SSM Testing of PSI SM coatings	Completion of prototype SSM testing.	Integration of device into working instrument. D 7.4 Provide inter-comparison tests results on relative performance of transmission and reflection polarisation devices. Contribute to joint report.
7.3	RISO			Assembly of SSM devices from the ILL, with the inclusion of collimation components. (D7.3)	Initial tests on SSM(Q1)

Final Report

8					
Neutron Energy Selection devices					
8.1	LLB	Design of Neutron Optical Gratings (NOG). Deposition of SM. Fabrication of the masks by electron beam lithography. (D8.1)	Fabrication and test of the first prototypes. Comparison with simulations. D8.3 Mid-term report on NOG and comparison with simulations	Optimisation of the gratings : thickness, spacings.	Installation of a real device on the reflectometer EROS. D8.5 Contribute to a report on the4 inter-comparison of NOG and monochromator performances and applicability.
8.2	ILL	Design of Gradient Crystal Monochromators. Evaluation of different growth technologies. Report on decision on methods and materials. (D8.2)	Fabrication of a large crystal and prototype monochromator (D8.4)	Monochromator testing and incorporation into instruments.	Further fabrication for additional instruments. D8.5 Contribute to a report on the4 inter-comparison of NOG and monochromator performances and applicability.
9					
Neutron Spin Echo Correction Devices					
9.1	JUELICH	Neutron Spin Echo Correction Lenses. Compute the layout an physical properties of the potential design models,	Complete tests on the key manufacturing steps involved. D9.1 Mid-term report on Neutron Spin Echo Correction Devices	Manufacture of completed design	Install and test them at the NSE instrument in FZJ (Jülich). D9.2 Mid-term report on Neutron Spin Echo Correction Devices
9.2	ILL				Test on the IN15 instrument

Table 3